UNIVERSITY OF CALIFORNIA, SAN DIEGO

Dissecting functions for the histone acetyltransferase Esa1
through suppression analysis

A dissertation submitted in partial satisfaction of the requirements for the degree
Doctor of Philosophy

in

Biology

by

Christie S. Chang

Committee in charge:

      Professor Lorraine Pillus, Chair
      Professor Douglass Forbes
      Professor Trey Ideker
      Professor Tracy Johnson
      Professor James Kadonaga
      Professor Victoria Lundblad

2010

UMI Number: 3397186

UMI®
Dissertation Publishing

ProQuest®

The Dissertation of Christie S. Chang is approved, and it is acceptable

in quality and form for publication on microfilm and electronically:

_____

_____

_____

_____

_____

_____
                                                    Chair

University of California, San Diego

2010

DEDICATION

To my family

TABLE OF CONTENTS

LIST OF ABBREVIATIONS

2μ	2-micron
5-FOA	5-fluoroorotic acid
CEN	centromeric
ChIP	chromatin immunoprecipitation
CID	CTD interacting domain
CPT	camptothecin
CTD	C-terminal domain
CUT	cryptic unstable transcript
DNA	deoxyribonucleic acid
HAT	histone acetyltransferase
HDAC	histone deacetylase
HU	hydroxyurea
IB	immunoblot
IP	immunoprecipitation
MMS	methyl methanesulfonate
NAD^+	nicotinamide adenine dinucleotide
NuA4	nucleosomal acetyltransferase of histone H4
rDNA	ribosomal DNA
RNA	ribonucleic acid
SC	synthetic complete
SGA	synthetic genetic array
SIR	silent information regulator
snoRNA	small nucleolar RNA
snRNA	small nuclear RNA
WT	wild-type
YPD	yeast extract-peptone-dextrose

LIST OF FIGURES

xiv

LIST OF TABLES

ACKNOWLEDGEMENTS

I would first like to thank Lorraine Pillus for her constant support throughout my time as a graduate student. She has been an integral part of my training, starting from my very first experiment in her lab, when she taught me about sterile technique. Since then, her advice and encouragement has helped develop my independence as a scientist. I would also like to thank my past mentors, Patricia Denny, Lily Mirels, and Abby Dernburg, who gave me the opportunity to do research with them before I decided on it as a career.

I would like to thank the Pillus lab, past and present members, for providing such a wonderful lab environment. Everyone has contributed positively to my growth as a scientist. Thanks for the invaluable advice and for critiquing my science over the many years. I am especially grateful for the friendships I've developed with my fellow graduate students Erin Scott and Melissa Koch. Having the two of them around has made lab enjoyable and fun.

Thanks to the following lab members for critical reading and editing of parts of my thesis: Renee Garza, Sandra Jacobson, Myriam Ruault, Melissa and Erin. Thanks also to Brian Wood, Rei Otsuka, and Jae Chung, undergraduate students I have mentored that have also contributed to various aspects of my project. I would also like to thank Astrid Clarke for her contributions to Chapter 2 and Erin Scott for her contributions to Appendix B.

I would like to thank all the people that have worked on the second floor of Pacific Hall, especially the Hampton and Kadonaga labs. Everyone has been great neighbors and extremely generous with their supplies and equipment.

I would like to thank the following people for sending strains and reagents: Michael Grunstein, David Stillman, Mitch Smith, Jeffrey Corden, David Brow, Jef Boeke. Thanks also to Michael David for use of the flow cytometer, Jenny DuRose and Maho Niwa for help with northern analysis, and Jennifer Chang for technical assistance in the quantitative RT-PCR experiments.

Finally, I would like to thank my family and friends. My parents have provided constant support and encouragement to me throughout my entire life. Thanks especially to my husband Brian. He has kept me driven and motivated throughout graduate school and much of my success is owed to him.

Chapter 2 is a manuscript in preparation that will be submitted for publication. Astrid Clarke performed the following experiments: Figure 2-1, Figure 2-2A, Figure 2-3A, Figure 2-8B, and Figure 2-10.

Chapter 3 is a reprint of Chang, C.S. and Pillus, L. 2009. Collaboration between the essential Esa1 acetyltransferase and the Rpd3 deacetylase is mediated by H4K12 histone acetylation in *Saccharomyces cerevisiae. Genetics* **183**(1):149-160. The paper was edited to be properly formatted for this chapter.

VITA

2003   B.A., Molecular and Cell Biology

              University of California, Berkeley

2006-2008   Teaching Assistant

              Department of Biology, University of California, San Diego

2010   Ph.D., Biology

              University of California, San Diego

PUBLICATIONS

Chang C.S. and Pillus L. 2009. Collaboration between the essential Esa1

acetyltransferase and the Rpd3 deacetylase is mediated by H4K12 histone acetylation in

Saccharomyces cerevisiae. Genetics **183**(1):149-60.

Lafon A, **Chang C.S.**, Scott E.M., Jacobson S.J., and Pillus L. 2007. MYST

opportunities for growth control: yeast genes illuminate human cancer gene functions.

Oncogene Aug 13;26(37):5373-84.

ABSTRACT OF THE DISSERTATION

Dissecting functions for the histone acetyltransferase Esa1
through suppression analysis

by

Christie S. Chang

Doctor of Philosophy in Biology

University of California, San Diego, 2010

Professor Lorraine Pillus, Chair

Posttranslational histone modifications contribute to chromatin-dependent

processes such as transcriptional regulation and repair of DNA damage. Catalysis of

these modifications is carried out by complexes that function in both targeting activities

to specific genes and in regulating genome-wide levels of modifications. One form of

histone modification is dynamic and reversible acetylation and deacetylation of lysines.

In *Saccharomyces cerevisiae*, Esa1 is an essential histone acetyltransferase that belongs

to the conserved MYST family. Esa1 is the catalytic subunit of two chromatin modifying

complexes with key roles in transcriptional regulation and DNA repair. In this thesis, three different genetic suppressors of *esa1* were identified and characterized, connecting the diverse nuclear functions of Esa1 with multiple cellular processes.

NAB3 encodes an RNA binding protein that processes 3'-ends of non-polyadenylated transcripts. Overexpression of *NAB3* suppressed the temperature-sensitivity of an *esa1* mutant and its defects in rDNA and telomeric silencing. Nab3 was discovered to function in transcriptional silencing at the rDNA locus, cell cycle progression, and DNA damage repair. These are all processes in which Esa1 participates, providing evidence that RNA processing by Nab3 is functionally linked to acetylation by Esa1.

Other genetic studies identified two closely-related histone deacetylases, Rpd3 and Hos2, that coordinate with Esa1 in its different functions. The first of these two studies demonstrates that Esa1 and Rpd3 coordinate acetylation of H4 lysine 12 (H4K12) to promote cell viability. *RPD3*, when deleted, suppressed mutant phenotypes of *esa1* including temperature-sensitivity and silencing defects. In particular, growth rescue of *esa1* by *rpd3* depended specifically on H4K12 acetylation, defining a crucial yet previously unsuspected role for this residue. Notably, of the two biochemically defined Rpd3 complexes, it was Rpd3L that mediated suppression, providing a new distinction from the smaller Rpd3S complex. In contrast to *RPD3*, deletion of *HOS2* suppressed *esa1*'s sensitivity to DNA damaging agents. Initial characterization thus indicates that Esa1 partners with Hos2, and not Rpd3, in response to DNA damage.

The work presented in this thesis applies the powerful tool of genetic suppression to important questions about biological roles for chromatin modifying enzymes.

Chapter 1.

Introduction

The emergence of lysine acetylation as a widespread posttranslational modification. N-epsilon lysine acetylation was discovered over 40 years ago as a reversible posttranslational modification that occurs on histones (Gershey et al. 1968) (Figure 1-1A). Since this initial discovery, histone acetylation and deacetylation has been widely studied for its contributions to transcriptional regulation.

Histone octamers are comprised of two of each of the four canonical histone proteins (H2A, H2B, H3, and H4). DNA is wrapped around this octamer to form the basic chromatin structural unit known as the nucleosome. This structure allows for DNA to be packaged into a condensed state for compaction into the nucleus. The amino acid sequence of each histone is highly conserved throughout all eukaryotes. The histone N-terminal tails protrude from the center of the nucleosome and are subject to several forms of posttranslational modification in addition to acetylation [reviewed in (Kornberg and Lorch 1999)]. For example, phosphorylation, methylation, ubiquitination, SUMOylation, ADP-ribosylation, and citrullination are all common ways that histones can be posttranslationally modified [reviewed in (Smith and Denu 2009)]. Multiple types of modifications can exist on a single nucleosome, and these can influence modifications on neighboring nucleosomes. The resulting combinatorial modifications provide an multitude of possible regulatory signals, thus highlighting the enormous range of functions for histone modifications (Jenuwein and Allis 2001).

2

Figure 1-1. Lysine acetylation and deacetylation. A) Acetylation and deacetylation of histones is a posttranslational modification carried out by enzymes known as histone acetyltransferases (HATs) and histone deacetylases (HDACs). B) Acetylation occurs on the epsilon amine group of the amino acid lysine. This reaction uses the acetyl group from acetyl-CoA and is carried out by HATs. Removal of the acetyl group, or deacetylation, is carried out by HDACs. The HDAC reaction shown is of an NAD^+-independent histone deacetylase.

A
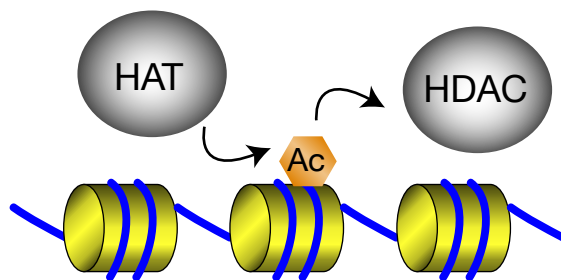
B
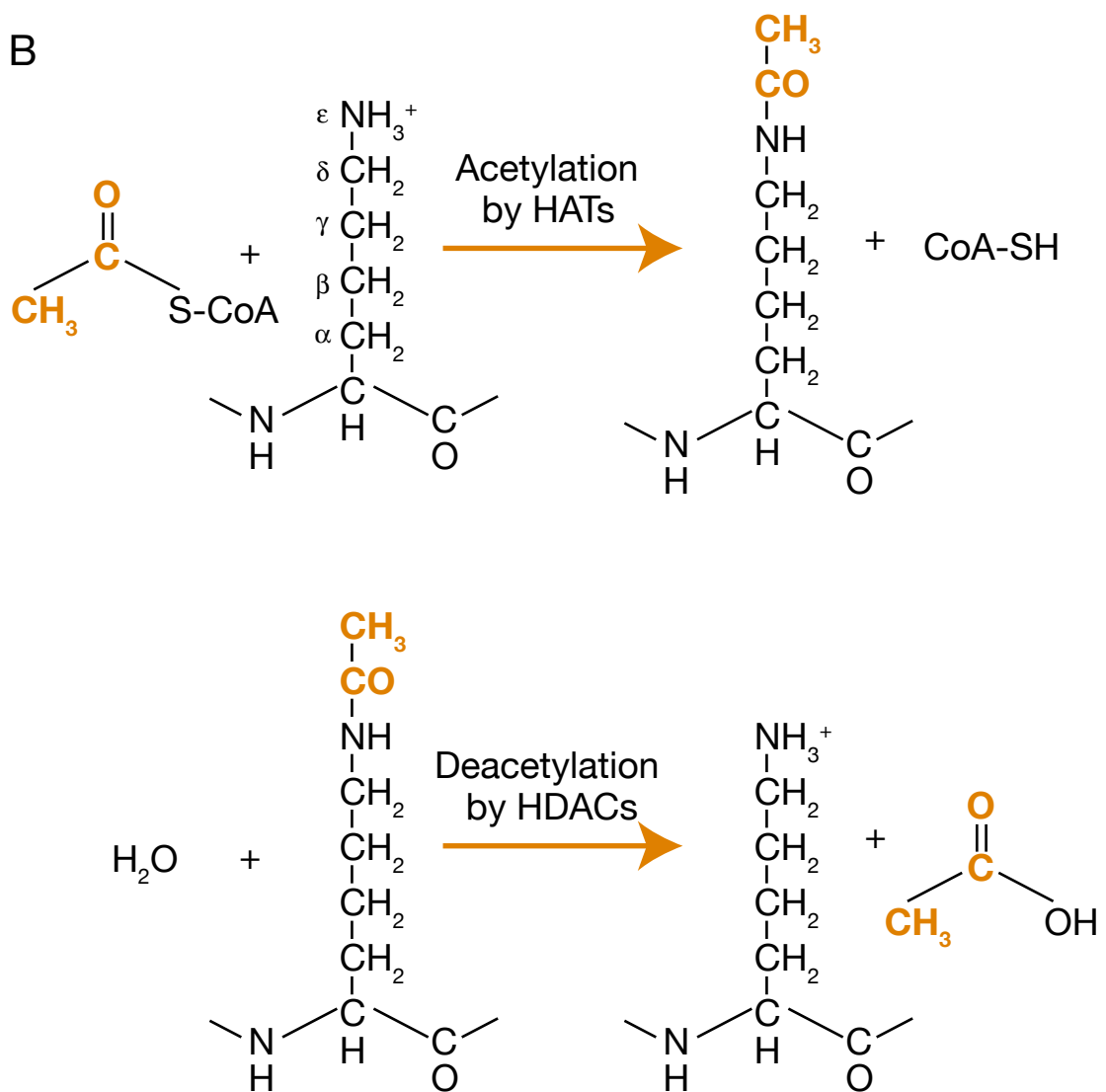
Tightly condensed chromatin structure can act as a barrier to proteins that require contact with DNA. For example, for transcription to occur efficiently, chromatin structure needs to be loosened so that transcription factors and polymerases have access to the DNA template [reviewed in (Kornberg and Lorch 1999)]. Histone modifications provide a regulatory mechanism for altering chromatin structure to facilitate processes such as transcription, DNA replication, and DNA repair. Some histone modifications have been shown to recruit or prevent binding of other proteins such as specific transcription activators or repressors, whereas others increase or decrease the histone octamer's interactions with DNA to maintain a more condensed or loose chromatin structure. For example, histone acetylation neutralizes the positive charge on lysines (Figure 1-1B), and is therefore thought to promote a more open chromatin structure by allowing for decreased interaction with DNA and accessibility of proteins [reviewed in (Henikoff 2005)].

It was realized early on that dynamic histone acetylation and deacetylation plays a prominent role in transcriptional activation and thus, efforts were made to identify the enzymes responsible for this reversible modification. These enzymes were named histone acetyltransferases (HATs) and histone deacetylases (HDACs) (Figure 1-1B). Multiple protein families of HATs and HDACs have been identified in many organisms. These chromatin modifying enzymes function in multiprotein complexes. Non-catalytic subunits of these complexes can aid in targeting activity or bridging connections with other cellular proteins [reviewed in (Shahbazian and Grunstein 2007)].

One example of how chromatin modifying complexes affect chromatin structure is the transcriptional silencing that occurs at telomeres. In the budding yeast

Saccharomyces cerevisiae, the SIR complex is critical for maintaining silent chromatin at the telomeres. The catalytic subunit Sir2, deacetylates histones which allows for binding and spreading of the two non-catalytic structural subunits Sir3 and Sir4. This action promotes formation of a highly-condensed state of chromatin known as heterochromatin [reviewed in (Rusche et al. 2003)].

Much of the focus on acetylation until recent years has been on defining its function as a posttranslational histone modification. It has become increasingly evident that HATs and HDACs also target nonhistone substrates. Only lately has there been a shift in attention to study the role of acetylation of these nonhistone proteins. For example, in yeast, acetylation of the gluconeogenic enzyme Pck1 was found to promote its enzymatic activity (Lin et al. 2009). More and more acetylated proteins are being identified, and each protein is added to a growing acetylome [reviewed in (Norris et al. 2009)]. In fact, in a recent study, almost every metabolic enzyme analyzed in human liver cells was found to be acetylated (Zhao et al. 2010). Therefore, not only is reversible acetylation an established mechanism for regulation of chromatin processes, but a much broader perspective of its role as a widespread posttranslational modification in the cell is emerging.

The MYST family of histone acetyltransferases. MYST HATs are a broadly conserved family of HATs defined by sequence homology to a shared MYST catalytic domain that consists of an acetyl-CoA binding motif and a zing finger. This MYST family is named after its founding members, *MOZ*, *YBF2/SAS3*, *SAS2*, and *TIP60* [reviewed in (Lafon et al. 2007)]. *SAS2* and *SAS3* are yeast genes first defined for their roles in transcriptional silencing, and *MOZ* was discovered as a recurrent translocation

partner in acute myeloid leukemias. Tip60 is a human protein that interacts with the HIV Tat activator. In addition to its interaction with an HIV protein, Tip60 along with other human MYST proteins are implicated in diseases such as cancer [reviewed in (Avvakumov and Côté 2007)]. Tip60 functions as a transcriptional co-activator the c-Myc oncoprotein and also acetylates the tumor suppressor p53 in response to DNA damage.

In *S. cerevisiae*, the three MYST HATs are Sas2, Sas3, and Esa1. Sas2 works in opposition to the HDAC Sir2, by acetylating K16 on histone H4 (H4K16) to prevent the spread of silent chromatin at the telomeres. Sas3 acetylates H3K14, and is thought to promote transcriptional activation or elongation, although its exact role is not understood completely. Esa1, the third and final MYST family member discovered in yeast, is the yeast homolog of human Tip60 [reviewed in (Lafon et al. 2007)], and is the focus of this thesis.

The essential yeast acetyltransferase Esa1 and its partners. Esa1 is the major essential histone acetyltransferase in *S. cerevisiae* (Smith et al. 1998; Clarke et al. 1999). To date, the only other known essential HAT in yeast is Taf1 (Mizzen et al. 1996). Although Taf1 displays strong *in vitro* HAT activity, it only contributes modestly to acetylation *in vivo* (Durant and Pugh 2006). Esa1 has a wide range of targets, and acetylates multiple lysines on H2A, H3, H4, as well as on the histone variant H2A.Z. Functional studies link Esa1's *in vivo* role predominantly to H4 (Clarke et al. 1999; Bird et al. 2002), although a decrease in acetylation at most lysines on all four core histones is observed at localized gene promoters (Suka et al. 2001).

Esa1 is the catalytic core of two distinct complexes, named NuA4 and piccolo (Allard et al. 1999; Boudreault et al. 2003). NuA4 (nucleosome acetyltransferase of H4) is the larger complex and is made up of 13 subunits. Many of these Esa1-associated factors are shared with other nuclear complexes. For example, the subunit Tra1 is found in SAGA and SLIK/SALSA, two complexes that contain the major H3 HAT Gcn5 (Grant et al. 1998). Four NuA4 subunits are also part of the SWR1 complex, which incorporates the histone variant H2A.Z into chromatin (Krogan et al. 2003; Mizuguchi et al. 2004). All except one of the 13 NuA4 components have counterparts in the human Tip60 complex, highlighting the conserved nature of the NuA4 complex between yeast and humans (Figure 1-2) [reviewed in (Doyon and Côté 2004)]. In yeast, the smaller piccolo complex is made up of only three proteins, all of which are also subunits of NuA4 (Figure 1-2) (Boudreault et al. 2003). *In vitro* assays show piccolo as the more active complex (Boudreault et al. 2003), yet the different *in vivo* functions of piccolo and NuA4 are not well-established. The biochemical composition and enzymatic activity of NuA4 and piccolo present a strong foundation for understanding Esa1's multiple cellular roles.

The diverse functions of the acetyltransferase Esa1. The essential nature of Esa1 highlights its importance in the cell, and the study of *esa1* conditional mutants has revealed that Esa1 functions in many chromatin-related nuclear processes. Esa1 is required for proper cell cycle progression, as evidenced by the observation that *esa1* mutants display a G2/M cell cycle block that is dependent on the checkpoint protein Rad9 (Clarke et al. 1999). H4 acetylation by Esa1 is critical in the repair of DNA double-strand breaks (Bird et al. 2002). Esa1 and members of NuA4 are recruited to sites of DNA damage (Bird et al. 2002; Downs et al. 2004), and *esa1* mutants are hyper-sensitive to

Figure 1-2. The NuA4 and piccolo complexes. Diagram of the complex members of NuA4 and piccolo. Esa1 is the catalytic subunit of both complexes. Top: NuA4 is comprised of 13 proteins. Underlined proteins are essential. Subunits in blue are also part of the Swr1 complex. Bottom: piccolo is made up of three subunits, all of which are also part of NuA4.

NuA4

piccolo
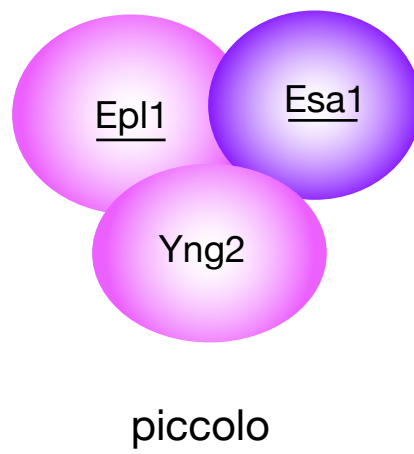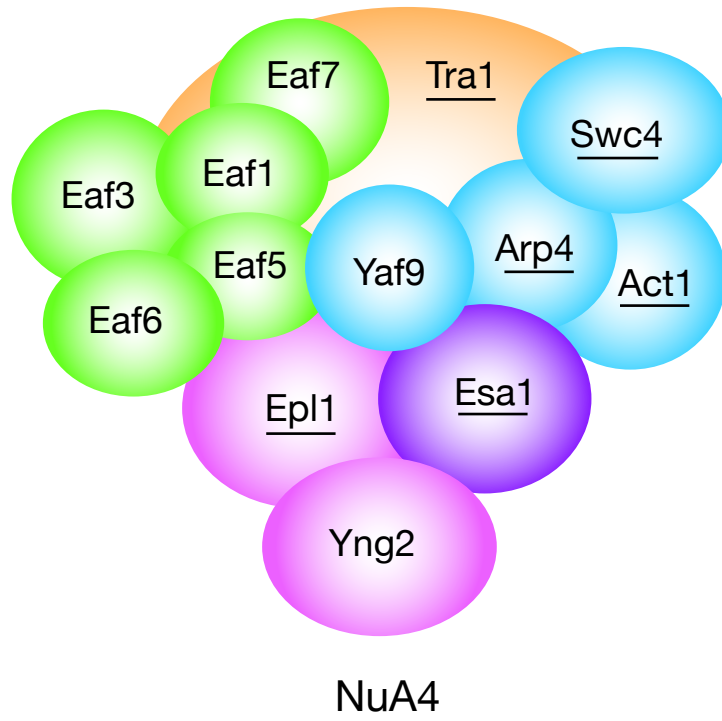
multiple types of DNA damaging agents such as camptothecin and methylmethane sulfonate (Bird et al. 2002).

Like many other chromatin modifying enzymes, Esa1 affects gene expression. Evidence exists for Esa1's role in promoting transcriptional activation as well as transcriptional silencing, although Esa1's precise function in both processes are not well understood. Esa1 is required for proper silencing at two of the three major silenced regions in the yeast genome, the telomeres and the ribosomal DNA (rDNA) repeats. Mutants of *esa1* display increased expression of reporter genes inserted at these loci. However, *esa1* mutants display no noticeable defect in mating, and therefore Esa1 does not influence silencing at the cryptic-mating type loci (Clarke et al. 2006).

As for Esa1's role in transcriptional activation, genome-wide chromatin immunoprecipitation studies have mapped Esa1 to the promoters of actively-transcribed genes (Robert et al. 2004). In addition, microarray analysis of *esa1* mutants to define expression profiles show that Esa1 contributes globally to transcriptional activation (Durant and Pugh 2006). However, these conclusions are driven by large datasets that have yet to be validated. The direct examination of transcriptional activation of specific genes by Esa1 also identified ribosomal protein genes as potential major targets for Esa1 (Reid et al. 2000).

Suppressor analysis as a powerful genetic tool. In the following chapters, the motivation behind each story stems from an observation of genetic suppression. Suppressor analysis is a widely used technique that allows for the identification of functional relationships between different proteins. The classical definition of a suppressor is a mutant that alters another mutant's phenotype to restore a more wild-type

phenotype. In addition to this type of suppressor, a variation is dosage suppression, where overexpression of a wild-type gene restores a mutant to a more wild-type function (Hawley and Walker 2003) (Figure 1-3).

Suppressor analysis can reveal that two proteins interact in several different ways [reviewed in (Prelich 1999)]. One common type of suppressor is known as a bypass suppressor. In this type of suppression, the suppressing mutation can bypass the defect caused by the original mutation, often indicating that the two genes function in related pathways (Hawley and Walker 2003). Another class of suppressors can uncover a physical interaction between two proteins. This type of suppression analysis is what led to the discovery of the mediator complex as a transcriptional co-factor of RNA polymerase II. Genes encoding mediator complex members are named *SRB* genes in yeast, since they were first isolated in a screen as <u>s</u>uppressors of <u>R</u>NA polymerase <u>B</u>. These mediator complex mutants could rescue the cold-sensitive phenotype of RNA polymerase II CTD truncation mutants (Nonet and Young 1989), and through biochemical analysis the Srb proteins were later shown to form a complex that physically binds to the CTD of RNA polymerase II [reviewed in (Carlson 1997)].

As mentioned earlier, a slight variation to classical suppression is another type known as high-copy suppression. Suppression of mutant phenotypes by high-copy suppression of a wild-type gene can reveal that these two genes encode proteins that function in similar pathways or that they physically interact (Hawley and Walker 2003). For example, in yeast, overexpression of *REC114* was found to suppress the cell cycle arrest phenotype of a *dmc1* mutant that arrests in prophase because of defective meiotic recombination resulting in unrepaired double-strand breaks. It was discovered that

Figure 1-3. Suppression analysis. A) An example of classical suppression. *mutant 1* causes a sick (green) phenotype. The addition of *mutant 2* in *mutant 1* suppresses this phenotype and restores the cell to a wild-type phenotype (yellow). Thus, *mutant 2* is a suppressor of *mutant 1*. B) An example of dosage (high-copy) suppression. *mutant 1* causes a sick (green) phenotype. Increased dosage of *Gene 2* in *mutant 1* suppresses this phenotype and restores the cell to a wild-type phenotype (yellow). Thus, *Gene 2* is a dosage suppressor of *mutant 1*. Inducible promoters or plasmids that are maintained at high-copy (2μ) are often used to increase dosage of a gene.

A
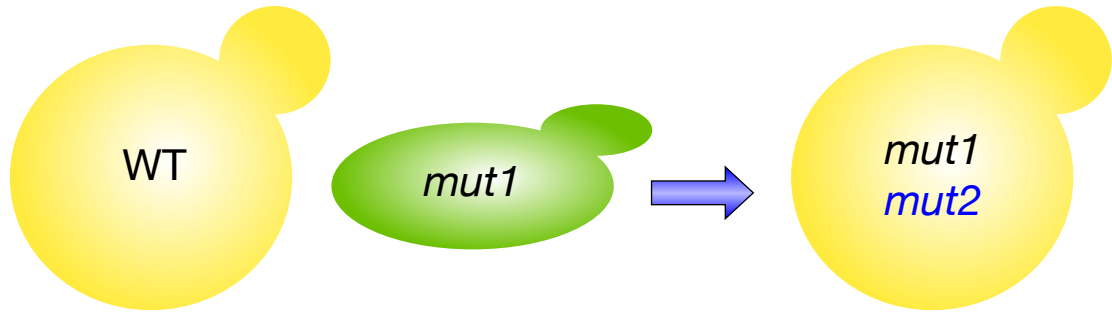
mutant 2 is a suppressor of *mutant 1*

B
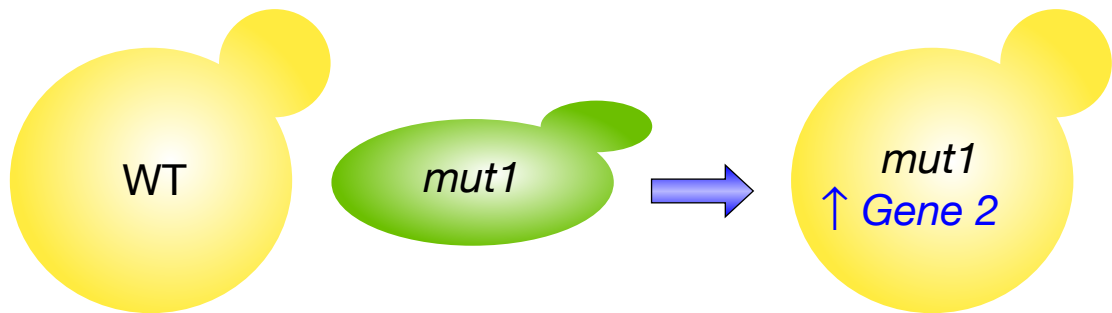
Gene 2 is a dosage suppressor of *mutant 1*

overexpression of *REC114* prevents the formation of these double-strand breaks, and is therefore able to bypass the *dmc1* cell cycle defect (Bishop et al. 1999), thus behaving as a bypass suppressor.

Suppressor analysis is relatively simple to carry out in budding yeast, as there are a limited number of genes to study and a large number of tools established for creation of mutants. Genomic libraries have been constructed on high-copy plasmids to allow for the ease of performing screens to identify high-copy suppressors. These libraries are an excellent resource for examining the effect of a dosage increase of thousands of genes in a particular mutant with relative technical simplicity (Rine 1991). However, it is important to keep in mind that the coverage of the library will determine the effectiveness of the screen.

A collection of deletion mutants covering the entire yeast genome is another of these valuable resources (Winzeler et al. 1999). Many genomic approaches in yeast have been developed to take advantage of this collection. One technique developed, termed synthetic genetic array (SGA) analysis, allows for the simple construction of double mutants using the deletion collection and your mutant of interest. The resulting double mutants are then analyzed in a growth-based assay for enhancement or suppression of a phenotype (Tong et al. 2001). Recently, SGA analysis was performed pair-wise for the majority of the yeast genome, creating a dataset of over 5 million genetic interactions (Costanzo et al. 2010). This dataset, in addition to others that have been generated with a focus on chromatin modifiers (Lin et al. 2008; Mitchell et al. 2008), provide an excellent starting point for suppression analysis.

One caveat to these genome-wide studies is that often only nonessential genes are included in the survey. Since conditional mutant alleles tend to be more problematic to manage, essential genes are often excluded. My thesis work focuses on suppressors of mutant phenotypes of the essential histone acetyltransferase gene *ESA1*.

Both multicopy dosage suppression and classical mutational suppression studies for *esa1* mutants are presented in this thesis. In Chapter 2, *NAB3*, which encodes an RNA processing factor, was isolated as a high-copy suppressor of multiple *esa1* mutant phenotypes. This link between *NAB3* and *ESA1* provides a connection between two separate nuclear processes centered around their nucleolar function and contributions to transcriptional silencing at the rDNA locus. This genetic interaction also revealed new roles for *NAB3* in cell cycle progression and DNA damage repair. In Chapters 3 and 4, deletion of *RPD3* and *HOS2*, two genes that encode related HDACs, was found to suppress different mutant phenotypes of *esa1*. Whereas deletion of *RPD3* rescued growth and silencing defects in *esa1* mutants (Chapter 3), deletion of *HOS2* rescued *esa1*'s DNA damage phenotypes (Chapter 4). The distinction between Esa1's interaction with Rpd3 and Hos2 indicates that Esa1 likely partners with different deacetylases in its multiple nuclear functions. Together with the wealth of current biochemical information, these genetic suppression studies presented in this thesis contribute to the increasing understanding of chromatin modifying complexes and their many cellular roles.

Chapter 2.

Suppression analysis of *ESA1* links the RNA processing factor Nab3 to transcriptional silencing and nucleolar functions

INTRODUCTION

Nucleosomes containing the core histones (H2A, H2B, H3, and H4) form the basic packaging unit of DNA that organizes chromatin into higher order structures. The N-terminal tails of histones are subject to multiple covalent modifications such as phosphorylation, methylation and acetylation. These modifications can alter gene expression locally at specific promoters or within large regions of chromatin [reviewed in (Jenuwein and Allis 2001)]. An increase in histone acetylation has been associated with both transcriptional activation as well as repression. Histone acetyltransferases (HATs), the enzymes that catalyze the acetylation reaction on histones, have been ascribed many cellular functions. Recently, nonhistone targets have also been identified for HATs [reviewed in (Sterner and Berger 2000)].

The HAT Esa1 in *Saccharomyces cerevisiae* functions in multiple cellular processes. Esa1 is a member of the highly conserved MYST family of acetyltransferases and is an essential HAT in yeast (Smith et al. 1998a; Clarke et al. 1999). Esa1 is the catalytic component of the NuA4 HAT complex, which primarily acetylates histone H4 and, to a lesser extent, H2A and its variant H2A.Z (Allard et al. 1999; Babiarz et al. 2006; Keogh et al. 2006). Many of the NuA4 components are essential (Galarneau et al. 2000; Loewith et al. 2000; Eisen et al. 2001), indicating that this complex plays at least one essential cellular role.

Evidence suggests that the expression of ribosomal protein genes is regulated by Esa1 function (Reid et al. 2000). Genome-wide expression analysis reveals widespread transcriptional changes in *esa1* mutants (Durant and Pugh 2006), and genome-wide binding profiles show Esa1 bound to the promoters of actively transcribed genes (Robert et al. 2004). Esa1 also functions in transcriptional silencing of the rDNA and at the telomeres (Clarke et al. 2006). The variety of targets identified thus far suggests Esa1 HAT activity regulates transcription of many genes, perhaps eliciting multiple responses.

Genetic analysis further indicates that Esa1 participates in diverse cellular functions. Characterization of temperature-sensitive alleles of *esa1* has revealed several intriguing phenotypes. First, *esa1* mutants display a G2/M cell cycle arrest at the restrictive temperature that is dependent upon the *RAD9* DNA-damage checkpoint (Clarke et al. 1999), indicating that Esa1 plays a role in cell cycle regulation. Esa1 also functions in repair of DNA damage. Esa1 localizes to double-strand breaks (Downs et al. 2004) and *esa1* mutants are hyper-sensitive to the DNA damaging agent camptothecin (Bird et al. 2002). Together, these results suggest Esa1p HAT activity is required for cell cycle regulation and genome integrity.

Suppression analyses are powerful for linking diverse biological functions. Overexpression of a key silencing protein and deacetylase, Sir2, was found to suppress *esa1* rDNA silencing defects, thereby suggesting that Sir2 and Esa1 may function coordinately to silence the rDNA array (Clarke et al. 2006). Several other studies have identified additional suppressors of *esa1* (Biswas et al. 2008; Lin et al. 2008; Chang and Pillus 2009). This chapter describes a dosage suppressor screen performed to uncover genes that, when expressed at high-copy, suppress the *esa1* temperature-sensitive

phenotype. These suppressors may be targets of Esa1 HAT activity or proteins that function coordinately with Esa1 in key cellular processes.

Of the four high-copy suppressors identified in this screen, *NAB3* was chosen for further focus for two reasons. First, only *NAB3* overexpression rescued the silencing defects of *esa1* mutants. Also, *NAB3* has known roles in RNA processing, and this functional connection to Esa1 may establish a link between two different nuclear processes.

Nab3 directs 3'-end processing of several classes of small non-coding RNAs. These include small-nuclear (sn) RNAs, small-nucleolar (sno) RNAs, and cryptic unstable transcripts (CUTs) [reviewed in (Lykke-Andersen and Jensen 2007)]. Nab3 and Nrd1, another essential RNA binding protein, recognize specific RNA sequences for 3'-end formation and transcription termination (Carroll et al. 2004).

In this chapter, suppression analysis revealed links between the RNA processing factor Nab3 and the histone acetyltransferase Esa1. In addition, new roles for Nab3 were discovered in nucleolar organization, rDNA silencing, DNA damage, and cell cycle progression.

RESULTS

Four suppressors of the *esa1-414* temperature sensitive phenotype. In order to identify genes that interact with *ESA1*, a dosage suppressor screen was performed utilizing a genomic *URA3*-marked 2-micron library. The library was transformed into an *esa1* temperature-sensitive strain and tested for growth at both permissive and restrictive temperatures. Plasmids were rescued from transformants that grew at the normally

restrictive temperature to determine the identity of suppressing genomic fragments. The results of this analysis revealed four *esa1* dosage suppressors; *LEU2*, *LYS20*, *NAB3*, and *VAP1* (Figure 2-1). *LEU2* and *LYS20* are non-essential genes required for the biosynthesis of leucine [reviewed in (Henry et al. 1984)] and lysine (Ramos et al. 1996), respectively. *VAP1* is also involved in amino acid metabolism, acting as a transporter of several amino acids including tyrosine, tryptophan, valine and leucine (Schmidt et al. 1994). *NAB3*, as mentioned above, is an essential gene involved in 3'-end processing of non-polyadenylated transcript [reviewed in (Lykke-Andersen and Jensen 2007)].

Increased dosage of *NAB3* suppresses *esa1*'s rDNA silencing defects. To understand the connection between the four suppressors and Esa1 functions, overexpression of the four genes were tested for suppression of *esa1* mutant defects other than temperature-sensitivity. One striking phenotype of *esa1* mutants is a strong rDNA silencing defect (Clarke et al. 2006). Previously, it has been shown that increased gene dosage of *SIR2* suppresses the *esa1* rDNA silencing defect (Clarke et al. 2006). Of the four suppressors, only increased dosage of *NAB3* suppressed the *esa1-414* rDNA silencing defect, restoring growth to near wild-type levels (Figure 2-2A). By contrast, *LEU2* and *VAP1* did not improve the rDNA silencing defect of the *esa1-414* strain whereas overexpression of *LYS20* slightly exacerbated *esa1*'s silencing defect (Figure 2-2A). Unlike increased gene dosage of *SIR2* (Smith et al. 1998b), *NAB3* did not improve wild-type rDNA silencing (Figure 2-2B). Since there appears to be a strong link between *NAB3* and *ESA1* in terms of silencing, we chose to characterize this particular suppressor in greater detail.

Figure 2-1. The *esa1* temperature-sensitive growth defect is partially suppressed by four genes expressed from 2-micron plasmids. Increased gene dosage of *LYS20* (pL1405), *VAP1* (pLP1406), *LEU2* (pLP1417), or *NAB3* (pLP1419) from a 2-micron plasmid moderately suppresses the *esa1-414* (LPY3291) growth defect at 35˚. The *esa1* growth defect at 35˚, demonstrated by vector (pLP1402) transformants, is completely restored in cells transformed with an *ESA1* plasmid (pLP796). Suppression was not observed at higher temperatures (data not shown).

control   growth

esa1-414 *LYS20*
            LYS20
            vector
            vector
            ESA1

esa1-414 *VAP1*
            VAP1
            vector
            vector
            ESA1

esa1-414 *LEU2*
            LEU2
            NAB3
            NAB3
            vector
            ESA1

28° SC-Trp-Ura   35° SC-Trp-Ura
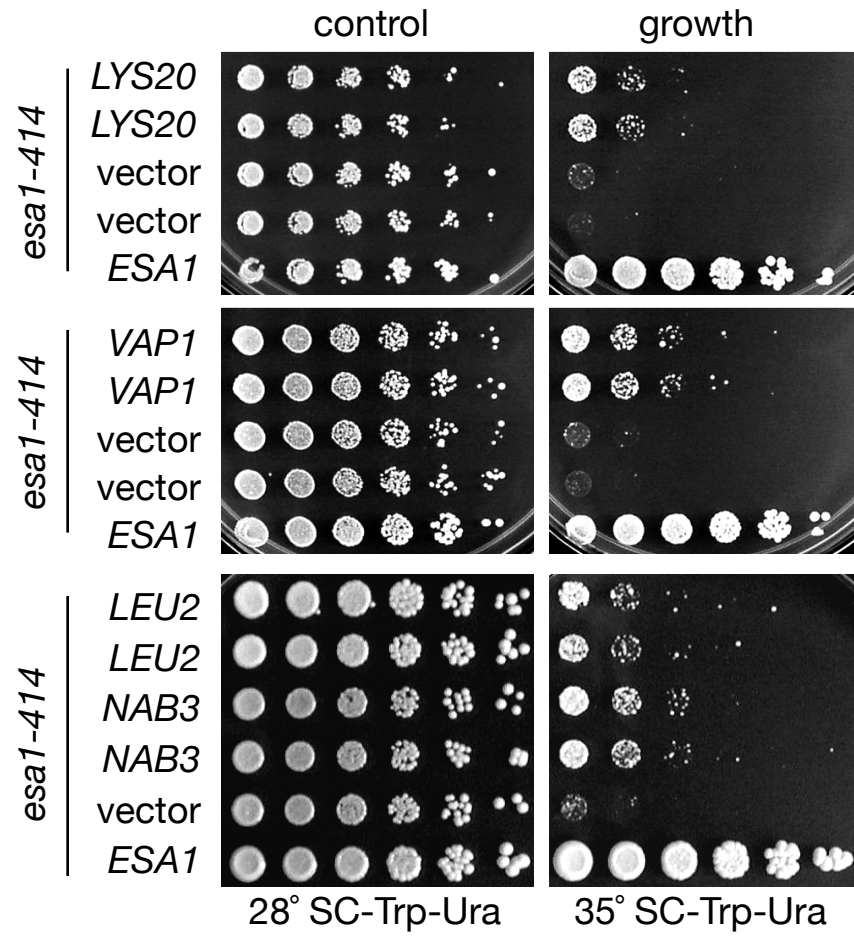
Figure 2-2. The *esa1* rDNA silencing defect is suppressed by increased gene dosage

of *NAB3*. A) Top: Diagram and location of rDNA::*ADE2-CAN1* silencing marker within

the rDNA array on chromosome XII. Bottom: The *esa1* (LPY4911) rDNA silencing

defect, demonstrated by vector transformants (pLP1402), is fully restored in cells

transformed with an *ESA1* plasmid (pLP796), and partially restored by *NAB3*

transformants (LPY1238). Increased dosage of *LYS20*, *LEU2*, or *VAP1* does not rescue

esa1's rDNA silencing defect. The *esa1* strain was transformed with *LYS20* (pLP1412),

LEU2 (pLP1417), *VAP1* (pLP1259), or *SIR2* (pLP37). Transformed strains using the 25S

rDNA*::ADE2-CAN1* reporter were grown on SC-Ade-Arg-Ura plates with and without

32 µg/ml of canavanine at 33˚. B) *NAB3* overexpression (pLP1238) has no effect on

rDNA silencing of WT strains (LPY4909).
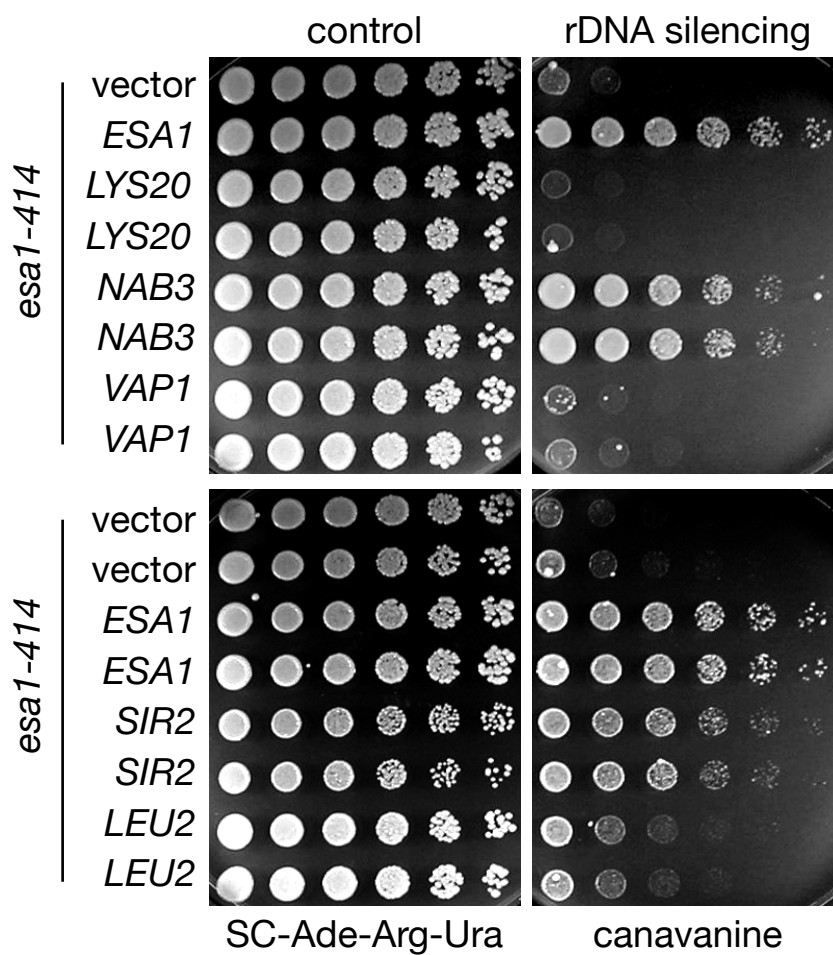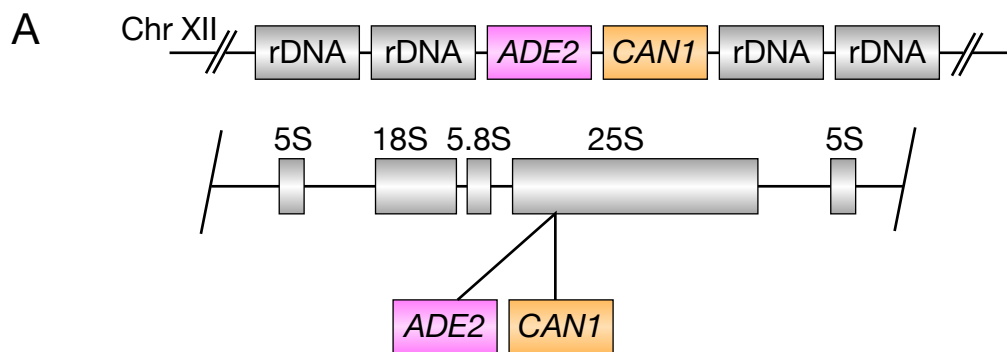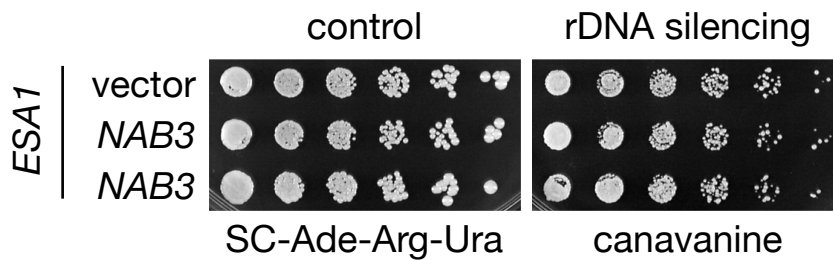
Increased dosage of *NAB3* suppresses a specific subset of *esa1* mutant phenotypes. In addition to being defective in rDNA silencing, *esa1* mutants are also defective in telomeric silencing (Clarke et al. 2006). Therefore, increased dosage of *NAB3* was tested for suppression of telomeric silencing defects in the *esa1* mutant using a telomeric *URA3* reporter gene located at the right arm of chromosome five (TELVR) (Renauld et al. 1993). Indeed, increased dosage of *NAB3* suppressed the telomeric silencing defects of *esa1* nearly to wild-type levels (Figure 2-3A). Similar to its effect on rDNA silencing, *NAB3* overexpression did not improve wild-type telomeric silencing (data not shown). Together, these results show that increased dosage of *NAB3* could improve both rDNA and telomeric silencing in *esa1* mutants.

Esa1 is required for the efficient repair of camptothecin-induced double-strand breaks. Mutants of *ESA1* are sensitive to camptothecin, a topoisomerase I inhibitor that triggers double-strand breaks (Bird et al. 2002). To test if *NAB3* suppresses *esa1*'s defects in response to DNA damage, overexpression of *NAB3* was tested for the ability to suppress *esa1*'s sensitivity to camptothecin. In response to camptothecin, *NAB3* overexpression exacerbated *esa1*'s mutant phenotypes (Figure 2-3B). This contrast to the *NAB3*-mediated suppression observed for the silencing defects of *esa1* highlights a difference between Nab3 and Esa1's functions in transcriptional silencing and DNA damage repair.

Global H4 lysine 5 acetylation is dramatically reduced in *esa1* mutants (Allard et al. 1999). To determine whether increased dosage of *NAB3* restores normal levels of histone acetylation to *esa1* mutants, a series of protein immunoblots with isoform-specific antibodies were performed to define the global acetylation state in *esa1* strains

Figure 2-3. Overexpression of *NAB3* rescues the telomeric silencing and exacerbates the camptothecin sensitivity of *esa1-414*. A) Top: Diagram of TELVR::*URA3* telomeric silencing marker on the right arm of chromosome V. Bottom: Increased gene dosage of *NAB3* suppresses the *esa1* telomeric silencing defect using the TELVR::*URA3* reporter. An *esa1* strain (LPY4919) was transformed with vector (pLP271), *ESA1* (pLP798), and *NAB3* (pLP1310) and plated on SC-Trp with and without 5-FOA at 33˚ to test for telomeric silencing. B) Increased gene dosage of *NAB3* exacerbates *esa1*'s sensitivity to the DNA damaging agent camptothecin. An *esa1* strain (LPY4774) was transformed with vector (pLP326), *ESA1* (pLP796), and *NAB3* (pLP2018) and tested for growth on SC-Ura plates with DMSO (control) and 20 µg/ml camptothecin.

A
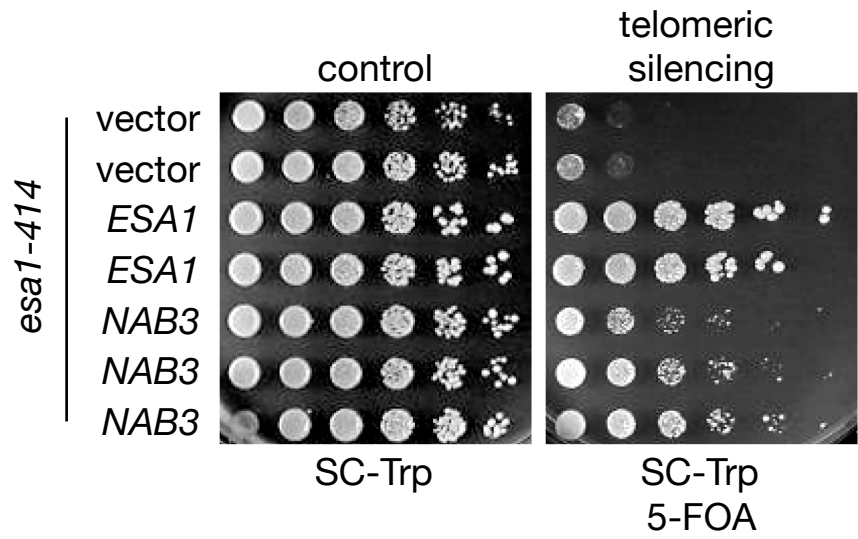
B
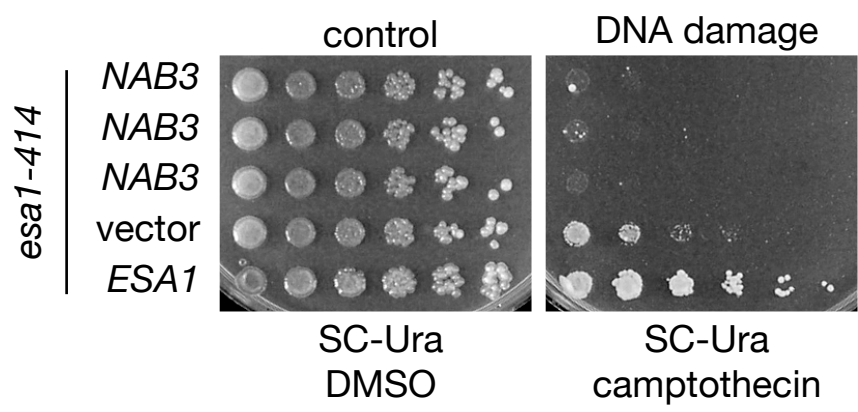
overexpressing *NAB3*. All the histone H3 and H4 lysine residues that Esa1 is known to target (Clarke et al. 1999) were tested in these experiments for changes in levels of acetylation (Figure 2-4A). Histone levels were determined to be constant among the different samples by probing with an antibody specific to the C-terminus of histone H3 (data not shown). This series of immunoblots shows that increased dosage of *NAB3* in *esa1* strains does not restore global acetylation levels at most of the known Esa1 targets. Therefore, *NAB3* overexpression does not rescue *esa1* mutants by restoring global acetylation defects at the histone H3 and H4 N-terminal tails.

Another possible mechanism for *NAB3* suppression is through Esa1's role in the cell cycle. Since Esa1 is required for cell cycle progression through G2/M, cell cycle profiles of *esa1* mutant strains with increased dosage of *NAB3* were examined by flow cytometry. Flow cytometry distinguishes cellular DNA content before (1C) and after (2C) replication. The *esa1* mutants have a well-defined G2/M cell cycle block, visualized as a decrease in the 1C peak and an accumulation of the 2C peak (Clarke et al. 1999). No change in the *esa1* cell cycle profile was observed with overexpression of *NAB3* (Figure 2-4B). Therefore, *NAB3* overexpression is not able to bypass the G2/M cell cycle block of *esa1* mutants. Thus, increased dosage of *NAB3* suppresses silencing defects associated with *esa1*, but not its high-copy suppression is limited to a defined subset of *esa1* phenotypes.

Nab3 does not affect transcriptional regulation of genes encoding histone acetyltransferase or deacetylase. Another hypothesis to explain the *NAB3* suppression is that increased *NAB3* changes the expression of a histone modifier that could counter the reduced activity of Esa1 in the *esa1* mutant. First, northerns were performed to check

28

**Figure 2-4. Overexpression of *NAB3* does not restore defects in global H4
acetylation defects and cell cycle progression of *esa1*.** A) Overexpression of *NAB3*
does not increase the bulk H4K5, H5K8, H4K12, H4K16, or H3K14 acetylation levels in
esa1 mutants. Whole cell extracts were made from wild-type (LPY5) and *esa1*
(LPY4774) strains with vector (pLP362) or 2-micron *NAB3* (pLP2018) grown at both
permissive (28˚) and elevated temperature (34˚). These were immunoblotted for amounts
of global H3 and H4 acetylation. B) Overexpression of *NAB3* does not influence *esa1*'s
G2/M cell cycle block. The same strains as in A) were grown at 28˚ and shifted to 37˚ for
four hours before fixing and staining with propidium iodide. Cell cycle profiles were
analyzed by flow cytometry.

A

strain: *ESA1*
vector: 2µ *NAB3*

B
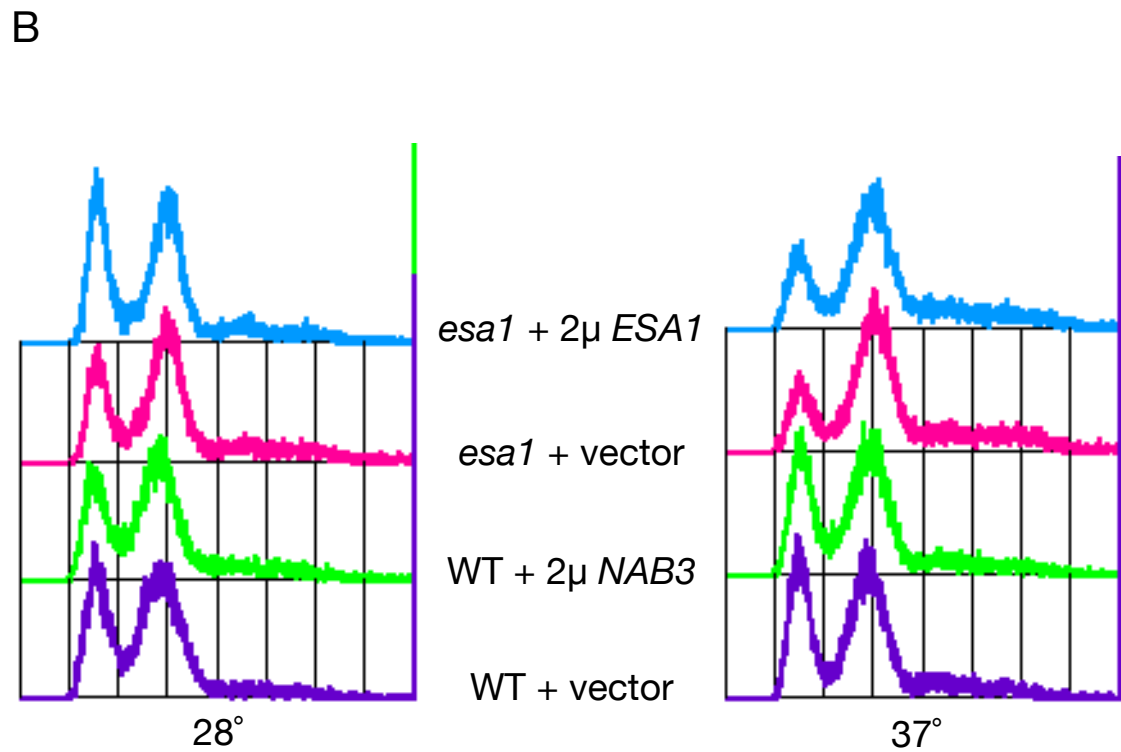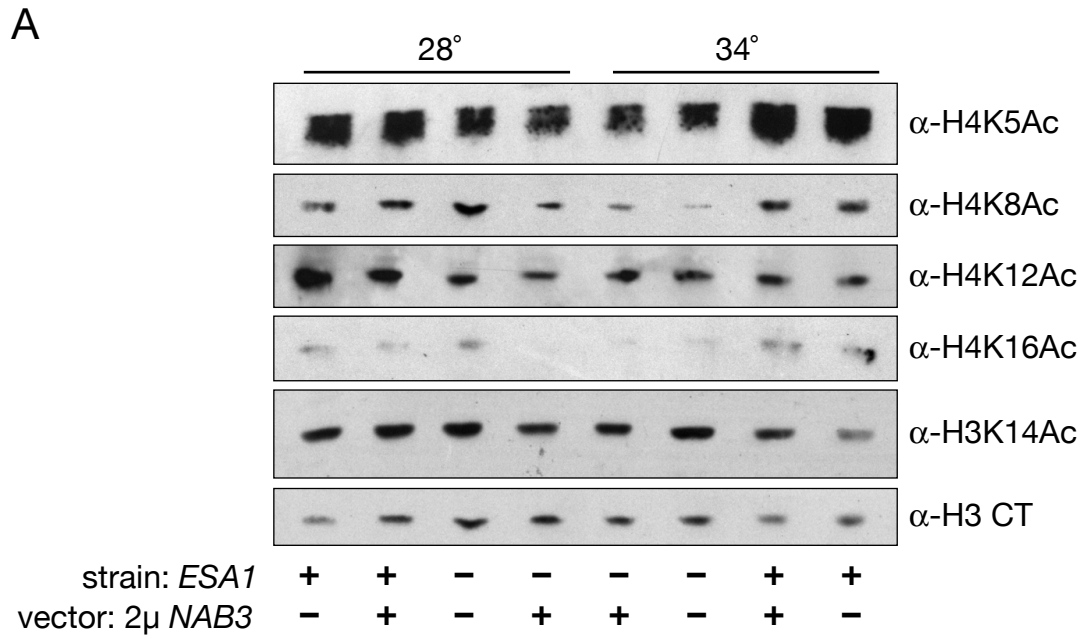
if *NAB3* dosage changed the abundance of *ESA1* transcripts, and *ESA1* levels were found to be constant even with increased dosage of *NAB3* and in the *nab3* mutant (Figure 2-5A). Thus, *NAB3* does not alter the transcriptional regulation of *ESA1*. In addition, protein immunoblots show that Nab3 levels are constant in an *esa1* mutant (data not shown).

It is also possible that *NAB3* affects transcription of a histone deacetylase (HDAC) that acts in opposition to Esa1. Transcriptional down-regulation of an HDAC may compensate for the lack of functional Esa1 and be able to restore the imbalance of acetylation in the cell. For example, deletion of the histone deacetylase gene *RPD3* suppresses the temperature-sensitivity and silencing defects of an *esa1* mutant (Chang and Pillus 2009). Evidence that *RPD3* may be regulated in a *NAB3*-dependent manner also comes from microarray data indicating that *RPD3* transcript levels are highly up-regulated in *nab3* mutants compared to wild-type strains (Mnaimneh et al. 2004). Changes in *RPD3* transcript and Rpd3 protein levels were examined by northern and immunoblots, respectively, to compare differences between wild-type and *esa1* strains with and without increased dosage of *NAB3*. No changes were observed in *RPD3* transcript levels by northern analysis when comparing between *nab3* and wild-type (Figure 2-5B), in contrast to the predicted change by microarray. Furthermore, using an antibody specific to Rpd3, Rpd3 levels were also examined, and again no *NAB3*-dependent changes were found (Figure 2-5B).

Another HDAC candidate of interest is Sir2, whose importance at the rDNA is already known (Rusche et al. 2003). *SIR2* overexpression has been shown to rescue silencing in an *esa1* mutant (Clarke et al. 2006). However, no *NAB3*-dependent

Figure 2-5. *NAB3* **overexpression does not result in detectable changes in** *ESA1* **and**

RPD3 **mRNA or Rpd3.** A) *NAB3* overexpression does not influence *ESA1* mRNA

levels. Total RNA was isolated from both WT (LPY5) and *esa1* (LPY4774) mutant

strains with *NAB3* overexpression (pLP2018) and without (pLP362). Samples were used

for northern analysis with *ESA1*-specific probe and results were obtained on a

phosphorimager. B) Top panel: same as in A) except with *RPD3*-specific probe. Bottom

panel: Lysates were made from strains in A) and an *rpd3* strain (LPY12154) with vector

(pLP362) and immunoblotted with anti-Rpd3. anti-PGK was used as a loading control.

differences in Sir2 levels were observed in wild-type and *esa1* mutant strains (data not shown).

Global analysis of *NAB3*- and *ESA1*-dependent gene targets. If *NAB3* down-regulates the same set of transcripts that are aberrantly expressed in *esa1* mutants, then overlapping genome-wide expression profiles from *esa1* and *nab3* mutants might reveal this relationship. Microarray data already exists for both *esa1* mutants (A. Clarke and S. Berger, unpublished) and *NAB3*-depletion strains constructed with a Tet-repressible promoter (Mnaimneh et al. 2004). One prediction is that transcripts highly expressed in *esa1* strains should also be highly expressed in *nab3* strains if Nab3 normally promotes the down-regulation of these genes. A simple scatter plot analysis of these two datasets against each other did not reveal an obvious correlation between genes that were either upregulated or downregulated in both mutants (Figure 2-6).

Nab3 is not acetylated by Esa1. Another proposed mechanism for *NAB3* mediated suppression is that Nab3 is a direct substrate for Esa1 acetyltransferase activity. Posttranslational modification of Nab3 might promote protein stability or RNA binding. A proteome-wide survey in yeast suggested that Esa1 could acetylate Nab3 *in vitro* (Lin et al. 2009). To examine whether this modification occurs *in vivo*, an antibody that recognizes proteins that have acetylated-lysines was used. Immunoprecipitation of Nab3 followed by immunoblot detection did not reveal any pool of Nab3 to be acetylated (Figure 2-7). Concurrently, acetylation of two NuA4/piccolo components, Esa1 and Epl1, was observed (Figure 2-7).

***nab3* mutants share phenotypes with *esa1* mutants.** To further characterize the role of *NAB3* function in relation to *ESA1*, *nab3* mutants were examined for known

Figure 2-6. Global analysis of *NAB3*- and *ESA1*-dependent gene targets. Scatter plot

of two expression profiles. The *esa1* microarray dataset used is from A. Clarke and S.

Berger (unpublished). The *nab3* microarray dataset used is from Mnaimneh et al. 2004.

For each gene locus analyzed by both expression microarrays, a point corresponding to

log ratios of intensity was plotted on the graph. The coordinates of each point (x, y)

correspond to the value from the *esa1* dataset (x-coordinate) and the value from the *nab3*

dataset (y-coordinate). Up arrows indicate genes that are upregulated in the mutant, and

down arrows indicate genes that are downregulated in the mutant. If a class of genes were

regulated by both Esa1 and Nab3, this should be reflected by a set of points in quadrants I

and III.
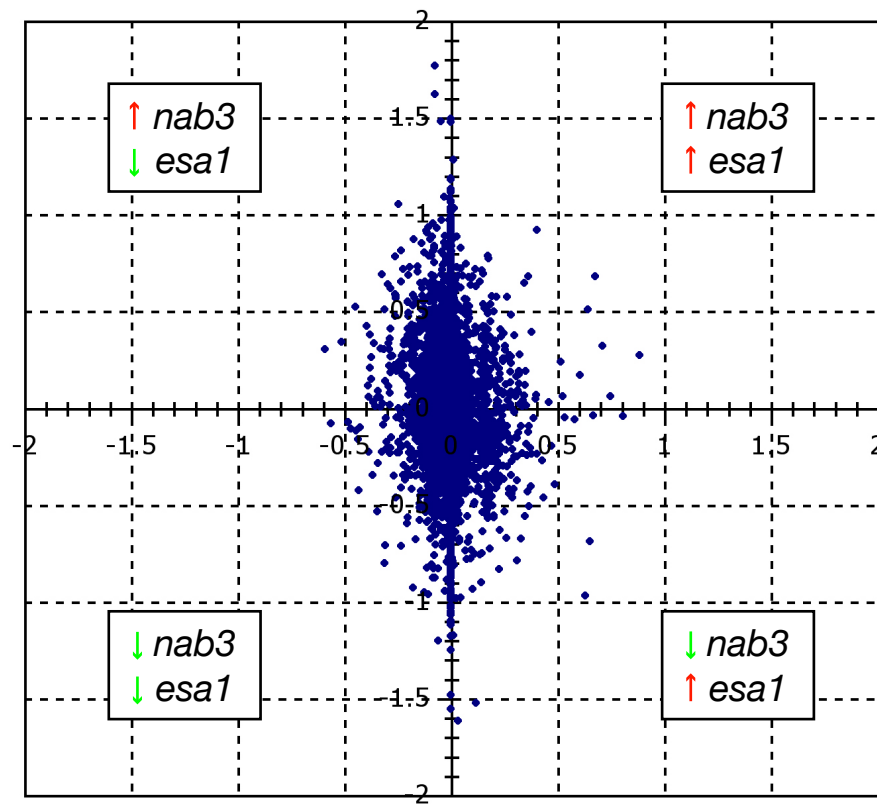
Figure 2-7. Nab3 is not acetylated *in vivo*. Untagged (LPY5) and chromosomally myc-tagged versions of Esa1 (LPY6121) and Nab3 (LPY14942) were immunoprecipitated followed by immunoblotting for anti-acetyl lysine to detect posttranslational acetylation. Acetylated-Esa1 and acetylated-Epl1 were readily detectable. A) Nab3-myc and Esa1-myc were immunoprecipitated and immunoblotted with anti-myc to confirm immunoprecipitations. B) Immunoprecipitated samples were immunoblotted with anti-acetyl lysine. Two bands correspond to detection of acetylation of Esa1-myc and Epl1. Epl1 identity verified by personal communication with J. Boeke. There was no detectable band in Nab3-myc lane.

A

IP: α-myc
IB: α-myc

no tag
Esa1-myc
Nab3-myc
no tag
Esa1-myc
Nab3-myc
no tag
Esa1-myc
Nab3-myc

→ Nab3-myc
→ Esa1-myc

input   IP   unbound

B

IP: α-myc
IB: α-acetyl lysine

no tag
Esa1-myc
Nab3-myc

→ Epl1
← Esa1-myc

IP
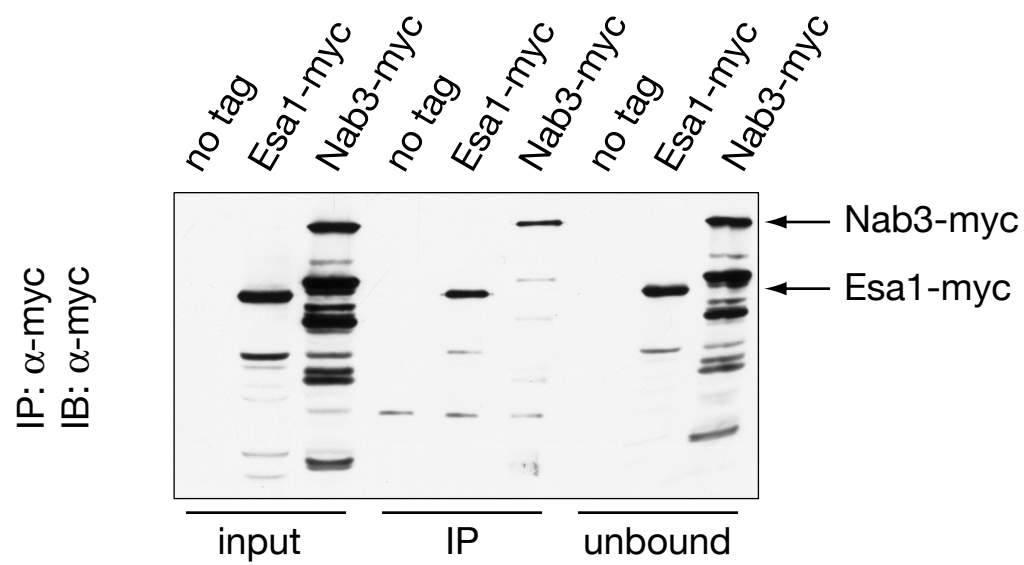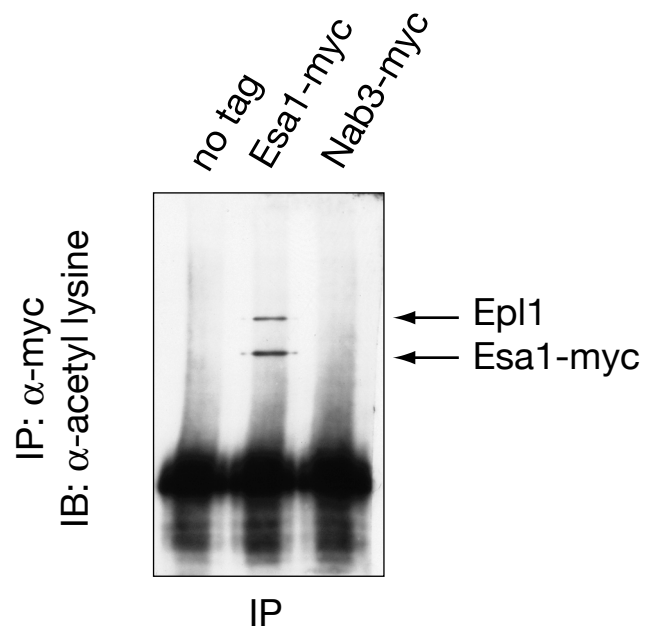
phenotypes of *esa1* mutants. The *nab3-10* mutant is a temperature-sensitive allele

described previously that contains a single amino acid substitution of F371L in its RRM

domain (Conrad et al. 2000). One hypothesis that would link Nab3 and Esa1 functions is

that Nab3 promotes an increase in global acetylation. When tested for changes in

acetylation of H4K5, the primary *in vivo* target of Esa1 (Clarke et al. 1999), global

acetylation in *nab3* mutants was maintained at wild-type levels (Figure 2-8A). Therefore,

Nab3 likely does not directly influence Esa1 global activity, although it is possible Nab3

alters localized targeting of Esa1.

The *nab3* mutant was next tested for defects in transcriptional silencing. Since

NAB3 overexpression suppressed both the telomeric and rDNA silencing defects in *esa1*,

it was likely that *nab3* mutants might contribute to silencing. Telomeric silencing assays

with *nab3* revealed normal and intact silencing (Figure 2-8B). However, when assayed

for rDNA silencing, *nab3* displayed a strong defect, similar to that observed in *esa1*

(Figure 2-9A). Together, these results suggest that Nab3 functions specifically in rDNA

silencing but not telomeric silencing, perhaps by coordinating with Esa1.

NAB3 overexpression did not suppress the DNA damage and cell cycle

phenotypes of *esa1* mutants (Figure 2-3B, Figure 2-4B). However, when *nab3* mutants

were examined for defects in DNA repair and cell cycle progression, the results revealed

a role for Nab3 in these processes. As seen in Figure 2-9B, *nab3* mutants displayed

sensitivity to the DNA damage agent camptothecin, although not to the same degree as

esa1. In addition, cell cycle profiles of *nab3* mutants showed a G2/M block that

resembles that of *esa1* mutants (Figure 2-9C). In addition to its defects in rDNA

Figure 2-8. *nab3* mutants have intact telomeric silencing and wild-type levels of bulk H4K5 acetylation. A) *nab3* mutants have wild-type levels of global H4K5 acetylation. WT (LPY5), *nab3* (LPY10622), and *esa1* (LPY4774) were grown at 28˚ and shifted to 37˚ for 2 hours before making whole cell extracts. These were then immunoblotted for global H4K5 acetylation levels. B) Unlike *esa1* mutants, *nab3* displays no telomeric silencing defect. WT (LPY4917), *sir2* (LPY4979), *esa1-L254P* (LPY5057), *esa1-414* (LPY4919), and *nab3-10* (LPY5406) strains with a TELVR::*URA3* reporter were plated on SC and 5-FOA to test for telomeric silencing.

A
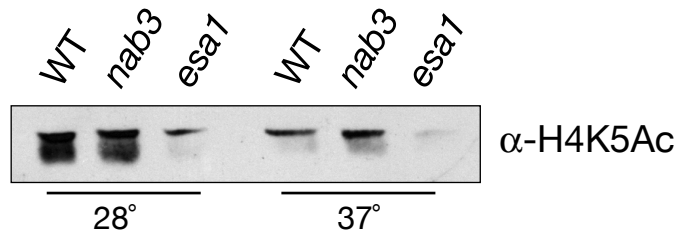
B
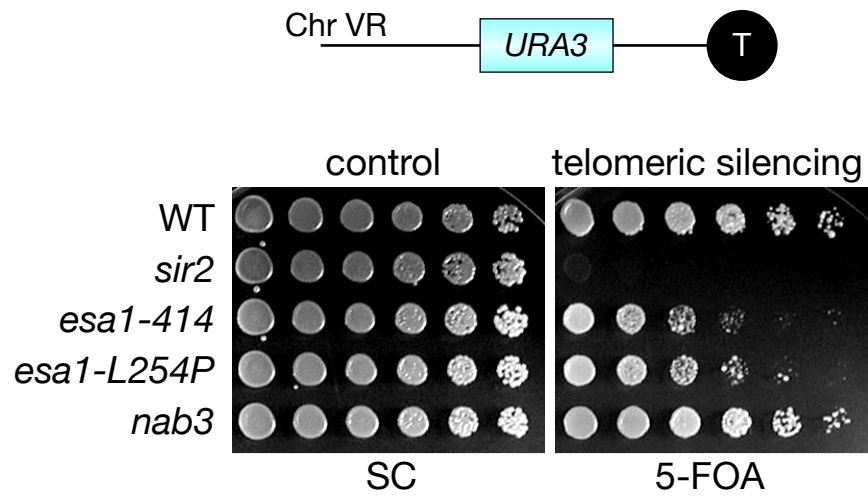
Figure 2-9. *nab3* mutants display defects in rDNA silencing, DNA damage repair, and cell cycle progression, similar to *esa1* mutants. A) The *nab3* mutant has an rDNA silencing defect. WT (LPY4909), *esa1* (LPY4911), and *nab3* (LPY5406) strains with the 25S rDNA::*ADE2-CAN1* reporter were assayed for rDNA silencing defects on 16 μg/ml canavanine. B) The *nab3* mutant is sensitive to the DNA damaging agent camptothecin. Serial dilutions of WT (LPY5), *esa1* (LPY4774), and *nab3* (LPY10622) were plated on DMSO (control) and 40 ug/ml camptothecin to test for drug sensitivity at 30˚. C) The same strains as in B) were fixed and stained with propidium iodide to analyze cell cycle profiles after being grown at 28˚ and shifted to 37˚ for four hours.

A

B

C
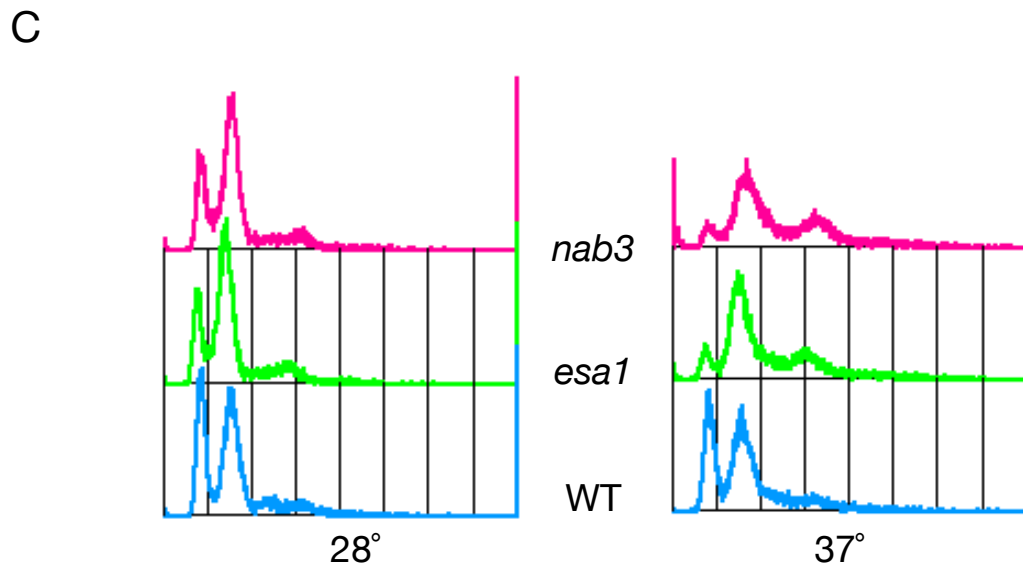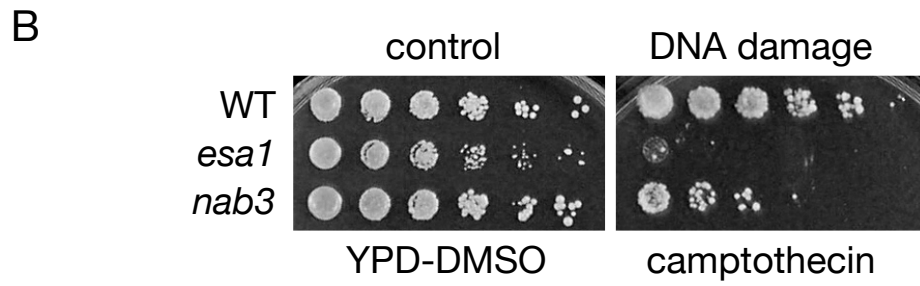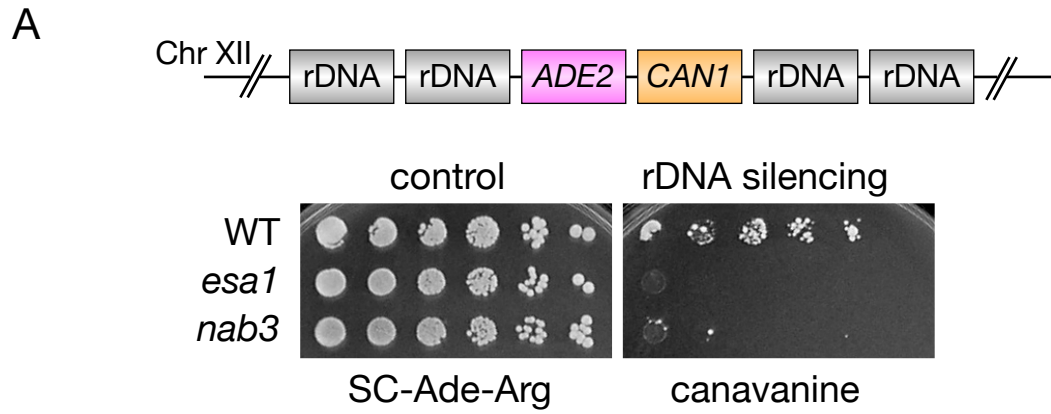
silencing, the identification of these phenotypes for *nab3* mutants uncovers a more extensive overlap in mutant phenotypes with *esa1*.

Nab3 localization is aberrant in *esa1* mutants. The nucleolus is a key compartment for RNA processing in the nucleus. Electron microscopy has shown *esa1* mutants to have disrupted nucleoli (Clarke et al. 1999) and *esa1* mutants display strong rDNA silencing defects and rDNA chromatin structure defects (Clarke et al. 2006). Because of Esa1's known connections to nucleolar function, and Nab3's newly identified role in rDNA silencing (Figure 2-9), Nab3 localization was observed in *esa1* mutants. Immunofluoresence was performed using an antibody directed against Nab3 in wild-type and *esa1* strains. In addition, Sir2 staining was visualized to demarcate the nucleolus.

Nabp3 nuclear localization has been previously described as both punctate and diffuse, partially overlapping with the nucleolus (Wilson et al. 1994) (Figure 2-10). At permissive temperature, Nab3 localization appeared normal in both wild-type and *esa1*. However, at restrictive temperature, Nab3 localization in *esa1* became diffuse and no longer co-localized in the nucleolus with Sir2-staining (Figure 2-10), indicating that Nab3 localization is aberrant in the *esa1* mutant. This change in Nab3 localization may contribute to the rDNA silencing and nucleolar structural defects observed in the *esa1* mutants, and provides a possible explanation as to why overexpression of *NAB3* rescues *esa1*'s rDNA silencing defect.

DISCUSSION

This study has identified four dosage suppressors of the *esa1* temperature-sensitive phenotype. Overexpression of *LEU2*, *LYS20*, *VAP1* and *NAB3* all partially

44

Figure 2-10. The localization of Nab3 is aberrant in the *esa1* mutant at restrictive temperature. A) Nab3 staining in wild-type cells (LPY4909) appears as punctate nuclear foci interspersed with diffuse nuclear staining at both permissive (28˚) and restrictive (37˚) temperature. Sir2 localization demarcates the nucleolus in a crescent shape and is normal at both temperatures in wild-type cells. Nab3 staining partly overlaps with Sir2 staining. B) At permissive temperature (28˚), Nap3 staining in the *esa1* mutant (LPY4911) appears similar to Nab3 staining in wild-type cells, with appropriate Sir2 nucleolar localization (inset, green). At restrictive temperature (37˚) in the *esa1* mutant, Nab3 staining is diffuse and does not overlap with Sir2.

A

DAPI	α-Nab3	

WT 28°

WT 37°

B

DAPI	α-Nab3	

esa1 28°

esa1 37°
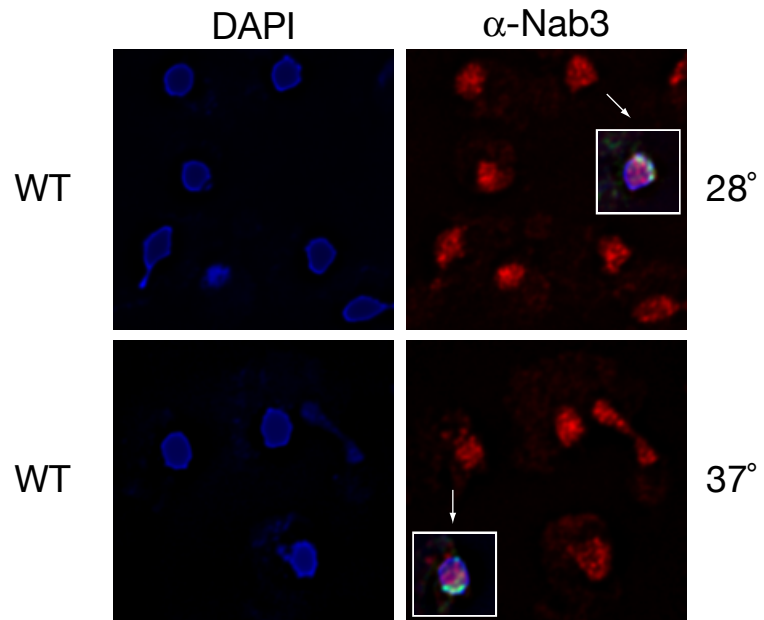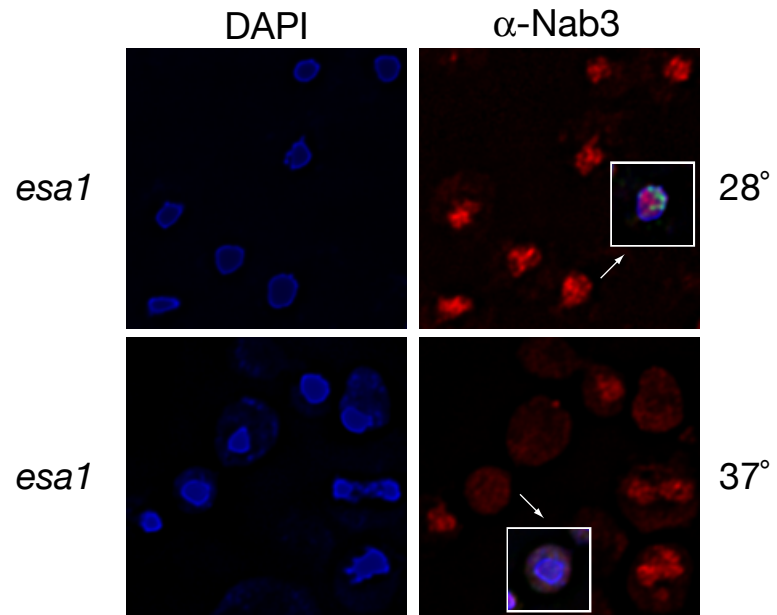
suppressed the growth defect of an *esa1* mutant. Of the four*, NAB3* was the only one that restored the rDNA and telomeric silencing defects of *esa1* mutants. Similar to *esa1* mutants, *nab3* mutants were defective in rDNA silencing. The nucleolar localization of Nab3 is disrupted in the *esa1* mutant, suggesting that Nab3 and Esa1's nucleolar functions are closely connected.

Genetic suppression has been a valuable tool in refining the understanding of Esa1's nuclear functions and interactions with other proteins. Aside from *NAB3*, the other three suppressors identified from the screen (*LEU2*, *LYS20*, and *VAP1*) are all involved in amino acid metabolism. Recent findings report the prevalence of lysine acetylation as a posttranslation modification in the regulation of metabolism (Zhao et al. 2010). This idea raises the possibility that the proteins encoded by the other three suppressors (Leu2, Lys20, and Vap1) are acetylated by Esa1 in yeast, and that acetylation of these metabolic proteins influences their critical functions.

NAB3 has previously been identified as a high-copy suppressor in other studies. The initial characterization of *NAB3* was through its isolation as a high-copy suppressor of a dominant allele of *CLN3*, a G1 cell cycle cyclin. *NAB3* overexpression suppressed the mating defect associated with this particular allele, and Nab3 was found to down-regulate transcript levels of *CLN3*. Overexpression of *NAB3* also was reported to suppress mutant alleles of a subunit of the Paf1 transcription elongation complex (Sheldon et al. 2005), which recruits the Set1 histone methyltransferase to chromatin.

It is apparent that Nab3 is critical for RNA processing events. Nrd1 is another RNA binding protein that is found in complex with Nab3, and also functions to direct 3'-end termination. Studies exploring connections between Nrd1 and Esa1 are described in

Appendix C. In addition to their role in processing non-coding RNAs, there is evidence that Nab3 and Nrd1 also participate in 3'-end formation of short protein-coding transcripts. Thus, a potential link between Nab3 and Esa1 may be that Nab3 binds to *ESA1* mRNA to direct 3'-end processing. In this study, Nab3 and its connections to Esa1 have been explored. These connections led to the discovery of previously unobserved phenotypes for *nab3* mutants, such as defects in transcriptional silencing at the rDNA, cell cycle progression, and repair of DNA damage. Future studies will provide a deeper understanding of how the cell coordinates acetylation by Esa1 and RNA processing (Figure 2-11).

MATERIALS AND METHODS

Dosage suppressor screen. A *URA3*-marked 2-micron genomic library (generously provided by P. Hieter) was transformed into two isolates of the *esa1-414* strain LPY3291 (*esa1Δ::HIS3* + pLP863) in six independent experiments, yielding a total of 130,000 screened transformants. Control plasmids pLP1402 (pRS202, vector backbone) or pLP796 (*ESA1/URA3*/2μ) were also transformed into LPY3291 for comparison of potential suppressors. Transformations were grown under permissive conditions on medium lacking tryptophan and uracil (SC-Trp-Ura) to select for both pLP863 and the *URA3*-marked library plasmids. Subsequently, transformation plates were replica-plated to SC-Trp-Ura plates, incubated at 28°, 35° and 37°, and colonies growing at 35° but not 37° were selected (to avoid uncovering *ESA1*). Positive suppressor candidates were tested for plasmid dependence by growing original transformants on 5-fluororotic acid (5-FOA), and the resulting resistant strains, which had lost the *URA3-*

48

Figure 2-11. The Esa1 acetyltransferase and the Nab3 RNA processing factor have tightly linked functions. Esa1 acetylates histones to facilitate chromatin-related processes. Nab3 and Nrd1 bind specific sequences on the 3'-ends of transcripts to direct their termination. Nrd1 interacts with the CTD of RNA polymerase II during transcription.
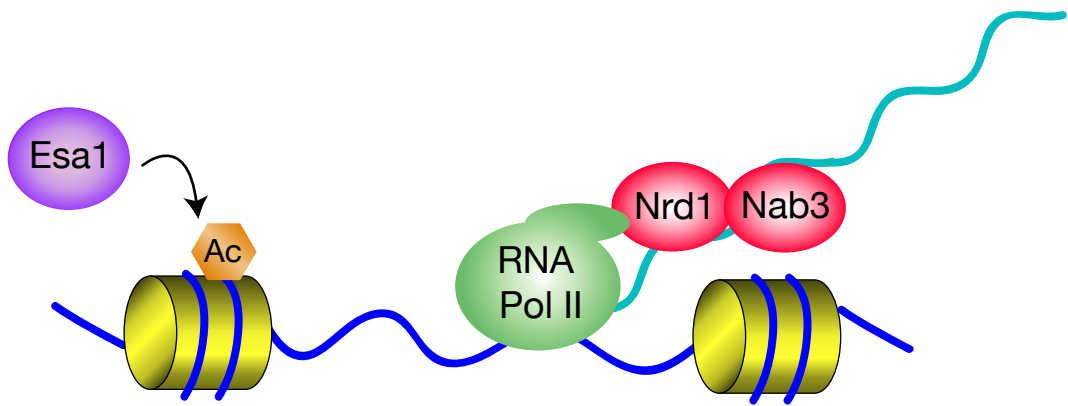
marked plasmid, were tested for temperature-sensitivity at 35˚. Suppressor strains that demonstrated temperature-sensitivity in this test were classified as plasmid-dependent and carried through plasmid rescue, as described below. These plasmids were retransformed into LPY3291 to confirm the suppressing phenotype.

Yeast plasmid rescue and sequencing. Suppressing plasmids were rescued from yeast and were sequenced to determine their genomic fragments using T3 and T7 primers, which anneal on either side of the library insert. Library fragments that contained multiple ORFs were subcloned to identify the gene responsible for suppression. Strategy for identification of the four suppressors is described in detail (Clarke 2001).

Yeast methods and strain construction. All yeast strains and plasmids used in this study are listed in Table 2-1 and Table 2-2. The silencing markers rDNA*::ADE2-CAN1* (Fritze et al. 1997) and TELVR*::URA3* (Renauld et al. 1993) were introduced through standard genetic crosses. All *nab3-10* strains originate from LPY5241 (provided by M. Swanson). Nab3 myc-tagging was carried out by amplification of pFA6a-13Myc-*kanMX6* and transformation into LPY5 using the method described (Longtine et al. 1998) to make LPY14942.

Growth dilution assays and silencing assays. Unless otherwise noted, dilution assays represent fivefold serial dilutions starting from an A_{600} of 1.0, with plates incubated at 30˚ on synthetic dropout media. rDNA silencing was assayed using the rDNA*::ADE2-CAN1* reporter as described (van Leeuwen and Gottschling 2002) by growing strains to saturation in SC-Ade-Arg medium and plating on SC-Ade-Arg (growth control) and SC-Ade-Arg with 16 or 32 μg/ml canavanine (to assay silencing). Cultures were grown in SC-Ade-Arg-Ura for strains with *URA3* plasmids. Assays

measuring telomeric silencing were carried out as described (van Leeuwen and Gottschling 2002) by growing strains to saturation in YPD medium and plating on SC (growth control) and SC with 0.1% 5-FOA (to assay silencing). Camptothecin sensitivity was assayed using camptothecin dissolved in DMSO added to phosphate buffered plates (pH7.5) to maintain maximal drug activity (Nitiss and Wang 1988). All images were captured after 2-4 days of growth.

Northern analysis, protein immunoblots, and immunoprecipitations. RNA isolation protocol using hot acid phenol. Total RNA was separated on 1.5% agarose gel, run at 100V for 4 hours. RNA was transferred to nitrocellulose, crosslinked, and incubated with P^{32}-labeled probe. Results were obtained by phosphorimager (Storm scanner). Extracts were prepared by bead beating as described previously (Clarke et al. 1999). Protein were separated on SDS-polyacrylamide gels (18% for detection of histones, 8% for Sir2 and Rpd3) and transferred onto nitrocellulose (0.2 μm). Primary anti-sera used were anti-H4K5Ac (1:5000 dilution, Serotec), anti-H4K8Ac (1:2500 dilution, Serotec), anti-H4K12Ac (1:2500 dilution, Serotec), anti-H4K16Ac (1:2500 dilution, Upstate), anti-H3K14Ac (1:2500 dilution, Upstate), and anti-Rpd3 (1:5000, generously provided by M. Grunstein). Secondary antibody used was goat anti-rabbit conjugated to horseradish peroxidase (Promega), and Western Lightning Chemiluminescence Reagent (Perkin Elmer) was used for detection on Kodak X-Omat film. Immunoprecipitations with anti-myc were performed as described in (Jacobson and Pillus 2009). Anti-acetyl lysine (Chemicon) was used at 1:1500 for immunoblots.

Flow cytometry. Cell cycle profiles were obtained by flow cytometry or propidium iodide stained cells on a FACScaliber machine (Becton Dickinson) and

analyzed on CellQuest software (Becton Dickinson). Cells were grown to an A_{600} of between 0.6-1.0, fixed in ethanol overnight, and stained with propidium iodide. Stained cells were sonicated to break up clumps before counting by flow cytometer. For each sample, 100,000 cells were counted and analyzed.

Nab3 and Sir2 immunofluorescence. Immunofluorescence was carried out as described (Gotta et al. 1997; Stone et al. 2000). The primary antibodies used were anti-Nab3 (mouse monoclonal 2F12, a kind gift from M. Swanson) and anti-Sir2 (rabbit polyclonal 2916, bleed 8). Texas Red-conjugated goat anti-mouse (Jackson Labs) was used as secondary antibody. Staining was visualized with an Applied Precision Deltavision optical sectioning deconvolution microscope.

Acknowledgements. Maurice Swanson provided the *nab3-10* strain and the Nab3 antibody. Michael Grunstein provided the Rpd3 antibody. Jenny DuRose and Maho Niwa assisted with northern analysis.

Chapter 2 is a manuscript in preparation that will be submitted for publication. Astrid Clarke performed the following experiments: Figure 2-1, Figure 2-2A, Figure 2-3A, Figure 2-8B, and Figure 2-10.

Table 2-1. Yeast strains used in Chapter 2

Strain	Genotype	Reference
LPY5 (W303-1a)	*MAT*a *ade2-1 can1-100 his3-11,15 leu2-3,112 trp1-1 ura3-1*	Thomas and Rothstein 1989
S288c	*MAT*a *his3Δ200 leu2-3, 112 trp1Δ1 ura3-52*	
LPY3291	S288c *MAT*a *esa1Δ::HIS3* + pLP863 (*esa1-414*)	Clarke et al. 1999
LPY4774	W303 *MAT*a *esa1-414*	
LPY4909	W303 *MAT*α rDNA*::ADE2-CAN1*	Clarke et al. 2006
LPY4911	W303 *MAT*α *esa1-414* rDNA*::ADE2-CAN1*	Clarke et al. 2006
LPY4917	W303 *MAT*α TELVR*::URA3*	Clarke et al. 2006
LPY4919	W303 *MAT*α *esa1-414* TELVR*::URA3*	Clarke et al. 2006
LPY5406	W303 *MAT*a *nab3-10* rDNA*::ADE2-CAN1*	
LPY6121	W303 *MAT*a *ESA1-13myc::kanMX*	
LPY10622	W303 *MAT*a *nab3-10*	
LPY12154	W303 *MAT*a *rpd3::kanMX*	
LPY14942	W303 *MAT*a *NAB3-13myc::kanMX*	

Unless otherwise noted, strains were constructed during the course of this study or are part of the standard lab collection.

Table 2-2. Plasmids used in Chapter 2

Plasmid (alias)	Description	Source/Reference
pLP362 (pRS426)	vector *URA3* 2μ	Sikorski and Hieter 1989
pLP1402 (pRS202)	library vector *URA3* 2μ	P. Hieter
pLP37	*SIR2 URA3* 2μ	
pLP271	vector *TRP1* 2μ	
pLP796	*ESA1 URA3* 2μ	Clarke et al. 2006
pLP798	*ESA1 TRP1* 2μ	
pLP1238	*NAB3 URA3* 2μ	
pLP1259	*VAP1 URA3* 2μ	
pLP1310	*NAB3 TRP1* 2μ	
pLP1412	*LYS20 URA3* 2μ	
pLP1405	*LYS20*-library clone *URA3* 2μ	
pLP1406	*VAP1*-library clone *URA3* 2μ	
pLP1417	*LEU2*-library clone *URA3* 2μ	
pLP1419	*NAB3*-library clone *URA3* 2μ	
pLP2018	*NAB3 URA3* 2μ	

Unless otherwise noted, plasmids were constructed during the course of this study or are part of the standard lab collection.

Chapter 3.

**Collaboration between the essential Esa1 acetyltransferase and the Rpd3
deacetylase is mediated by H4K12 histone acetylation**

INTRODUCTION

The genome of eukaryotic cells is packaged in chromatin, where the DNA is
organized into a nucleosomal subunit structure. Nucleosomes consist of DNA wrapped
around a histone octamer that contains two copies of each of the four core histones (H2A,
H2B, H3, and H4), each of which can be post-translationally modified with multiple
types of chemical and protein additions. The addition and removal of these modifications
are catalyzed by histone modifying enzymes that function in a wide range of nuclear
processes.

One dynamic histone modification is the acetylation and deacetylation of lysine
residues. Enzymes that add an acetyl group to a lysine residue are known as histone
acetyltransferases (HATs), and the enzymes that remove acetyl groups are called histone
deacetylases (HDACs). The opposing activities of these two types of enzymes control the
status of histone acetylation in the cell. For example, in the budding yeast *S. cerevisiae*,
regulation of H4 lysine 16 (H4K16) acetylation is critical in maintaining transcriptionally
silent chromatin at the telomeres and regulating replicative life span, via activities of the
HAT Sas2 and the HDAC Sir2 (Kimura et al. 2002; Suka et al. 2002; Dang et al. 2009).

Roles for the other acetylated lysines on H4 are less clearly defined. Some
information has come from studying these modifications on a genome-wide level.
Through one microarray expression study, it became apparent that H4K5, H4K8, and

H4K12 might contribute non-specifically but jointly to transcription. Each lysine, when individually mutated to an unacetylatable amino acid, results in minimal changes in genome-wide transcription. However, when combined to make double or triple lysine mutants, they display additive effects on transcription (Dion et al. 2005). In addition to participating in transcriptional control, H4 acetylation is critical for other nuclear processes, including DNA replication and repair (Megee et al. 1995; Bird et al. 2002; Choy and Kron 2002). Esa1 and Rpd3 are yeast enzymes with opposing activities toward H4 lysine acetylation, and are also members of two highly conserved families of histone modifying enzymes [reviewed in (Doyon and Côté 2004; Yang and Seto 2008)].

Rpd3 is one of the founding members of class I HDACs, which include the human proteins HDAC1, 2, 3, and 8 that are often overexpressed in human cancer cells. Indeed, HDAC inhibitors are being actively used and studied as therapeutic agents for multiple types of cancer [reviewed in (Yang and Seto 2008)]. In yeast, Rpd3 deacetylates lysines on both H3 and H4 (Rundlett et al. 1996) and is involved in a wide-range of nuclear processes. On a global scale, Rpd3 is responsible for transcriptional regulation of a large number of genes (Bernstein et al. 2000; Sabet et al. 2004; Alejandro-Osorio et al. 2009). For many, but not all of these genes, transcriptional regulation occurs through modification of the lysines on the H3 and H4 N-termini (Sabet et al. 2004). When examined at specific loci, Rpd3 represses transcription of *INO1* and *IME2* by deacetylating histones at the promoters of these genes (Kadosh and Struhl 1998b; Rundlett et al. 1998). In contrast, there are several transcripts that require Rpd3 for their activation (De Nadal et al. 2004; Sertil et al. 2007). For example, Rpd3 is required for expression of the DNA damage inducible genes *HUG1* and *RNR3* (Sharma et al. 2007).

In line with Rpd3 having a role in DNA repair, *rpd3* mutants are defective in nonhomologous end-joining (Jazayeri et al. 2004). Mutants of *rpd3* increase silencing at the telomeres, ribosomal DNA (rDNA) repeats, and *HM* cryptic mating-type loci (De Rubertis et al. 1996; Rundlett et al. 1996; Vannier et al. 1996; Sun and Hampsey 1999), although the mechanism for this is unknown. Rpd3 also contributes to cell cycle control, in that *rpd3* mutants undergo early DNA replication origin firing (Vogelauer et al. 2002; Aparicio et al. 2004).

Rpd3 exists in two biochemically defined complexes, named Rpd3S (small) and Rpd3L (large) to reflect their relative sizes (Carrozza et al. 2005b; Keogh et al. 2005). The identification of the subunits in each of the two Rpd3-containing complexes has begun to reveal a separation in Rpd3 complex functions. Rpd3L is likely responsible for Rpd3's role at gene promoters, as Rpd3 is recruited to chromatin via the Rpd3L-specific subunit Ume6, which recognizes specific upstream promoter sequences (Kadosh and Struhl 1997; Carrozza et al. 2005a). Rpd3L-specific mutants also display increased rDNA, telomeric, and *HM* loci silencing (Vannier et al. 1996; Zhang et al. 1998; Sun and Hampsey 1999; Loewith et al. 2001; Carrozza et al. 2005a; Keogh et al. 2005), and replication timing defects (Knott et al. 2009) similar to *rpd3Δ* itself, indicating that Rpd3L is responsible for Rpd3's role in silencing and regulation of replication initiation. The smaller Rpd3S complex is recruited to methylated H3K36 within coding sequences to repress intragenic transcription initiation (Carrozza et al. 2005b; Keogh et al. 2005), a role not shared by Rpd3L.

Whereas Rpd3 is a class I HDAC, Esa1 is part of the evolutionarily conserved MYST family of HATs. Tip60, the human homolog of Esa1, is associated with many

human diseases, including HIV, Alzheimer's and multiple cancers. Tip60 acetylates the

tumor suppressor p53 and acts as a transcriptional co-activator for c-Myc and NF-κB

[reviewed in (Avvakumov and Côté 2007)]. In yeast, Esa1 is essential for viability (Smith

et al. 1998; Clarke et al. 1999), although Esa1's essential function may not be limited to

its catalytic activity (Decker et al. 2008). Esa1 acetylates specific lysine residues on

histones H2A, H3, H4 (Smith et al. 1998; Clarke et al. 1999), and the histone variant

H2A.Z (Babiarz et al. 2006; Keogh et al. 2006; Millar et al. 2006). Similar to Rpd3, Esa1

is the catalytic subunit of two chromatin modifying complexes that have shared subunits.

The larger of these is known as NuA4, whereas the smaller is piccolo (Allard et al. 1999;

Boudreault et al. 2003). *In vitro* activity assays indicate that piccolo is the more active

acetyltransferase complex on chromatin, but separate roles for the two complexes have

not been established *in vivo* (Boudreault et al. 2003).

Through the study of conditional *esa1* mutants, Esa1 has been discovered to play

an important role in many nuclear processes. Esa1 functions in cell cycle progression

(Clarke et al. 1999) and DNA repair (Bird et al. 2002). Esa1 also contributes both to

transcriptional activation and repression. Esa1 binding has been observed at the

promoters of many transcriptionally active genes (Robert et al. 2004), and specifically at

ribosomal protein genes, where Esa1 is needed for their transcriptional activation (Reid et

al. 2000). In a somewhat opposing role, Esa1 is required for transcriptional silencing at

the telomeres and the rDNA. Specifically, Pol II reporter genes that are normally

repressed when inserted at the telomeres and the rDNA display increased expression in

esa1 mutants (Clarke et al. 2006).

In this study, we defined an *in vivo* collaboration between the histone acetyltransferase Esa1 and the histone deacetylase Rpd3. Genetic dissection of the functional interactions revealed that the collaboration is mediated specifically through the Rpd3L complex. Deletion of *RPD3* suppressed multiple phenotypes of *esa1* mutants, including temperature-sensitivity, rDNA and telomeric silencing defects, and restored global H4 acetylation defects. Deletion of genes encoding Rpd3L-specific subunits Pho23 or Sds3 likewise promoted suppression of *esa1* phenotypes, suggesting that Esa1 coordinates acetylation specifically with Rpd3L. Consistent with this interpretation, deletion of the Rpd3S subunit encoded by *RCO1* did not suppress *esa1* phenotypes. Finally, suppression of the growth defect in the *esa1* mutant by deletion of Rpd3L subunits was specifically dependent on acetylation of lysine 12 on histone H4, thereby pointing to a crucial yet previously unsuspected role for this specific residue.

RESULTS

Deletion of the histone deacetylase gene *RPD3* suppressed the growth defect of *esa1*. Histone acetylation and deacetylation are opposing chemical modifications that must be balanced for transcriptional regulation. The interplay between HATs and HDACs is complicated by the presence of numerous enzymes, some of which have very specific substrates, whereas others share overlapping histone targets. In attempting to dissect these relationships, large-scale studies have uncovered an intricate network of genetic interactions between multiple HATs and HDACs (Collins et al. 2007; Lin et al. 2008; Mitchell et al. 2008).

In a study directly examining Esa1's functions in rDNA silencing, a surprising relationship was discovered between Esa1 and the class III HDAC Sir2 (Clarke et al. 2006). When either *ESA1* or *SIR2* is overexpressed, each suppresses the rDNA silencing defects of the other mutant. For example, overexpression of *ESA1* rescues the rDNA silencing defect of the *sir2* mutant (Clarke et al. 2006).

Neither increased dosage nor deletion of *SIR2*, however, had any effect on the growth defect of the *esa1-414* temperature-sensitive mutant at elevated temperatures. In searching for other genes encoding chromatin modifying enzymes that might functionally interact with *esa1* mutants, deletion of *RPD3* was discovered to specifically suppress this growth defect (Figure 3-1)*.*

To ask if deletion of genes encoding other HDACs could also support viability of the temperature-sensitive *esa1-414* allele at restrictive temperatures, double mutants of *esa1-414* were constructed in combination with a series of HDAC mutants. Along with the class III family deacetylase Sir2, deletion of genes encoding HDACs of classes I and II were tested. Rpd3, Hos1, Hos2, and Hda1 are all yeast HDACs of classes I and II that share 25-50% protein sequence identity. Of these, only *RPD3* deletion supported growth of *esa1* mutants at elevated temperatures (Figure 3-1). Mutation of the other genes either had no effect or in the case of *hos2*, exacerbated the severity of the *esa1* growth defect. Some of these results are parallel to interactions reported in a genome-wide study (Lin et al. 2008).

The *esa1-414* temperature-sensitive mutant contains a frameshift mutation that results in an early truncation of the protein, and displays reduced HAT activity both *in vitro* and *in vivo* (Clarke et al. 1999). To test the allele-specificity of the suppression,

Figure 3-1. Deletion of the histone deacetylase gene *RPD3* suppresses the growth

defect of *esa1-414*. Deletion of *RPD3* suppressed the temperature-sensitivity of the *esa1-*

414 allele, whereas deletion of other genes encoding histone deacetylases did not. Top

panel: serial dilutions of wild-type (LPY5), *esa1* (LPY4774), *esa1 rpd3* (LPY12156),

rpd3 (LPY12154), *esa1 sir2* (LPY11160), and *sir2* (LPY11) are shown on SC at the

restrictive temperature for *esa1* (35˚), compared to growth at the permissive temperature

(30˚). Bottom panel: serial dilutions of wild-type (LPY5), *esa1* (LPY4774), *esa1 hos1*

(LPY13712), *esa1 hos2* (LPY13585), *esa1 hda1* (LPY13478), *hos1* (LPY13706), *hos2*

(LPY13583), and *hda1* (LPY13472) on SC at restrictive and permissive temperatures.

Note that some of these interactions overlap with published results from a genome-wide

study (Lin et al. 2008), yet others are distinct. The differences may be due to strain

background- or allele-specific effects (personal communication, Y. Lin and J. Boeke).

control   growth

| WT |
| esa1 |
| esa1 rpd3 |
| rpd3 |
| esa1 sir2 |
| sir2 |

30° SC   35° SC

control   growth

| WT |
| esa1 |
| esa1 hos1 |
| esa1 hos2 |
| esa1 hda1 |
| hos1 |
| hos2 |
| hda1 |

30° SC   35° SC
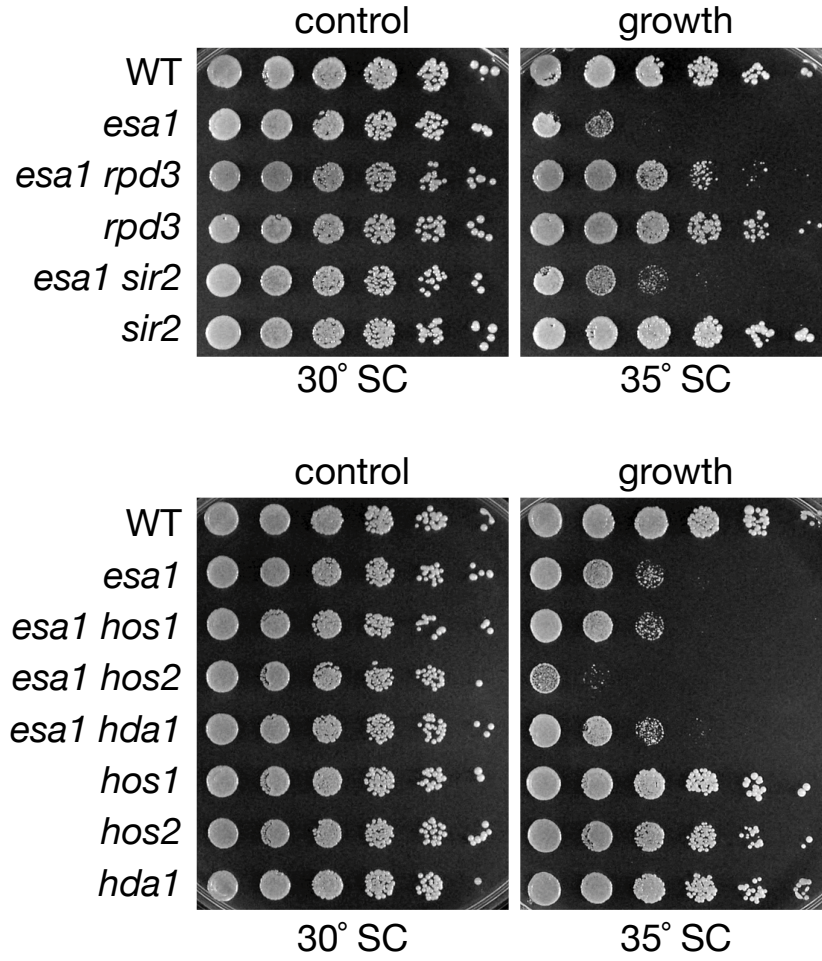
RPD3 was deleted in another *esa1* temperature-sensitive allele, *esa1-L254P*, and was also found to suppress the *esa1* growth defect at restrictive temperature (Figure 3-2A). The *esa1-L254P* allele contains a point mutation that resides near the HAT domain, and similar to *esa1-414*, is temperature-sensitive and lacks *in vitro* and *in vivo* HAT activity (Clarke et al. 1999). Thus, *rpd3* suppression of the *esa1* growth defect is not allele-specific and may be a general property for catalytically compromised Esa1. Furthermore, using the *RPD3* catalytically-dead allele, *rpd3-H150A-H151A* (Kadosh and Struhl 1998a) in combination with the *esa1* mutant showed results consistent with the *rpd3Δ* (Figure 3-2B). Therefore, the growth rescue observed is due to loss of histone deacetylase activity by Rpd3, and not some other function of Rpd3.

To test if *RPD3* deletion could bypass the non-viable *esa1Δ* phenotype, two tests were conducted. In the first, a plasmid shuffle was performed with a wild-type *ESA1* plasmid in the *esa1Δ rpd3Δ* double mutant. This strain was unable to grow under conditions that select for loss of the wild-type *ESA1* plasmid (Figure 3-2C). In the second test, an *esa1Δ/ESA1 rpd3Δ/rpd3Δ* diploid was sporulated, dissected, and examined for viability. All genotypically *esa1Δ rpd3Δ* double mutants were inviable. Some double mutants germinated and were able to undergo a small number of divisions, but none continued dividing to form colonies (data not shown), similar to *esa1Δ* itself (Clarke et al. 1999). This analysis confirmed the plasmid shuffle result, demonstrating that *rpd3* did not suppress the inviable *esa1Δ*.

Suppression of *esa1*'s growth defect was mediated exclusively by the Rpd3L complex. Rpd3S and Rpd3L, the two Rpd3-containing HDAC complexes, each have shared subunits as well as a number of distinct subunits (Carrozza et al. 2005a; Carrozza

Figure 3-2. Allele-specificity of *esa1 rpd3* temperature-sensitive suppression. A)

Suppression of *esa1*'s growth defect by *rpd3* was not *esa1* allele-specific. Serial dilutions

of wild-type (LPY5), *esa1-L254P* (LPY12160), *esa1-L254P rpd3* (LPY12164), and *rpd3*

(LPY12154) were plated on SC at the permissive and restrictive temperatures. B) *esa1*

rpd3 carrying either wild-type *RPD3* (LPY14359), catalytically inactive *rpd3-H150A-*

H151A (LPY14360), or vector (LPY14356) on a *HIS3* plasmid were plated at permissive

and restrictive temperatures on SC-His to assay for growth. C) Deletion of *RPD3* did not

bypass the need for *ESA1*. The following strains, wild-type (LPY12200), *esa1Δ*

(LPY12204), *esa1Δ rpd3* (LPY12206) and *rpd3* (LPY12202), all carried a wild-type

URA3/ESA1 plasmid (pLP796). These strains were subjected to a plasmid shuffle by

counterselection on 5-FOA.

A

control　　　　growth

WT
esa1-L254P
esa1-L254P rpd3
rpd3

30° SC　　　　35° SC

B

esa1 rpd3　　control　　　　growth
RPD3
rpd3-H150A-H151A
vector

30° SC-His　　　35° SC-His

C

esa1Δ	*esa1Δ* *rpd3Δ*
WT	*rpd3Δ*

SC-Ura　　　　5-FOA
2μ/*ESA1*/*URA3*　　(plasmid shuffle)
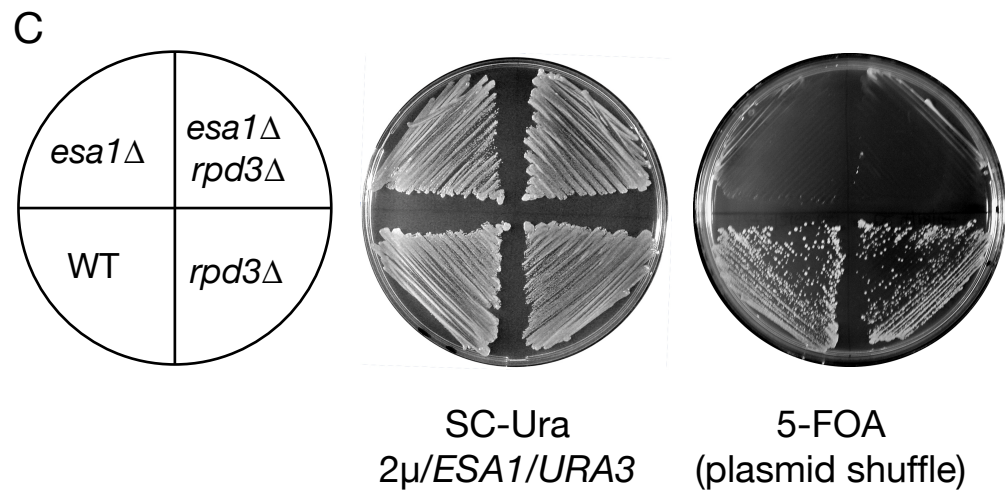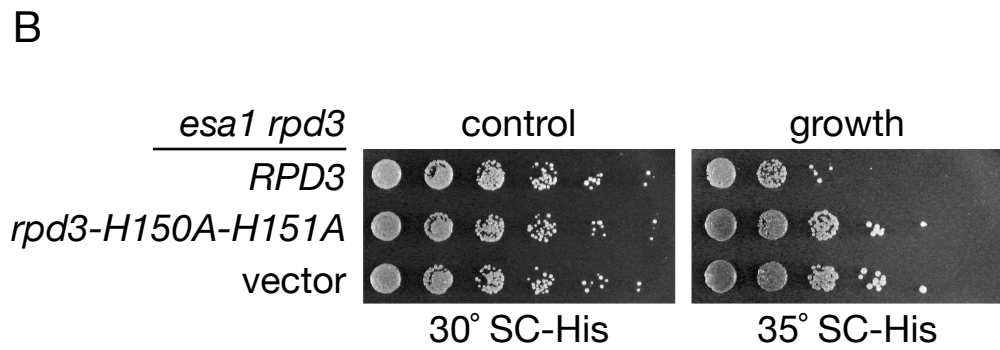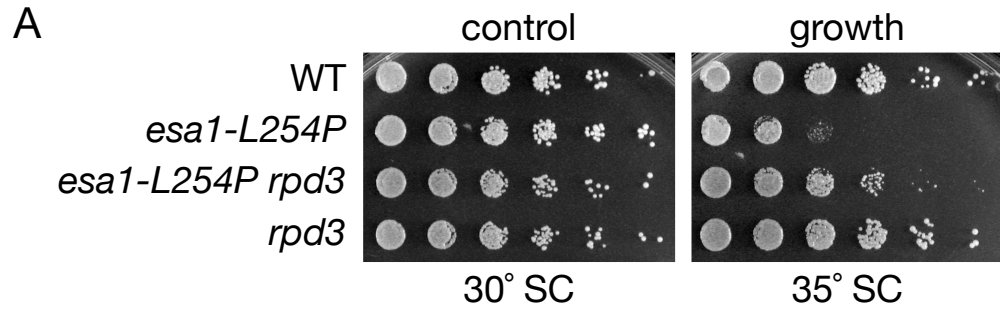
et al. 2005b; Keogh et al. 2005) (Figure 3-3A). Both Rpd3S and Rpd3L also contain

proteins that function in additional nuclear complexes. By evaluating subunits that are

unique to Rpd3S and Rpd3L, the complexes were dissected genetically to determine if

deletion of both is required, or if instead the suppression observed in the *esa1 rpd3*

double mutant is mediated through one specific complex. Double mutants were

constructed with *esa1* and genes specific to each of the two complexes. These double

mutants were then tested for suppression of *esa1*.

Rpd3S, the smaller of the two complexes, has only two subunits (Eaf3, Rco1) that

distinguish it from Rpd3L (Carrozza et al. 2005b; Keogh et al. 2005). However, Eaf3 is

not unique to Rpd3S since it is also a component of NuA4 (Eisen et al. 2001), an Esa1-

containing complex. Loss of *EAF3* disrupts both NuA4 and Rpd3S, thus *RCO1* was

chosen instead to disrupt Rpd3S. The Rco1 protein contains a PHD finger, and is required

for the complex integrity of Rpd3S (Carrozza et al. 2005b). As shown in Figure 3-3B (top

panel), deletion of *RCO1* in an *esa1* mutant did not suppress the *esa1* growth defect. In

fact, the *esa1 rco1* double mutant displayed a slightly exacerbated growth defect

compared to that of *esa1*. Therefore, the suppression of *esa1*'s growth defect is not

mediated through Rpd3S.

Rpd3L contains several subunits distinct from those in Rpd3S. Some are involved

in the function of other transcriptional complexes, such as Cti6, which recruits the SAGA

HAT complex to chromatin for transcriptional activation (Papamichos-Chronakis et al.

2002). In contrast, Sds3 is a subunit unique to Rpd3L. Sds3 is essential for the integrity

of the Rpd3L complex, and Rpd3L dissociates in *sds3* mutants, thereby resulting in a loss

of all Rpd3L histone deacetylase activity (Lechner et al. 2000; Carrozza et al. 2005a).

Figure 3-3. Rpd3L is the Rpd3-containing complex responsible for suppression of the growth defect in the *esa1* mutant. A) Cartoon highlighting the unique and shared members of the Rpd3S and Rpd3L complexes. B) Deletion of *RCO1*, specific to Rpd3S, did not suppress *esa1*'s growth defect at restrictive temperature. Deletion of *PHO23* and *SDS3*, both specific to Rpd3L, mimicked the suppression seen in *esa1 rpd3*. Serial dilutions of wild-type (LPY5), *esa1* (LPY4774), *esa1 rco1* (LPY12652), *rco1* (LPY12645), *esa1 sds3* (LPY12956), *sds3* (LPY12958), *esa1 pho23* (LPY12729), and *pho23* (LPY12732), were plated on SC at permissive (30˚) and restrictive temperatures (35˚). Cartoon of complexes is modified from (Roguev and Krogan 2007).

A

Rpd3L

Rpd3S

B

control

growth

esa1

esa1 rco1

rco1

WT

esa1

esa1 sds3

sds3

esa1 pho23

pho23

30° SC

35° SC
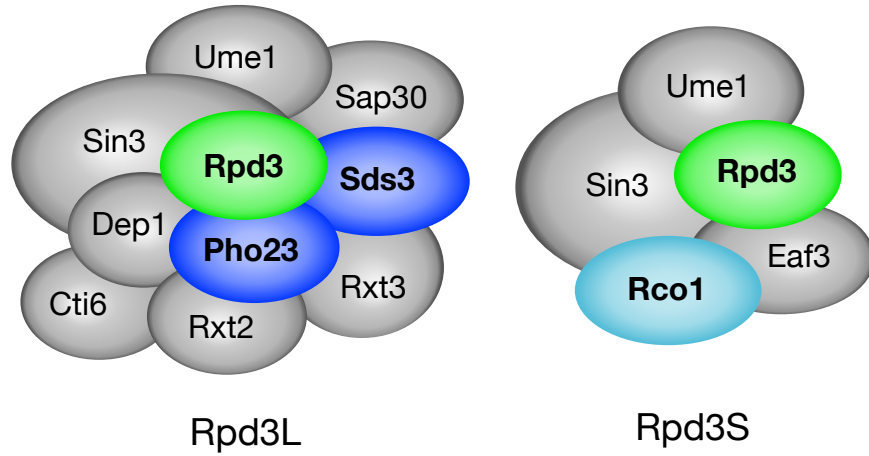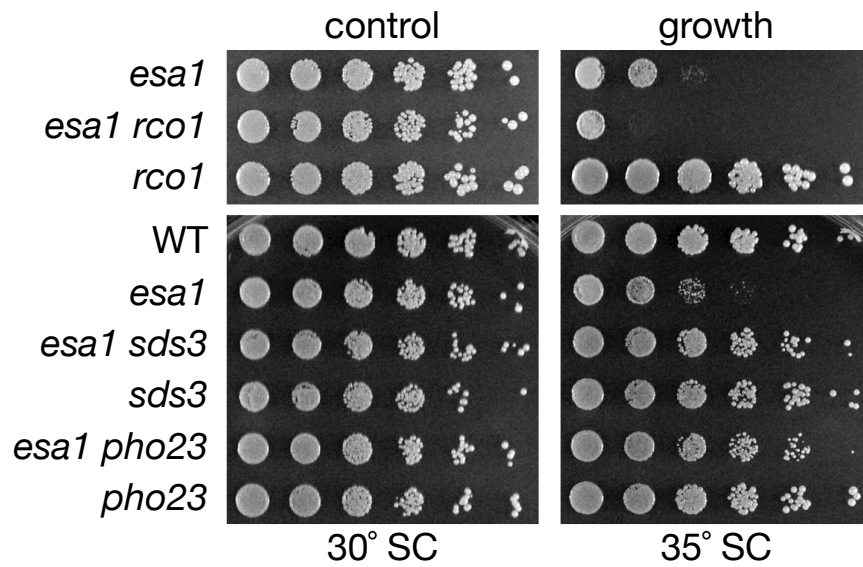
Deletion of *SDS3* in an *esa1* mutant mimicked the suppression seen in *esa1 rpd3* (Figure 3-3B, bottom), providing evidence that suppression of *esa1* is mediated through Rpd3L.

Pho23 is another Rpd3L-specific protein with a PHD finger and is one of three yeast proteins that belong to the ING tumor suppressor family (Loewith et al. 2001). In contrast to the *sds3Δ* mutant, the Rpd3L complex is structurally intact in *pho23Δ* cells and has normal levels of *in vitro* histone deacetylase activity (Carrozza et al. 2005a). Deletion of *PHO23* in the *esa1* mutant mimicked the suppression seen in both the *esa1 rpd3* and *esa1 sds3* double mutants (Figure 3-3B, bottom). This minor disruption in the Rpd3L complex is able to suppress *esa1*'s growth defect and supports the idea that Pho23 may have a key targeting function that works in opposition to other PHD finger proteins that exist in NuA4 and piccolo.

Comparing the growth at elevated temperatures of *esa1 rco1* mutants to the *esa1 sds3* and *esa1 pho23* strains thus demonstrates that the rescue of *esa1*'s growth defect by deletion of *RPD3* is mediated by the Rpd3L complex and not by Rpd3S. This specificity of suppression further establishes functional and not merely structural distinctions between the two Rpd3 complexes. To determine if the specificity of suppression extended to the diverse biological roles of Esa1, a broader analysis of defective *esa1* functions was evaluated.

Disruption of Rpd3L suppressed silencing phenotypes of the *esa1* mutant. Mutants of *ESA1* have a wide range of phenotypes, including defects in cell cycle control, transcriptional silencing, and the DNA damage response (Clarke et al. 1999; Bird et al. 2002; Clarke et al. 2006). To determine the involvement of Rpd3L in contributing to

these phenotypes, the *esa1 rpd3* double mutants along with the complex-specific double

mutants were examined for the integrity of these functions using *in vivo* assays.

First, rDNA silencing was assayed in the *esa1 rpd3* double mutant. Rpd3 has a

previously reported increase in rDNA silencing (Sun and Hampsey 1999), confirmed here

with the observation that *rpd3* increased repression of a *CAN1* reporter integrated at a

single 25S rDNA locus (Figure 3-4). In contrast, *esa1* mutants are defective in silencing

at the rDNA (Clarke et al. 2006) (Figure 3-4). Deletion of *RPD3* in combination with

esa1 suppressed this rDNA silencing defect. Deletion of *RPD3* in the *esa1* mutant not

only rescued the rDNA silencing defect, but increased silencing in the double mutant to

that seen in an *rpd3* single mutant (Figure 3-4, top). This same trend was observed when

the catalytic residues of *RPD3* were mutated in combination with *esa1* (Figure 3-6). The

complex-specific double mutants were next tested for rDNA silencing. The previous

observations that Rpd3L-specific mutants display increased rDNA silencing (Sun and

Hampsey 1999; Loewith et al. 2001; Keogh et al. 2005) were confirmed. Consistent with

the suppression of *esa1*'s growth defect, rDNA silencing was suppressed only when

Rpd3L was disrupted in *esa1* and not when Rpd3S was disrupted (Figure 3-4, compare

sds3 and *pho23* to *rco1* mutants).

Telomeric silencing was next assayed and revealed suppression patterns parallel

to those for rDNA silencing. The *esa1* mutant is defective in silencing a *URA3* reporter

gene integrated at telomere VR (Clarke et al. 2006) (Figure 3-5). The *rpd3* and Rpd3L-

specific mutants displayed increased silencing (Figure 3-5), confirming previous reports

(Vannier et al. 1996; Zhang et al. 1998; Loewith et al. 2001; Carrozza et al. 2005a;

Keogh et al. 2005). When genes encoding Rpd3L subunits were deleted in combination

Figure 3-4. Disruption of Rpd3L suppresses the rDNA silencing defect of *esa1*. Wild-type (LPY4909), *esa1* (LPY4911), *esa1 rpd3* (LPY12147), *rpd3* (LPY12145), *esa1 sds3* (LPY13517), *sds3* (LPY13513), *esa1 pho23* (LPY13859), *pho23* (LPY13854), *esa1 rco1* (LPY13505), and *rco1* (LPY13501) all have the rDNA::*ADE2-CAN1* reporter to test for rDNA silencing on plates containing canavanine. Decreased growth on canavanine indicates a defect in rDNA silencing.
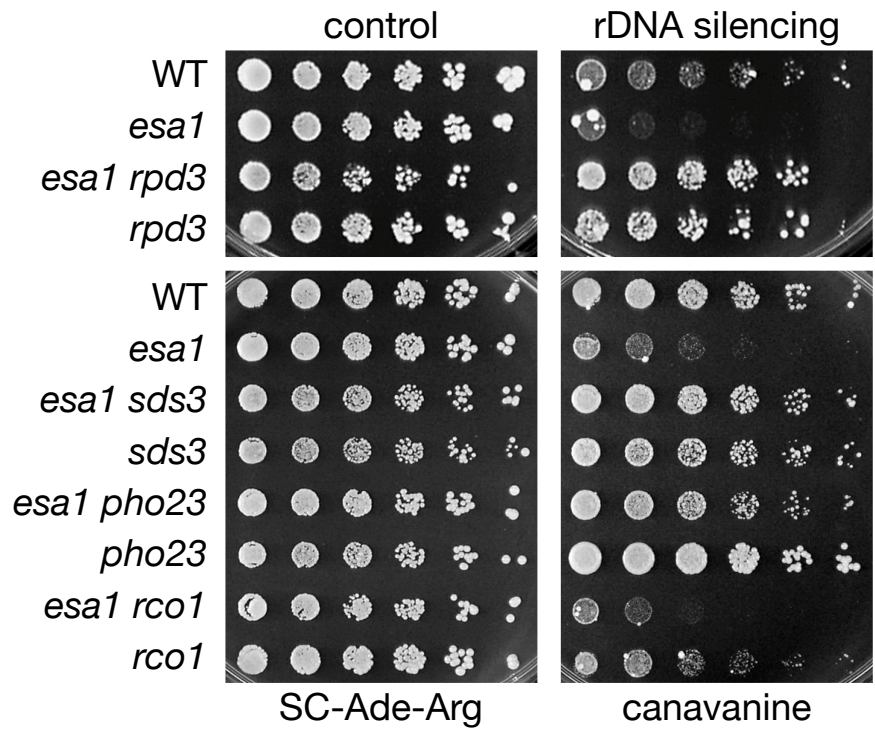
Figure 3-5. Disruption of Rpd3L suppresses *esa1* telomeric silencing. Wild-type

(LPY4917), *esa1* (LPY4919), *esa1 rpd3* (LPY12211), *rpd3* (LPY12093), *esa1 sds3*

(LPY13540), *sds3* (LPY13536), *esa1 pho23* (LPY13769), *pho23* (LPY13765), *esa1 rco1*

(LPY13528), and *rco1* (LPY13524) all have the TELVR*::URA3* silencing marker to test

for telomeric silencing on plates containing 5-FOA. Decreased growth on 5-FOA

indicates a defect in telomeric silencing.

Chr VR ____ [*URA3*] ____ (T)

control

telomeric
silencing

WT
esa1
esa1 rpd3
rpd3

WT
esa1
esa1 sds3
sds3
esa1 pho23
pho23
esa1 rco1
rco1

SC

5-FOA
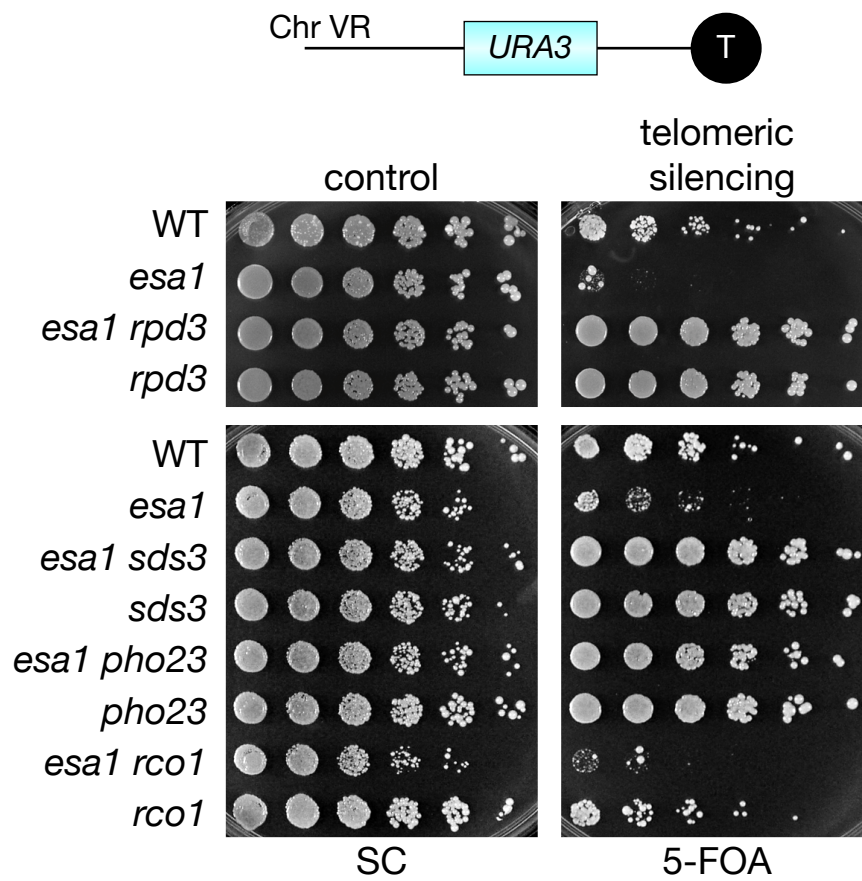
Figure 3-6. *RPD3* mutant lacking catalytic activity suppresses rDNA and telomeric silencing defects of *esa1*. A) *esa1 rpd3* double mutant strains with rDNA::*ADE2-CAN1* reporter carrying either wild-type *RPD3* (LPY14660), catalytically inactive *rpd3-H150A-H151A* (LPY14661), or vector (LPY14659), were assayed for rDNA silencing on SC-Ade-Arg-His plates with canavanine (32 μg/ml). B) *esa1 rpd3* with TELVR*::URA3* carrying wild-type *RPD3* (LPY14365), *rpd3-H150A-H151A* (LPY14366), and vector (LPY14364), were assayed for telomeric silencing on SC-His 5-FOA plates.

A
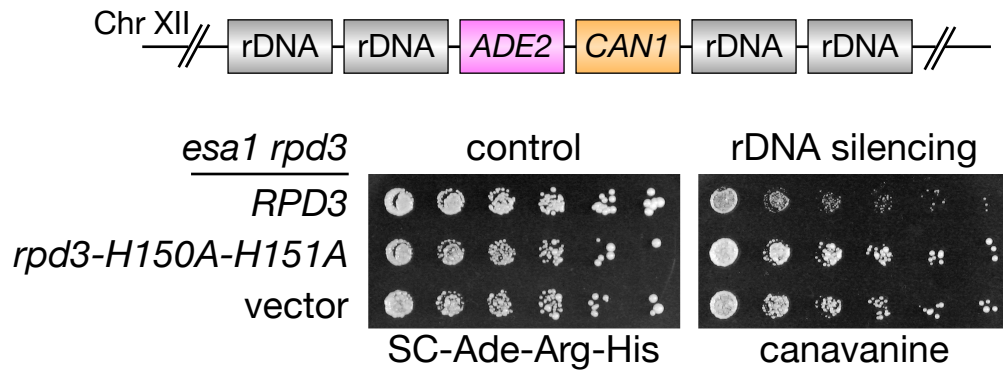
B
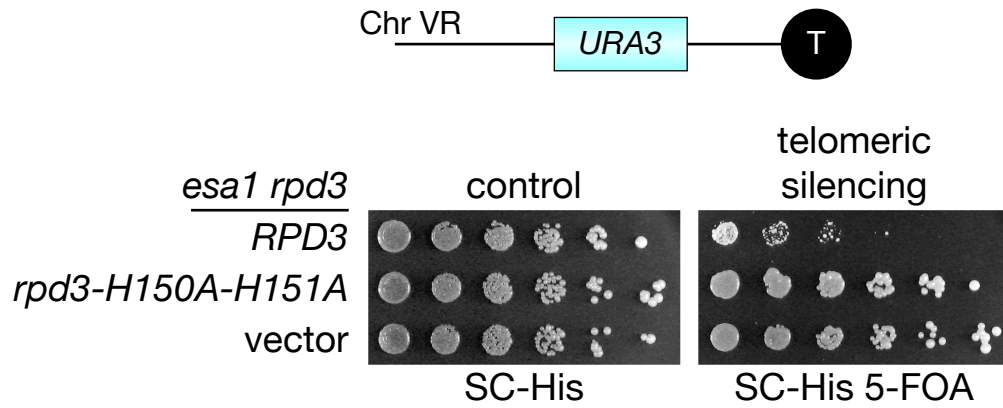
with *esa1*, they all restored telomeric silencing to *esa1* mutants, whereas deletion of the Rpd3S-specific *RCO1* had no effect on *esa1*'s reduced telomeric silencing (Figure 3-5, Figure 3-6). Therefore, Esa1 and Rpd3L share a critical opposing role in silencing at both the rDNA and telomeres.

Rpd3L disruption did not suppress the DNA damage phenotype of the *esa1* mutant. Whereas the growth and silencing phenotypes of *esa1* are consistent with Esa1's transcriptional functions, Esa1 also has a role in DNA double-strand break repair. This is readily observed in that *esa1* mutants are sensitive to camptothecin (Bird et al. 2002), a phenotype associated with defects in DNA repair and genome integrity. Camptothecin causes double-strand breaks by inhibiting topoisomerase I (Hsiang et al. 1985). Rpd3 also contributes to double-strand break repair, and *rpd3* mutants are sensitive to phleomycin, another DNA damaging agent (Jazayeri et al. 2004).

When tested in plate assays, an *rpd3* single mutant displayed increased sensitivity to camptothecin, and *rpd3* did not suppress *esa1's* sensitivity to camptothecin (Figure 3-7). In fact, the *esa1 rpd3* double mutant had increased sensitivity to camptothecin compared to *esa1* alone. Deletion of Rpd3L- and Rpd3S-specific subunits either exacerbated or had a minimal effect on camptothecin sensitivity in the *esa1* mutant (Figure 3-7).

Esa1 and Rpd3 are among several chromatin modifiers that are recruited to the repair of double-strand breaks resulting from DNA damage (Downs et al. 2004; Tamburini and Tyler 2005; Lin et al. 2008). Camptothecin sensitivity in *esa1* cells is thought to result from a failure of Esa1 and NuA4 recruitment to double-strand breaks.

Figure 3-7. Rpd3L disruption does not suppress *esa1*'s camptothecin sensitivity.

Wild-type (LPY5), *esa1* (LPY4774), *esa1 rpd3* (LPY12156), *rpd3* (LPY12154), *esa1 pho23* (LPY12729), *pho23* (LPY12732), *esa1 sds3* (LPY12956), *sds3* (LPY12958), *esa1 rco1* (LPY12652), and *rco1* (LPY12645), were plated on a control YPD plate containing DMSO and a plate containing 20 μg/ml of camptothecin in DMSO.
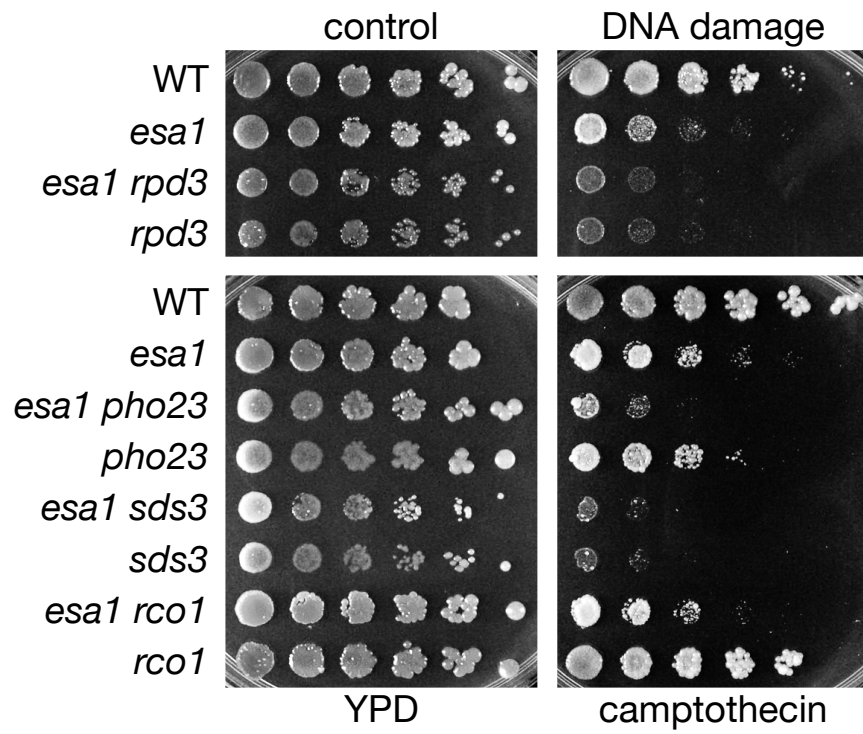
Therefore, *rpd3* as a suppressor of *esa1* is unlikely to involve Esa1's role in acetylation at sites of DNA damage.

In addition to the silencing and DNA damage phenotypes, *rpd3* mutants have reduced mating efficiency and are cycloheximide sensitive (Vidal and Gaber 1991). To examine if mutation of *ESA1* could reciprocally suppress *rpd3* phenotypes, the *esa1 rpd3* and the complex-specific double mutants were examined for changes in mating efficiency and cycloheximide sensivitity. Mutation of *ESA1* in *rpd3* had no effect on the reduced mating efficiency of *rpd3*, and the same was seen for the Rpd3L-specific mutants *pho23* and *sds3* (Figure 3-8A). The mating defect of *rpd3* mutants appeared specific to Rpd3L, shown by the reduced mating of *pho23* and *sds3* compared to wild-type mating in *rco1* (Figure 3-8A). Reduced mating efficiency has been observed previously for *sap30*, another Rpd3L-specific mutant (Zhang et al. 1998).

To determine if mutation of *ESA1* could suppress *rpd3*'s cycloheximide sensitivity, growth of the *esa1 rpd3* double mutant was examined on cycloheximide-containing plates. No suppression was observed; in fact the *esa1* mutant displayed a previously unreported modest cycloheximide resistance (Figure 3-8B). Together, *rpd3* in the context of Rpd3L can suppress many but not all *esa1* mutant phenotypes. The nature of this functional interaction is not, however, reciprocal because *esa1* mutants do not suppress the *rpd3* defects tested.

Deletion of *RPD3* restored global histone acetylation levels of shared target residues in the *esa1* mutant. To test whether the genetic relationship discovered between *esa1* and *rpd3* was observed at the molecular level of histone modification, global histone acetylation was evaluated using isoform-specific antisera for lysines

Figure 3-8. Mutant phenotypes of *rpd3* are not suppressed by *esa1* mutation. A)

Mutation of *ESA1* had no effect on *rpd3*'s mating defect. Wild-type (LPY5), *esa1*

(LPY4774), *esa1 rpd3* (LPY12156), *rpd3* (LPY12154), *esa1 pho23* (LPY12729), *pho23*

(LPY12732), *esa1 sds3* (LPY12956), *sds3* (LPY12958), *esa1 rco1* (LPY12652), and

rco1 (LPY12645) were patched onto YPD and mated to tester α strain (LPY78) by

replica plating. A non-mating *sir2* strain (LPY11) was used as a control. B) Mutation of

ESA1 had no effect on *rpd3*'s cycloheximide sensitivity. Wild-type (LPY5), *esa1*

(LPY4774), *esa1 rpd3* (LPY12156), and *rpd3* (LPY12154) strains were tested for growth

on YPD plates containing 250 ng/ml cycloheximide.

A

B
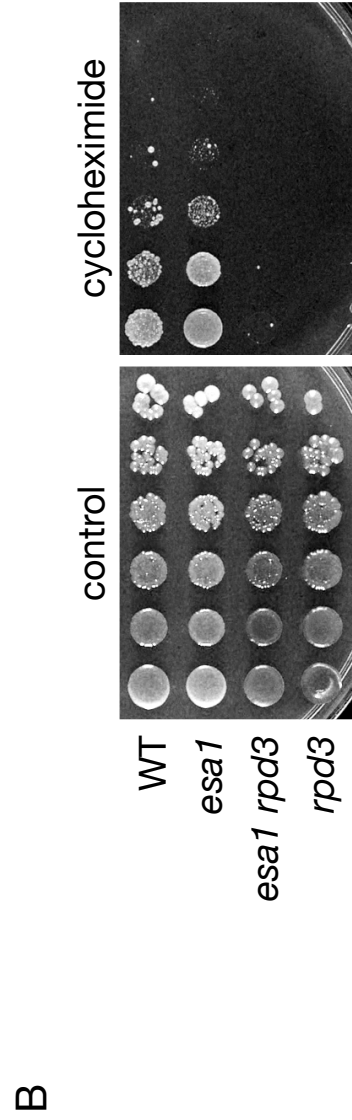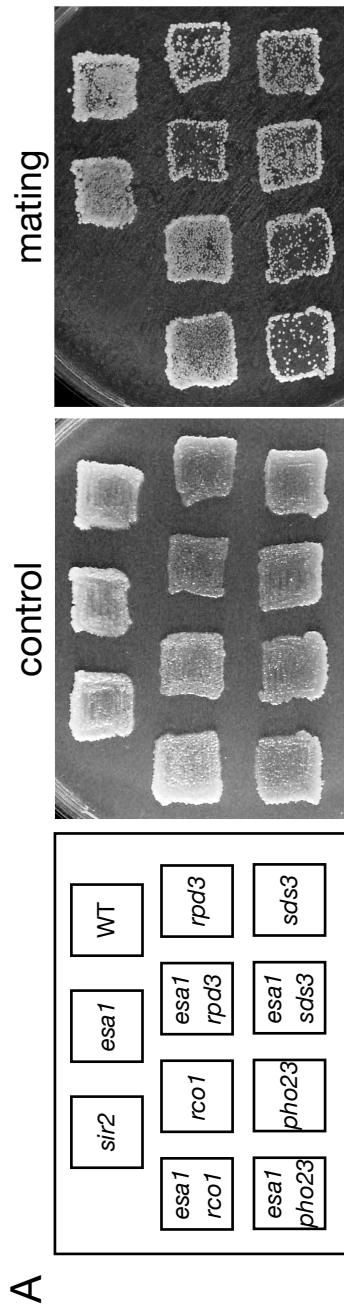
targeted by Esa1 and Rpd3. The enzymatic activities of Esa1 and Rpd3 both target specific lysines on the N-terminal tail of histone H4 (Figure 3-9A). Esa1 has global effects *in vivo* on H4K5 acetylation (Clarke et al. 1999) and also acetylates multiple lysines on H4 at sites within the rDNA (Clarke et al. 2006) and at specific gene promoters (Suka et al. 2001). Rpd3 globally deacetylates H4K5 and H4K12 (Rundlett et al. 1996) and is responsible for deacetylation of most histone tail lysine residues at specific gene promoters (Suka et al. 2001).

Lysates were collected from cells grown at permissive and slightly elevated temperatures that maintained viability. Immunoblots were performed on these lysates and probed with antisera specific for each acetylated lysine. As a control, histone levels were assayed and found comparable among all strains, as shown by probing for the C-terminus of H3 (Figure 3-9B, top panel). As expected, *esa1* mutants displayed decreased bulk histone acetylation, most dramatic for H4K5 (Clarke et al. 1999) and H4K12, and *rpd3* mutants had slightly increased acetylation of H4K5 and H4K12 compared to wild-type, consistent with earlier reports (Rundlett et al. 1996) (Figure 3-9B). In the non-catalytic mutants (*rco1*, *sds3*, and *pho23*), global histone acetylation changes were not observed (Figure 3-10). This result might be expected since an Rpd3 complex is still present in each of these mutants. Thus, it was not surprising that there were only very subtle changes in acetylation in these mutants when combined with *esa1* (Figure 3-10). Additionally, at two H4 lysines that are not shared targets of Esa1 and Rpd3, H4K8 and H4K16, acetylation was not changed in the *esa1 rpd3* double mutant.

Finally, in the *esa1 rpd3* double mutant, there was almost a complete restoration of the *esa1* global acetylation defect at both permissive and elevated temperatures that

Figure 3-9. Deletion of *RPD3* restores global acetylation levels of specific histone H4 residues in *esa1* mutants. A) Diagram of the histone H4 N-terminal tail highlighting sites of acetylation modifications. B) Deletion of *RPD3* restored global acetylation of H4K5 and H4K12, but not H4K8 and H4K16. Whole cell protein extracts from wild-type (LPY5), *esa1* (LPY4774), *esa1 rpd3* (LPY12156), and *rpd3* (LPY12154) cells at both permissive (30˚) and restrictive (34˚) temperature were immunoblotted with an antiserum specific to the C-terminus of H3 to control for histone levels, and with H4 antisera to detect the amount of bulk histone acetylation at each lysine residue.

A

B

Figure 3-10. Deletion of non-catalytic subunits of Rpd3 complexes does not change global acetylation of H4K5 or H4K12. Whole cell extracts were prepared from Wild-type (LPY5), *esa1* (LPY4774), *esa1 sds3* (LPY12956), *sds3* (LPY12958), *esa1 rpd3* (LPY12156), *rpd3* (LPY12154), *esa1 pho23* (LPY12729), *pho23* (LPY12732), *esa1 rco1* (LPY12652), and *rco1* (LPY12645) and immunoblotted for global acetylation changes at H4K5 and H4K12.

H4K5Ac

H4K12Ac

H4K5Ac

H4K12Ac
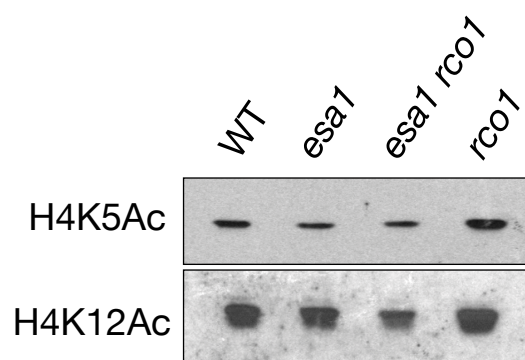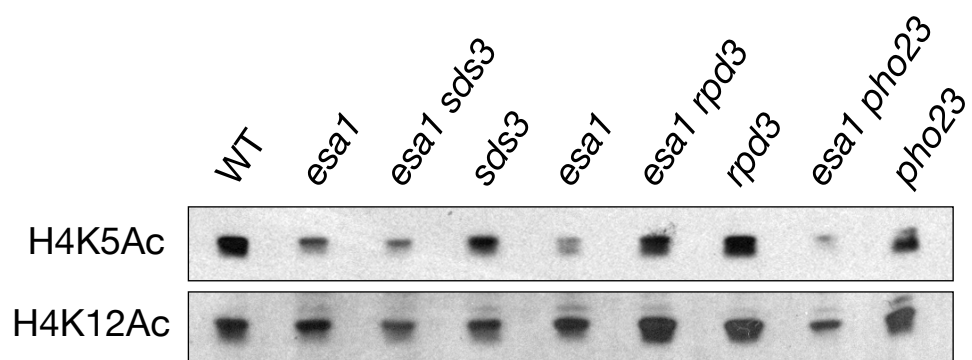
was strongest for H4K12 (Figure 3-9B). There was also an intermediate effect on acetylation at H4K5. Together, these results provide a molecular basis for the growth defect and silencing suppression observed in the *esa1 rpd3* double mutant (Figures 3-1, 3-4, 3-5).

Suppression of *esa1*'s growth defect by deletion of *RPD3* is mediated through H4K12 acetylation. Because the most dramatic change in global histone acetylation in *esa1 rpd3* was at H4K12 (Figure 3-9B), it seemed likely that this particular residue was most critical for the functional interaction between the two enzymes. To evaluate the possibility, mutants were constructed in which each target lysine was changed to alanine, an amino acid residue that cannot be acetylated. The ability of *rpd3* to suppress *esa1*'s growth defect was then tested with each histone lysine mutant. In wild-type cells, the H4K12A mutant by itself did not display any growth defects, nor did it affect growth in the *esa1* or *rpd3* single mutant. However, H4K12A in combination with the *esa1 rpd3* double mutant displayed a dramatic reduction in growth at elevated temperature compared to the *esa1 rpd3* double mutant (Figure 3-11, top). The other H4 lysine mutants (H4K5A, H4K8A, and H4K16A) had minimal effects on the growth of the *esa1 rpd3* double mutant (Figure 3-11, bottom). The dependence on H4K12 was also observed in the *esa1 rpd3-H150A-H151A* catalytic mutant (Figure 3-12). Therefore, the suppression observed in the *esa1 rpd3* double mutant is specifically dependent on H4K12, and not H4K5, K8, or K16.

H4K12 was also found to be the key acetylated lysine in suppression of *esa1* by disruption of the Rpd3L complex. As shown in Figure 3-13, when each lysine was individually mutated in the *esa1 sds3* and *esa1 pho23* double mutants, only the H4K12A

Figure 3-11. Suppression of *esa1*'s growth defect by *rpd3* is dependent on H4K12.

Strains are deleted for all copies of H3 and H4 and carry a *TRP1* plasmid with either

wild-type H4 or H4 with one mutated lysine residue. Plasmid retention was required for

survival. Serial dilutions of the following strains were plated at permissive (30˚) and

restrictive temperature (35˚) on SC. Top panel: growth of H4K12A mutants in

combination with *esa1 rpd3*. Wild-type (LPY12383), H4K12A (LPY12394), *esa1*

(LPY12384), *esa1* H4K12A (LPY12071), *esa1 rpd3* (LPY12707), *esa1 rpd3* H4K12A

(LPY12714), *rpd3* (LPY12695), *rpd3* H4K12A (LPY12702). Bottom panel: growth of

esa1 rpd3 mutants in combination with each lysine individually mutated to alanine. *esa1*

rpd3 (LPY12707), *esa1 rpd3* H4K5A (LPY12708), *esa1 rpd3* H4K8A (LPY12711), *esa1*

rpd3 H4K12A (LPY12714), *esa1 rpd3* H4K16A (LPY12717).
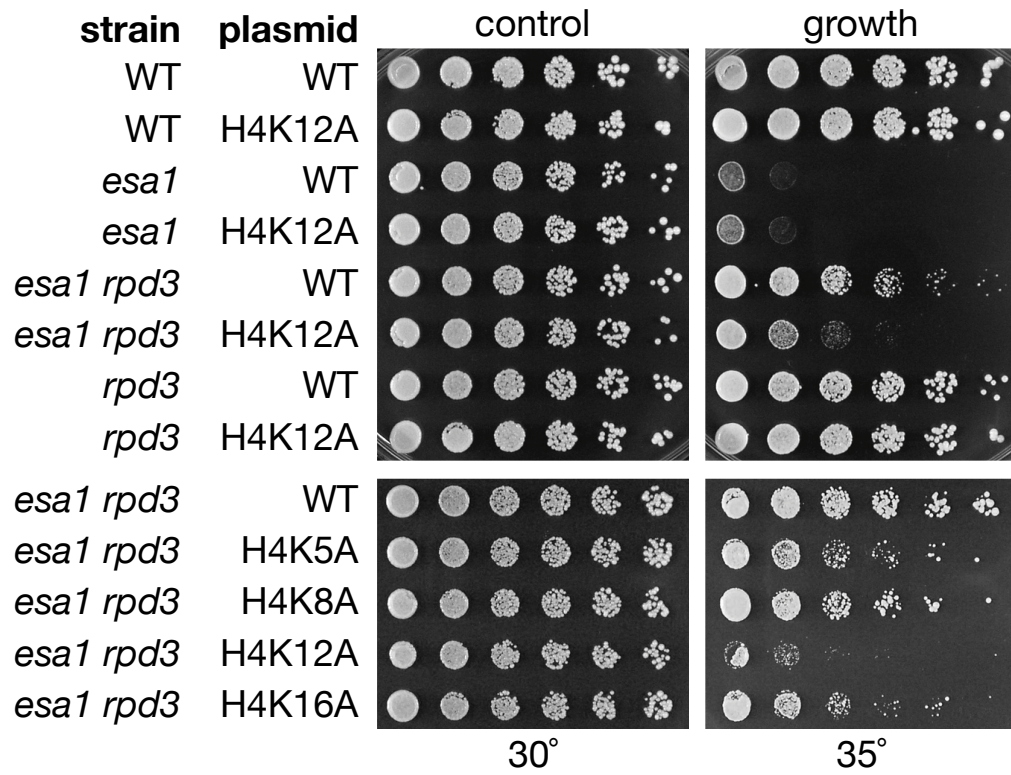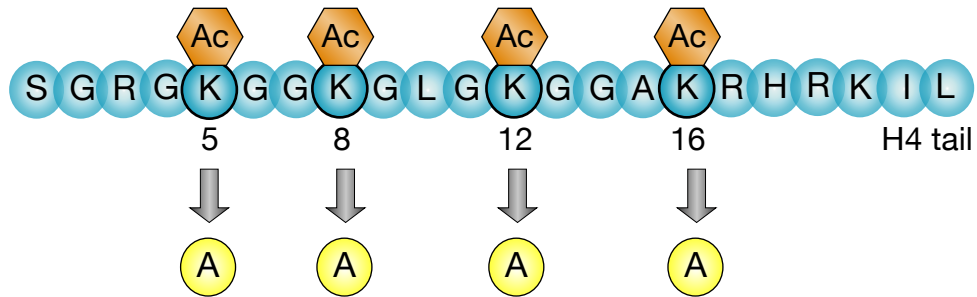
Figure 3-12. Growth rescue of *esa1* mutant by catalytcally inactive *rpd3-H150A-H151A* is dependent on H4K12. *esa1 rpd3* strains carrying different H4 lysine mutant plasmids were transformed with a *HIS3* plasmid containing *rpd3-H150A-H151A*. These were plated on SC-His at permissive and restrictive temperatures to assay for growth. All strains are *esa1 rpd3-H150A-H151A* with wild-type H4 (LPY14675), H4K5A (LPY14676), H4K8A (LPY14677), H4K12A (LPY14678), or H4K16A (LPY14679)
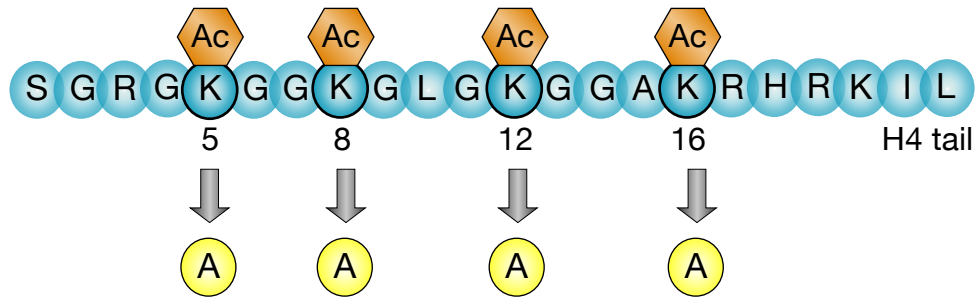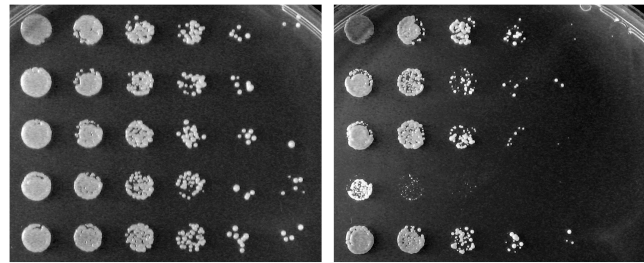
Figure 3-13. Suppression of *esa1*'s growth defect by deletion of Rpd3L-specific subunits is dependent on H4K12. Top panel: two-fold dilutions, starting at an A_{600} of 0.1, were plated on SC-Trp for assaying growth of *esa1 sds3* in combination with each lysine individually mutated to alanine. Strains are *esa1 sds3* (LPY14175), *esa1 sds3* H4K5A (LPY14176), *esa1 sds3* H4K8A (LPY14177), *esa1 sds3* H4K12A (LPY14178), and *esa1 sds3* H4K16A (LPY14179). Bottom panel: as above except in *esa1 pho23* mutant. Strains are *esa1 pho23* (LPY14165), *esa1 pho23* H4K5A (LPY14166), *esa1 pho23* H4K8A (LPY14167), *esa1 pho23* H4K12A (LPY14168), and *esa1 pho23* H4K16A (LPY1416
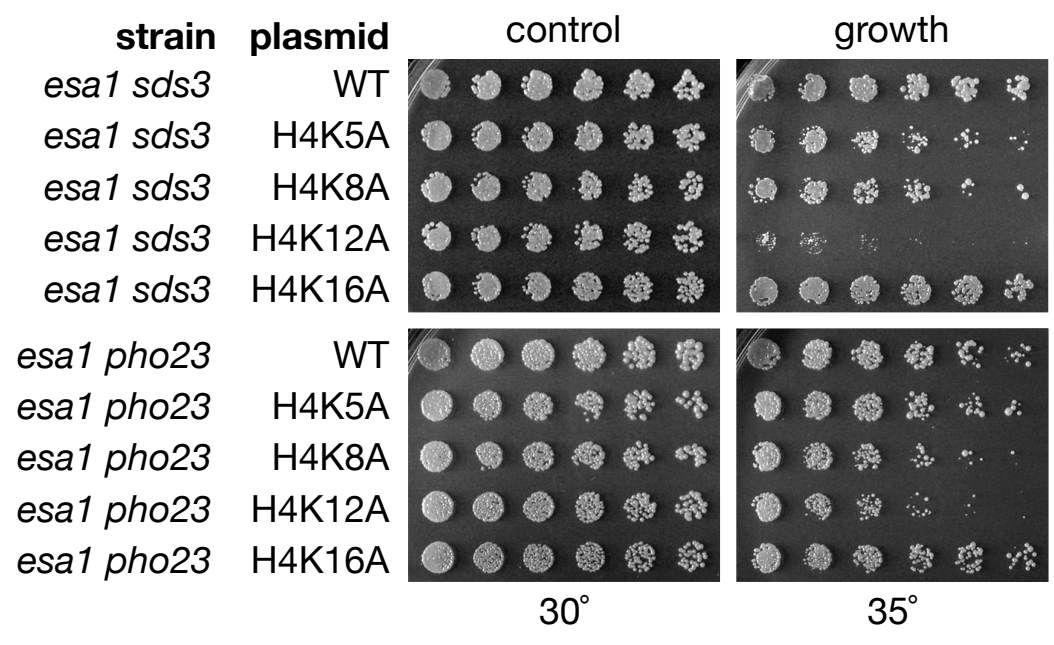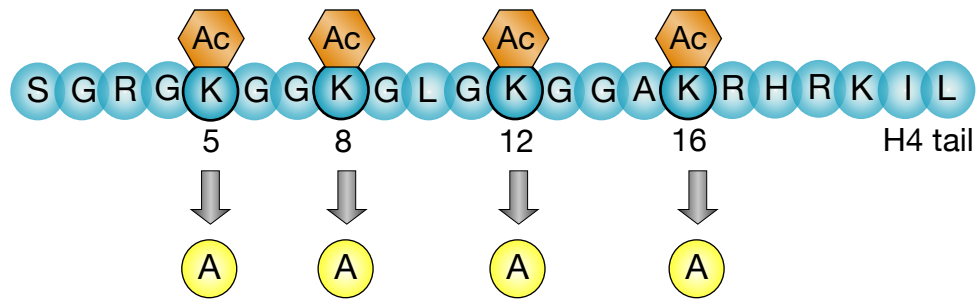
substitution resulted in a loss of suppression, albeit to a more modest degree than in *esa1 rpd3*. Although the dependence on H4K12 appears subtle in the *esa1 pho23* double mutant, this slight effect was observed reproducibly. Notably, in the protein immunoblots H4K5 showed a moderate acetylation increase in the *esa1 rpd3* double mutant compared to *esa1* (Figure 3-9B), yet the H4K5A mutant had little impact on the growth of *esa1 rpd3*, *esa1 sds3*, or *esa1 pho23* (Figure 3-11, 3-13).

Thus H4K5 and H4K12 are common targets of global acetylation and deacetylation by both Esa1 and Rpd3. However, the distinction observed here between the growth of *esa1 rpd3* in H4K5A versus H4K12A mutants points to H4K12 as the critical shared target of Esa1 and the Rpd3L complex for regulating growth and viability (Figure 3-16A).

DISCUSSION

The findings presented here tightly link Esa1's acetyltransferase activity and Rpd3's deacetylase activity in critical cellular processes. Loss of Rpd3L specifically alleviated many of the cell's needs for fully functional Esa1 activity, a property not shared by the Rpd3S complex, nor by other class I-III deacetylases (summarized in Table 3-1). This exclusive relationship between Esa1 and Rpd3L centers on their shared histone target H4K12. In addition, Esa1 works specifically with the Rpd3L complex in maintaining silencing at the rDNA and telomeres, but not in repairing camptothecin-induced double-strand breaks (Figure 3-16, Table 3-1).

Esa1 and Rpd3 have both previously been shown to be required for rDNA and telomeric silencing. Esa1 is enriched at the rDNA by chromatin immunopreceiptation and

Esa1-dependent changes in H4 acetylation are seen at the rDNA (Clarke et al. 2006).

Unlike its role in growth, the *rpd3*-mediated suppression of *esa1*'s rDNA and telomeric

silencing defects was not dependent on H4K12 acetylation (Figure 3-14, 3-15). Hence

suppression at these loci is mechanistically distinct. Rpd3L's role in rDNA and telomeric

silencing involves boundary formation (Zhou et al. 2009) and is dependent on the histone

deacetylase Sir2 that targets H4K16 (Sun and Hampsey 1999; Raisner and Madhani

2008). Therefore the observed dependence on H4K16 acetylation (Figure 3-14, 3-15) was

not surprising. This dependence on Sir2 and H4K16 deacetylation has led to the idea that

Rpd3 has an indirect effect in silencing, possibly through altering Sir2 activity (Sun and

Hampsey 1999) or the expression of other genes involved in silencing. Because *esa1*'s

rDNA and telomeric silencing defects were suppressed by disruption of Rpd3L (Figure 3-

4, 3-5), and were dependent on H4K16 acetylation (Figure 3-14, 3-15), it is likely that

Esa1 and Rpd3L's role in silencing is upstream of Sir2 (Figure 3-16B).

It is becoming evident that histone modifying enzymes also target many non-

histone substrates [reviewed in (Sterner and Berger 2000)]. Indeed, recent data indicate

that such non-histone substrates exist for NuA4 (Lin et al. 2009), including Yng2, which

is also a substrate of Rpd3 (Lin et al. 2008). Further studies should provide additional

insight into the range and roles of non-histone substrates in Esa1 and Rpd3 functions,

perhaps revealing a more direct link for their influence on rDNA and telomeric silencing.

In this case however, we have shown that H4K12 is a key shared target for the

contributions of Esa1 and Rpd3 to cell growth and viability.

A critical role for dynamic acetylation and deacetylation of H4K12 by Esa1

and Rpd3L. The cell contains numerous HATs and HDACs that together acetylate many

Figure 3-14. rDNA silencing suppression is not dependent on a single H4 lysine. A)

Top panel: same strains from Figure 3-13 were plated on SC-Ade-Arg with 32 µg/ml

canavanine to test for rDNA silencing defects with the rDNA::*ADE2-CAN1* reporter.

Bottom panel: *esa1 sds3* (LPY14296), *esa1 sds3* H4K5A (LPY14297), *esa1 sds3* H4K8A

(LPY14298), *esa1 sds3* H4K12A (LPY14299), *esa1 sds3* H4K16A (LPY14300) all have

the rDNA::*ADE2-CAN1* silencing reporter, and were assayed as above. B) Strains from

part (A) top panel, were transformed with catalytically-inactive *rpd3-H150-H151A*

(transformed strains are LPY14685, LPY14686, LPY14687, LPY14688, and LPY14689,

in order) and assayed for silencing on SC-Ade-Arg-His plates with 32 µg/ml canavanine.

Chr XII rDNA — rDNA — *ADE2* — *CAN1* — rDNA — rDNA

A

strain	plasmid	control	rDNA silencing
esa1 rpd3	WT		
esa1 rpd3	H4K5A		
esa1 rpd3	H4K8A		
esa1 rpd3	H4K12A		
esa1 rpd3	H4K16A		
esa1 sds3	WT		
esa1 sds3	H4K5A		
esa1 sds3	H4K8A		
esa1 sds3	H4K12A		
esa1 sds3	H4K16A		

SC-Ade-Arg   canavanine

B

rpd3-H150A-H151A

strain	plasmid	control	rDNA silencing
esa1 rpd3	WT		
esa1 rpd3	H4K5A		
esa1 rpd3	H4K8A		
esa1 rpd3	H4K12A		
esa1 rpd3	H4K16A		

SC-Ade-Arg-His   canavanine

99

Figure 3-15. Telomeric silencing suppression is not dependent on a single H4 lysine.

esa1 rpd3 (LPY14301), *esa1 rpd3* H4K5A (LPY14302), *esa1 rpd3* H4K8A (LPY14303), *esa1 rpd3* H4K12A (LPY14304), *esa1 rpd3* H4K16A (LPY14305) were plated on 5-FOA plates to test for telomeric silencing using the TELVR*::URA3* silencing marker.

Chr VR   URA3   T

		control	telomeric silencing
strain	**plasmid**		
esa1 rpd3	WT		
esa1 rpd3	H4K5A		
esa1 rpd3	H4K8A		
esa1 rpd3	H4K12A		
esa1 rpd3	H4K16A		
		SC	5-FOA

101
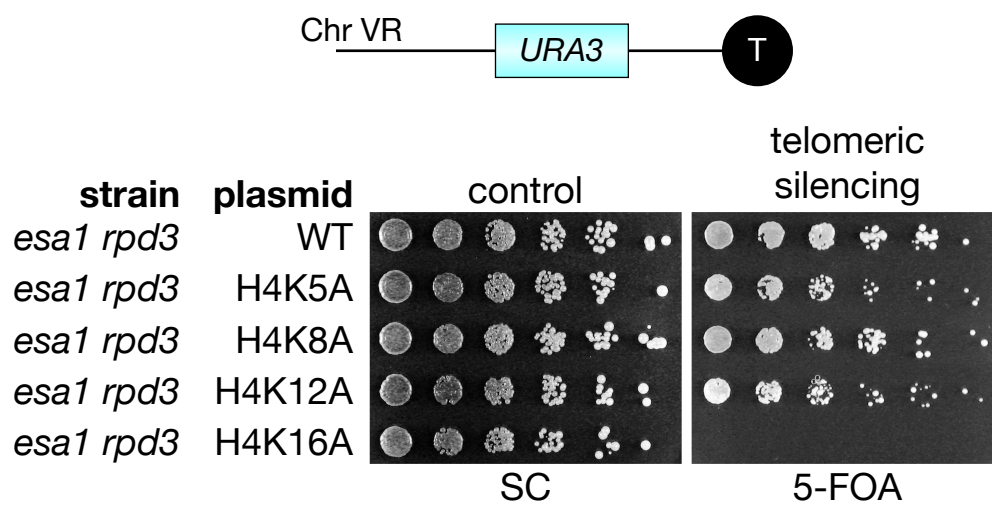
Figure 3-16. A model depicting a critical role for Esa1 and Rpd3L in coordinating the dynamic acetylation of H4K12. A) Esa1 and Rpd3L control H4K12Ac for general transcriptional targets contributing to cell viability and growth. B) Esa1 and Rpd3L contribute to rDNA and telomeric silencing. This relationship is not mediated specifically through H4K12 acetylation, but likely through a number of other targets. Sir2 deacetylation of H4K16 appears downstream of the role for Esa1 and Rpd3L. C) Esa1 and Rpd3S, but not Rpd3L, may control acetylation at sites of DNA damage.

A   growth
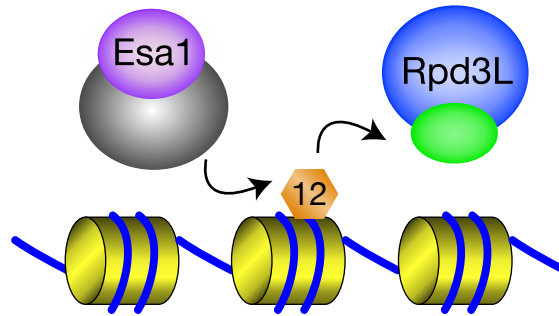
B   silencing
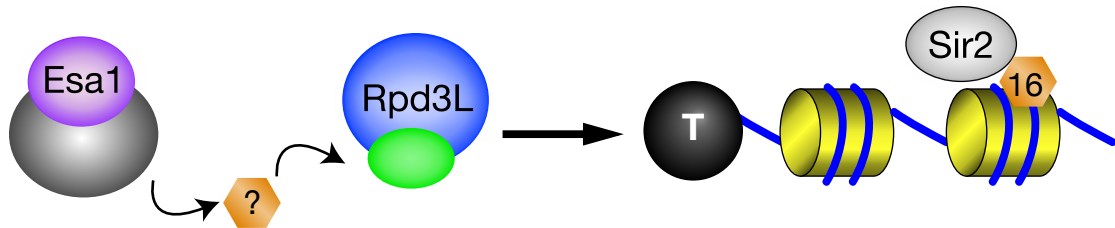
C   damage
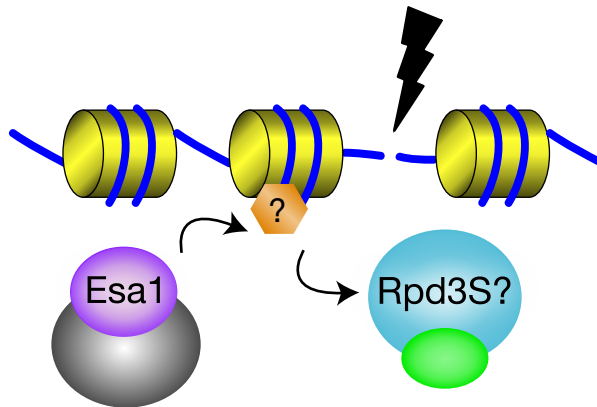
lysine residues on histones. The intricacies of histone acetylation and deacetylation result from several features: each HAT and HDAC often targets multiple lysine residues, different HATs and HDACs have overlapping acetylation targets, and other post-translational modifications may influence activity or substrate recognition. For example, a simple mutation of H4K12 did not suppress *esa1* defects (Figure 3-11), even though it is a key target of Esa1. This is because Esa1 has many other histone targets, including other lysines on H4, H2A, and H2A.Z, and lack of acetylation of these also contributes to *esa1*'s growth defect.

Defining roles for specific histone acetylation sites is further complicated by the genome-wide data that acetylation of H4K5, H4K8, and H4K12 are redundant in transcription (Dion et al. 2005). One point in support of this idea is that the H4K12A single mutant displayed no obvious growth defects (Figure 3-11). A previous study defined the H3 and H4 N-termini as the functional targets of Rpd3 in regulation of transcription (Sabet et al. 2004). The connections between Esa1, Rpd3L, and H4K12 presented here strengthen this functional importance through further identification of a key specific lysine (H4K12) in the H4 N-terminus, and the acetyltransferase responsible (Esa1). Since in the absence of Esa1 and Rpd3L, H4K12 acetylation became particularly important for cell viability (Figure 3-11, 3-13), these specific links define a model whereby control of H4K12 acetylation is essential for transcriptional regulation of a subset of genes by Esa1 and Rpd3L for cell viability (Figure 3-16A).

Among the several genome-wide ChIP datasets that define Esa1 and Rpd3 binding (Reid et al. 2000; Kurdistani et al. 2002; Robert et al. 2004), little overlap has been observed between regions strongly enriched for Esa1 and those enriched for Rpd3.

This may be due to the fact that Esa1 and Rpd3 both exist in multiple complexes in the cell, creating noise in the datasets. Esa1-bound loci would include both NuA4 and piccolo, thereby conflating their occupancy sites. Likewise, genome-wide ChIP that has been performed does not allow discrimination between sites of Rpd3L versus Rpd3S occupancy. When analyzed at specific loci, Rpd3S functions at downstream regions (Carrozza et al. 2005b; Keogh et al. 2005), thus it is likely that the genome-wide binding of Rpd3 found at downstream regions can be attributed to Rpd3S and binding at promoters can be attributed to Rpd3L. However, because the genomic binding maps were generated with non-tiling arrays, resolving the differences in Rpd3L and Rpd3S binding with available datasets is not possible. The differences in function between Rpd3L and Rpd3S in relation to Esa1 provide a new tool for refining understanding of the two complexes.

Distinguishing complexes and their functional interactions. Esa1 and Rpd3 each act as the catalytic subunit of two multiprotein histone modifying complexes. The two Rpd3 complexes, Rpd3S and Rpd3L, are composed of distinct subunits that allow them to be genetically dissected. Several recent papers have examined different roles for Rpd3S and Rpd3L (Carrozza et al. 2005a; Carrozza et al. 2005b; Keogh et al. 2005; Biswas et al. 2008; Knott et al. 2009). We have established that disruption of Rpd3L function is specifically responsible for the genetic suppression of *esa1* mutants for cell viability and silencing phenotypes (Figure 3-3, 3-4, 3-5).

Two different roles for histone modifying enzymes in the DNA damage response have been uncovered. One role is to participate in the transcriptional response through the activation of DNA repair genes. For example, Esa1 and Rpd3 are both required for

transcriptional activation of the damage-inducible genes *HUG1* and *RNR3* (Sharma et al. 2007). The identification of these as shared targets for activation raises a useful distinction because *rpd3* cannot suppress *esa1*'s sensitivity to DNA damage. It seems likely therefore that Esa1 and Rpd3 target genes relevant to changes in H4K12 acetylation are those that Esa1 activates and Rpd3 represses. Identification of these genes should prove of great interest.

The other function for histone modifying enzymes in DNA repair is more direct: chromatin modification targeted to the site of DNA damage. Along with several other HATs and HDACs, Esa1, some members of NuA4, and Rpd3 itself all bind at double-strand breaks, followed by changes in acetylation of nearby chromatin (Bird et al. 2002; Downs et al. 2004; Tamburini and Tyler 2005; Lin et al. 2008). Our observations showing that deletion of Rpd3L-specific subunits does not suppress repair defects of *esa1* mutants make it unlikely that Rpd3L functions together with Esa1 at sites of DNA damage. However, since Rpd3 is present at double-strand breaks and is required for nonhomologous end-joining (Jazayeri et al. 2004; Tamburini and Tyler 2005), perhaps Rpd3S and Esa1 coordinate acetylation at sites of DNA damage (Figure 3-16C).

By constructing specific double deletion mutants, it was possible to refine understanding of Rpd3S and Rpd3L functions beyond earlier reports. In contrast, Esa1 exists in the NuA4 and piccolo complexes, yet because piccolo is a subcomplex of NuA4, it has not yet been possible to disrupt piccolo without also disrupting NuA4 function. Therefore, it remains to be determined whether *rpd3* suppression of *esa1* is mediated through NuA4 or piccolo.

Future studies should provide additional insight into distinctions between NuA4 and piccolo that may allow this question to be answered. One idea comes from studies examining the chromatin modifying complexes SLIK/SALSA and SAGA. These complexes share most subunits, including the histone acetyltransferase Gcn5. It was found that the shared subunit Spt7, exists in a C-terminally truncated form in the smaller SLIK/SALSA complex, allowing for construction of specific *SPT7* alleles that favor a specific complex (Sterner et al. 2002; Wu and Winston 2002). Analogous to this shift between SLIK/SALSA and SAGA, the discovery of specific alleles of piccolo components that favor activity of one complex over another may allow for future dissection of Esa1's interactions with Rpd3.

One possibility is that NuA4 and Rpd3S, which share the chomodomain protein Eaf3, work together, whereas piccolo and Rpd3L are also a functional pair. Some data supporting this idea can be extrapolated from genome-wide studies. For example, double mutants of *RPD3* and genes encoding NuA4-specific subunits show reduced fitness, whereas a double deletion mutant of *RPD3* and *EPL1*, which is in both piccolo and NuA4, shows synthetic rescue (Lin et al. 2008). However, because deletion of *EPL1* disrupts both piccolo and NuA4, it is difficult to make a clear distinction between the two.

The composition of NuA4, piccolo, Rpd3L, and Rpd3S is evolutionarily conserved [reviewed in (Doyon and Côté 2004; Yang and Seto 2008)]. One particular class of proteins in both is the PHD finger-containing ING family of tumor suppressors. Yng2 is a yeast ING protein that is a subunit of both piccolo and NuA4 (Loewith et al. 2000), whereas Pho23 is another yeast ING protein that is a subunit of Rpd3L (Loewith

et al. 2001; Carrozza et al. 2005a). The precise functions of Yng2 and Pho23 in their

complexes are unknown, but analogous to the opposing activities between Esa1 and

Rpd3, Yng2 and Pho23 have opposite effects on p53-dependent transcriptional activation,

shown in an experiment where human p53 was expressed in yeast to drive transcription

(Nourani et al. 2003). This opposing effect on activity of a human protein in transcription

emphasizes the conserved nature underlying the partnership between the Esa1 and Rpd3

complexes reported here. In addition, the identification of H4K12 as a critical shared

acetylation target uncovers the importance of the dynamic acetylation and deacetylation

of a particular histone residue in the context of Esa1 and Rpd3L function.

Dynamic and reciprocal histone modifications are increasingly recognized as key

regulatory switches. This principle was highlighted in a recent study investigating histone

ubiquitination in metazoan development. Coordinate control of H2B ubiquitination in

Drosophila by the ubiquitin ligase dBRE1 and the ubiquitin protease Scrawny was found

to be essential for regulating gene silencing to promote cellular differentiation (Buszczak

et al. 2009). Our studies identify links between Esa1 and Rpd3L specifically in the

acetylation and deacetylation of H4K12. Further, they reveal a critical distinct

characteristic of the Rpd3L complex in relation to Esa1, and identify roles for specific

histone residues in promoting cell viability. Future functional dissection of Rpd3 and

Esa1 multiprotein complexes will deepen understanding of how such chromatin modifiers

control important and diverse cellular processes.

MATERIALS AND METHODS

Yeast strains and plasmids. All strains and plasmids are listed in Tables 3-2 and

3-3. Except where noted with specific allele designations, all mutations used are null

alleles constructed using standard molecular methods. The *rpd3::kanMX* (LPY12154),

hda1::kanMX (LPY13472), *hos1::kanMX* (LPY13706), and *hos2::kanMX* (LPY13583)

mutants were constructed using marker swap plasmids M3926, M3929, and M3925 as

described in (Voth et al. 2003) on *rpd3::LEU2* (DY1539) (Kasten et al. 1997),

hda1::TRP1 (DY4891), *hos1::HIS3* (DY6073), *hos2::TRP1* (DY4549) (all generous gifts

from D. Stillman) and then backcrossed prior to use. The *pho23Δ::kanMX* (LPY12732),

sds3Δ::kanMX (LPY12958), and *rco1Δ::kanMX* (LPY12645) mutants were constructed

by amplification (oligonucleotides listed in Table 3-4) of the *kanMX* cassettes from

Saccharomyces Genome Deletion Project strains, transformed into W303-1a (LPY5) and

backcrossed prior to use. All double and triple mutants and the silencing markers

rDNA*::ADE2-CAN1* (Fritze et al. 1997) and TELVR*::URA3* (Renauld et al. 1993) were

introduced through standard genetic crosses. Construction of the *RPD3* catalytic mutant

plasmid, *rpd3-H150A-H151A*, is described in (Ruault and Pillus 2006). Histone mutant

strains, derived from MSY1905 (a generous gift from M. M. Smith) (Ruault and Pillus

2006) are chromosomally deleted for both *HHF-HHT* loci, and initially contained wild-

type histones on the plasmid pJH33 (*CEN URA3 HTA1 HTB1 HHF2 HHT2*) (Ahn et al.

2005). For mutant construction, strains were transformed with a *TRP1* plasmid containing

the relevant H4 (*HHF2*) mutation, and then subjected to a plasmid shuffle by

counterselection on 5-FOA to remove pJH33. Histone mutant plasmids were constructed

by site-specific mutagenesis using oligonucleotides listed in Table 3-4. Histone mutant

strains with telomeric silencing reporter initially contained pLP2224 (*HHF2 HHT2 HIS3* CEN), and were transformed with *TRP1* plasmid carrying relevant H4 (*HHF2*) mutation. Loss of pLP2224 was screened on SC-His plates.

      Growth dilution assays and silencing assays. Unless otherwise noted, all dilution assays represent five-fold serial dilutions, starting from an A_{600} of 1.0 after growth to saturation in 3 ml of liquid synthetic complete (SC) medium. Growth and silencing plates were incubated at 30˚. Suppression of *esa1*'s growth defect on SC plates was assayed at the restrictive temperature of 35˚. The rDNA silencing assays were performed with strains containing the rDNA*::ADE2-CAN1* reporter as described (van Leeuwen and Gottschling 2002). Strains were grown in SC-Ade-Arg medium to saturation, normalized as above, and plated on SC-Ade-Arg (growth control) and SC-Ade-Arg plates containing 32 µg/ml of canavanine (to assay rDNA silencing). Telomeric silencing assays were performed with the TELVR*::URA3* reporter as described (Renauld et al. 1993; van Leeuwen and Gottschling 2002). Strains were grown in SC medium and plated on both SC (growth control) and SC with 0.1% 5-FOA (to assay telomeric silencing). Camptothecin (CPT) sensitivity was assayed using CPT dissolved in DMSO added to plates buffered with 100 mM potassium phosphate (pH 7.5) to maintain maximal drug activity (Nitiss and Wang 1988). Growth control plates contained equal concentrations of DMSO and phosphate buffer. All images were captured after 2-4 days of growth.

      Qualitative mating assays. *MAT*a strains were patched onto YPD, grown up overnight at 30˚ and replica plated onto a minimal medium plate spread with a lawn of

mating-type tester *MATα* (LPY78). Plates were grown at 30° for 2-3 days prior to data collection.

Protein immunoblots. Whole cell extracts were prepared from cells grown to A_{600} of 0.6-1.0 at 30°. In the temperature shift experiment, cells were grown first at 30° and then shifted to 34° for six hours. Extracts were prepared by bead-beating as described previously (Clarke et al. 1999). Briefly, cells were resuspended in phosphate buffered saline with protease inhibitors and lysed by vortexing with glass beads. Whole cell extracts were then denatured by boiling in sample loading buffer and separated from the insoluble pellet by centrifugation. Proteins were separated on 18% SDS-polyacrylamide gels and transferred to nitrocellulose (0.2 μm). Primary antisera used were anti-H4K5Ac (1:5000 dilution, Serotec), anti-H4K8Ac (1:2500 dilution, Serotec), anti-H4K12Ac (1:2500 dilution, Serotec), anti-H4K16Ac (1:2500 dilution, Upstate) and anti-H3 CT (1:10,000 dilution, Upstate). Goat anti-rabbit conjugated to horseradish peroxidase (Promega) was used as a secondary antibody, and signal was detected with Western Lightning® Chemiluminescence Reagent (Perkin Elmer) on Kodak™ X-Omat™ film.

Acknowledgements. David Stillman provided the original *hda1*, *hos1*, *hos2*, and *hos3* strains, and Mitch Smith provided the original histone mutant strain.

Chapter 3 is a reprint of Chang, C.S. and Pillus, L. 2009. Collaboration between the essential Esa1 acetyltransferase and the Rpd3 deacetylase is mediated by H4K12 histone acetylation in *Saccharomyces cerevisiae*. *Genetics* **183**(1):149-160. The paper was edited to be properly formatted for this chapter.

Table 3-1. Summary of Results: effects of second mutation on *esa1* mutant.

esa1 phenotype	*rpd3Δ*§	*rpd3-H150A-H151A*§	*sds3Δ*‡	*pho23Δ*‡	*rco1Δ*†
growth suppression (dependence on K12)	+ (yes)	+ (yes)	+ (yes)	+ (yes)	–
rDNA silencing (dependence on K12)	+ (no)	+ (no)	+ (no)	+	–
TEL silencing (dependence on K12)	+ (no)	+	+	+	–
CPT suppression	–		–	–	–/+
restore global H4Ac	+		–/+	–/+	–/+

+ indicates suppression of *esa1* phenotype
– indicates exacerbation of *esa1* phenotype
–/+ indicates no change
§ catalytic (Rpd3) subunit
‡ Rpd3L subunit
† Rpd3S subunit

Table 3-2. Yeast strains used in Chapter 3

Strain	Genotype	Reference
LPY5 (W303-1a)	*MAT*a *ade2-1 can1-100 his3-11,15 leu2-3,112 trp1-1 ura3-1*	Thomas and Rothstein 1989
LPY11	W303 *MAT*a *sir2::HIS3*	
LPY78	*MAT*α *his4*	P. Schatz
LPY4774	W303 *MAT*a *esa1-414*	
LPY4909	W303 *MAT*α rDNA*::ADE2-CAN1*	Clarke et al. 2006
LPY4911	W303 *MAT*α *esa1-414* rDNA*::ADE2-CAN1*	Clarke et al. 2006
LPY4917	W303 *MAT*α TELVR*::URA3*	Clarke et al. 2006
LPY4919	W303 *MAT*α *esa1-414* TELVR*::URA3*	Clarke et al. 2006
LPY11160	W303 *MAT*α *esa1-414 sir2::HIS3*	
LPY11816	W303 *MAT*α *hht1-hhf1Δ::kanMX hht2-hhf2Δ::kanMX hta2-htb2Δ::HPH* rDNA*::ADE2-CAN1* + pJH33	
LPY11817	W303 *MAT*α *esa1-414 hht1-hhf1Δ::kanMX hht2-hhf2Δ::kanMX hta2-htb2Δ::HPH* rDNA*::ADE2-CAN1* + pJH33	
LPY12071	LPY11817 + pLP2146 (no pJH33)	
LPY12093	W303 *MAT*α *rpd3::kanMX* TELVR*::URA3*	
LPY12145	W303 *MAT*α *rpd3::kanMX* rDNA*::ADE2-CAN1*	
LPY12147	W303 *MAT*α *esa1-414 rpd3::kanMX* rDNA*::ADE2-CAN1*	
LPY12154	W303 *MAT*a *rpd3::kanMX*	
LPY12156	W303 *MAT*a *esa1-414 rpd3::kanMX*	
LPY12160	W303 *MAT*a *esa1-L254P*	
LPY12164	W303 *MAT*a *esa1-L254P rpd3::kanMX*	
LPY12200	W303 *MAT*a + pLP796	
LPY12202	W303 *MAT*a *rpd3::kanMX* + pLP796	
LPY12204	W303 *MAT*a *esa1Δ::HIS3* + pLP796	
LPY12206	W303 *MAT*a *esa1Δ::HIS3 rpd3::kanMX* + pLP796	
LPY12211	W303 *MAT*α *esa1-414 rpd3::kanMX* TELVR*::URA3*	

Table 3-2. Yeast strains used in Chapter 3 (continued)

Strain	Genotype	Reference
LPY12228	W303 *MATα rpd3::kanMX hht1-hhf1Δ::kanMX hht2-hhf2Δ::kanMX hta2-htb2Δ::HPH* rDNA*::ADE2-CAN1* + pJH33	
LPY12230	W303 *MATα esa1-414 rpd3::kanMX hht1-hhf1Δ::kanMX hht2-hhf2Δ::kanMX hta2-htb2Δ::HPH* rDNA*::ADE2-CAN1* + pJH33	
LPY12236	W303 *MAT*a *esa1-414 rpd3::kanMX hht1-hhf1Δ::kanMX hht2-hhf2Δ::kanMX hta2-htb2Δ::HPH* + pJH33	
LPY12383	LPY11816 + pLP1775 (no pJH33)	
LPY12384	LPY11817 + pLP1775 (no pJH33)	
LPY12394	LPY11816 + pLP2146 (no pJH33)	
LPY12645	W303 *MAT*a *rco1Δ::kanMX*	
LPY12652	W303 *MAT*a *esa1-414 rco1Δ::kanMX*	
LPY12695	LPY12228 + pLP1775 (no pJH33)	
LPY12702	LPY12228 + pLP2146 (no pJH33)	
LPY12707	LPY12230 + pLP1775 (no pJH33)	
LPY12708	LPY12230 + pLP2181 (no pJH33)	
LPY12711	LPY12230 + pLP2145 (no pJH33)	
LPY12714	LPY12230 + pLP2146 (no pJH33)	
LPY12717	LPY12230 + pLP1990 (no pJH33)	
LPY12729	W303 *MAT*a *esa1-414 pho23Δ::kanMX*	
LPY12732	W303 *MAT*a *pho23Δ::kanMX*	
LPY12956	W303 *MAT*a *esa1-414 sds3Δ::kanMX*	
LPY12958	W303 *MAT*a *sds3Δ::kanMX*	
LPY13124	W303 *MATα esa1-414 sds3Δ::kanMX hht1-hhf1Δ::kanMX hht2-hhf2Δ::kanMX hta2-htb2Δ::HPH* rDNA*::ADE2-CAN1* + pJH33	
LPY13139	W303 *MAT*a *esa1-414 pho23Δ::kanMX hht1-hhf1Δ::kanMX hht2-hhf2Δ::kanMX hta2-htb2Δ::HPH* + pJH33	
LPY13183	W303 *MAT*a *esa1-414 sds3Δ::kanMX hht1-hhf1Δ::kanMX hht2-hhf2Δ::kanMX hta2-htb2Δ::HPH* + pJH33	
LPY13472	W303 *MAT*a *hda1::kanMX*	

Table 3-2. Yeast strains used in Chapter 3 (continued)

Strain	Genotype	Reference
LPY13478	W303 *MAT*a *esa1-414 hda1::kanMX*	
LPY13501	W303 *MAT*α *rco1Δ::KanMX* rDNA*::ADE2-CAN1*	
LPY13505	W303 *MAT*α *esa1-414 rco1Δ::kanMX* rDNA*::ADE2-CAN1*	
LPY13513	W303 *MAT*α *sds3Δ::kanMX* rDNA*::ADE2-CAN1*	
LPY13517	W303 *MAT*α *esa1-414 sds3Δ::kanMX* rDNA*::ADE2-CAN1*	
LPY13524	W303 *MAT*α *rco1Δ::kanMX* TELVR*::URA3*	
LPY13528	W303 *MAT*α *esa1-414 rco1Δ::kanMX* TELVR*::URA3*	
LPY13536	W303 *MAT*α *sds3Δ::kanMX* TELVR*::URA3*	
LPY13540	W303 *MAT*α *esa1-414 sds3Δ::kanMX* TELVR*::URA3*	
LPY13583	W303 *MAT*a *hos2::kanMX*	
LPY13585	W303 *MAT*a *esa1-414 hos2::kanMX*	
LPY13706	W303 *MAT*a *hos1::kanMX*	
LPY13712	W303 *MAT*a *esa1-414 hos1::kanMX*	
LPY13765	W303 *MAT*α *pho23Δ::kanMX* TELVR*::URA3*	
LPY13769	W303 *MAT*α *esa1-414 pho23Δ::kanMX* TELVR*::URA3*	
LPY13854	W303 *MAT*α *pho23Δ::kanMX* rDNA*::ADE2-CAN1*	
LPY13859	W303 *MAT*α *esa1-414 pho23Δ::kanMX* rDNA*::ADE2-CAN1*	
LPY13862	W303 *MAT*a *hat1Δ::kanMX*	
LPY13866	W303 *MAT*a *esa1-414 hat1Δ::kanMX*	
LPY13869	W303 *MAT*a *hat1Δ::kanMX rpd3::kanMX*	
LPY13871	W303 *MAT*a *esa1-414 hat1Δ::kanMX rpd3::kanMX*	
LPY14030	W303 *MAT*a *pho23Δ::kanMX rpd3::kanMX*	
LPY14034	W303 *MAT*a *esa1-414 pho23Δ::kanMX rpd3::kanMX*	
LPY14041	W303 *MAT*a *esa1-414 rpd3::kanMX sds3Δ::kanMX*	
LPY14050	W303 *MAT*a *rpd3::kanMX sds3Δ::kanMX*	
LPY14165	LPY13139 + pLP1775 (no pJH33)	
LPY14166	LPY13139 + pLP2181 (no pJH33)	
LPY14167	LPY13139 + pLP2145 (no pJH33)	
LPY14168	LPY13139 + pLP2146 (no pJH33)	
LPY14169	LPY13139 + pLP1990 (no pJH33)	

Table 3-2. Yeast strains used in Chapter 3 (continued)

Strain	Genotype	Reference
LPY14175	LPY13183 + pLP1775 (no pJH33)	
LPY14176	LPY13183 + pLP2181 (no pJH33)	
LPY14177	LPY13183 + pLP2145 (no pJH33)	
LPY14178	LPY13183 + pLP2146 (no pJH33)	
LPY14179	LPY13183 + pLP1990 (no pJH33)	
LPY14247	W303 *MAT*a *esa1-414 rpd3::kanMX hht1-hhf1Δ::kanMX hht2-hhf2Δ::kanMX hta2-htb2Δ::HPH* TELVR*::URA3* + pLP2224	
LPY14296	LPY13124 + pLP1775 (no pJH33)	
LPY14297	LPY13124 + pLP2181 (no pJH33)	
LPY14298	LPY13124 + pLP2145 (no pJH33)	
LPY14299	LPY13124 + pLP2146 (no pJH33)	
LPY14300	LPY13124 + pLP1990 (no pJH33)	
LPY14301	LPY14247 + pLP1775 (no pLP2224)	
LPY14302	LPY14247 + pLP2181 (no pLP2224)	
LPY14303	LPY14247 + pLP2145 (no pLP2224)	
LPY14304	LPY14247 + pLP2146 (no pLP2224)	
LPY14305	LPY14247 + pLP1990 (no pLP2224)	
LPY14356	LPY12156 + pLP60	
LPY14359	LPY12156 + pLP1945	
LPY14360	LPY12156 + pLP1946	
LPY14364	LPY12211 + pLP60	
LPY14365	LPY12211 + pLP1945	
LPY14366	LPY12211 + pLP1946	
LPY14659	LPY12147 + pLP60	
LPY14660	LPY12147 + pLP1945	
LPY14661	LPY12147 + pLP1946	
LPY14675	LPY12236 + pLP1775 + pLP1946 (no pJH33)	
LPY14676	LPY12236 + pLP2181 + pLP1946 (no pJH33)	
LPY14677	LPY12236 + pLP2145 + pLP1946 (no pJH33)	
LPY14678	LPY12236 + pLP2146 + pLP1946 (no pJH33)	
LPY14679	LPY12236 + pLP1990 + pLP1946 (no pJH33)	

Table 3-2. Yeast strains used in Chapter 3 (continued)

Strain	Genotype	Reference
LPY14685	LPY12707 + pLP1946	
LPY14686	LPY12708 + pLP1946	
LPY14687	LPY12711 + pLP1946	
LPY14688	LPY12714 + pLP1946	
LPY14689	LPY12717 + pLP1946	

Unless otherwise noted, strains were constructed during the course of this study or are part of the standard lab collection.

Table 3-3. Plasmids used in Chapter 3

Plasmid (alias)	Description	Source/Reference
pJH33	*HTA1 HTB1 HHF2 HHT2 URA3* CEN	Ahn et al. 2005
pLP1775	*HHF2 HHT2 TRP1* CEN	S. L. Berger
pLP2181	*hhf2-K5A HHT2 TRP1* CEN	
pLP2145	*hhf2-K8A HHT2 TRP1* CEN	
pLP2146	*hhf2-K12A HHT2 TRP1* CEN	
pLP1990	*hhf2-K16A HHT2 TRP1* CEN	
pLP2224	*HHF2 HHT2 HIS3* CEN	
pLP796	*ESA1 URA3* 2μ	Clarke et al. 2006
pRS313 (pLP60)	vector *HIS3* CEN	Sikorski and Hieter 1989
pLP1945	*RPD3*-13myc *HIS3* CEN	Ruault and Pillus 2006
pLP1946	*rpd3-H150A-H151A*-13myc *HIS3* CEN	Ruault and Pillus 2006

Unless otherwise noted, plasmids were constructed during the course of this study or are part of the standard lab collection.

Table 3-4. Oligonucleotide sequences used in Chapter 3

Oligo #	Name	Sequence (5'-3')
921	H4K5A sense	TCCGGTAGAGGT**GC**AGGTGGTAAAGG
922	H4K5A antisense	CCTTTACCACCT**GC**ACCTCTACCGGA
898	H4K8A sense	GTAAAGGTGGT**GC**AGGTCTAGGAAAAGG
899	H4K8A antisense	CCTTTTCCTAGACCT**GC**ACCACCTTTAC
900	H4K12A sense	AAGGTCTAGGA**GC**AGGTGGTGCCAAGC
901	H4K12A antisense	GCTTGGCACCACCT**GC**TCCTAGACCTT
788	H4K16A sense	GGAAAAGGTGGTGCC**GC**GCGTCACAGAAAG ATT
789	H4K16A antisense	AATCTTTCTGTGACGC**GC**GGCACCACCTTTT CC
950	*PHO23* KO forward	CTTCGCCCAGCACATTGTCC
951	*PHO23* KO reverse	CGGCGATTAGACTGAGCTGC
974	*SDS3* KO forward	CACTCAAGCGATGATCGTTTCG
975	*SDS3* KO reverse	CTACAGTGGCATTAGTTGCAGC
956	*RCO1* KO forward	GCCAATCTGGCTTCCCTAATAGC
957	*RCO1* KO reverse	GGCAACATTCAGCATATCCAGG
1086	*HAT1* KO forward	GCGACCATTTCATCAAGAGC
1087	*HAT1* KO reverse	GCTACCATGGTGTGTCACTT
882	*kanMX* forward	ATTACGGCTCCTCGCTGCAG
883	*kanMX* reverse	CAGCCATTACGCTCGTCATC
1142	*LEU2* reverse	AATCTGGAGCAGAACCGTGG
236	*kanMX* forward	GATGACGAGCGTAATGGCTG

Nucleotides in **bold underline** in the above sequences are mutagenic, compared to the wild-type sequence. For all the knockout pairs, PCR was performed on genomic DNA isolated from haploid deletion strains dissected from the heterozygous diploid collection from the *Saccharomyces* Genome Deletion Project.

Chapter 4.

Identification of a functional interaction between the histone deacetylase Hos2 and the histone acetyltransferase Esa1 in response to DNA damage

INTRODUCTION

The essential histone acetyltransferase Esa1 functions in many nuclear processes. In addition to being required for viability, Esa1 participates in transcriptional silencing and activation, cell cycle progression, and the repair of DNA damage [reviewed in (Lafon et al. 2007)]. Chapter 3 described the identification of the histone deacetylase Rpd3, and its functions with Esa1 in contributing to cell viability. It was discovered that acetylation by Esa1 and deacetylation by Rpd3 of a specific lysine, K12 in histone H4 (H4K12), was critical for growth. One conclusion from Chapter 3 was that Rpd3 likely does not collaborate with Esa1 to repair damage-induced double-strand breaks, since deletion of *RPD3* did not rescue *esa1*'s sensitivity to the DNA damaging agent camptothecin (Figure 3-7). This chapter describes how Hos2, an Rpd3-related histone deacetylase, was identified as a potential partner to Esa1 in response to DNA damage.

Many chromatin modifying enzymes are thought to influence the repair of DNA damage. Their roles can either be the direct modification of histones at DNA breaks or through regulation of the transcriptional response to DNA damage. There is evidence for several HATs and HDACs in both of these categories. For example, Esa1 and members of NuA4 localize to double-strand breaks during both homologous recombination and non-homologous end joining repair (Bird et al. 2002; Downs et al. 2004; Tamburini and Tyler 2005). Many other chromatin modifiers have been localized to double-strand

breaks, including the histone acetyltransferase Gcn5, and the deacetylases Rpd3, Sir2, and Hst1 (Tamburini and Tyler 2005). Also, Rpd3, Hos2, and Esa1 each contribute to transcriptional activation of the damage-inducible genes *HUG1* and *RNR3* (Sharma et al. 2007).

In *S. cerevisiae*, the five members of the class I/II HDAC family are Hda1, Rpd3, Hos1, Hos2, and Hos3 (Rundlett et al. 1996). The remaining HDACs in yeast are part of the conserved family of class III NAD$^+$-dependent HDACs (Brachmann et al. 1995; Blander and Guarente 2004). All five yeast class I/II HDACs share extensive homology in many regions (Figure 4-1). For example, Hos2 shares 48% identity and 73% similarity to Rpd3 (*Saccharomyces* Genome Database, WU-BLAST). Like Rpd3, Hos2 is a class I HDAC and belongs to the same family of deacetylases as human HDAC1, 2, 3, and 8. Hos2 was initially identified by sequence homology to Rpd3 and Hda1 (Rundlett et al. 1996). It was subsequently found in specific chromatographic fractions of purified yeast proteins that displayed histone deacetylase activity (Suka et al. 1998).

Specific lysine targets of Hos2 have not been well characterized. Neither *in vitro* histone deacetylase assays nor *in vivo* studies to evaluate increases in bulk histone acetylation levels have been performed to identify preferential activity of Hos2 toward specific lysines residues on any of the histones. When examined at candidate genes by chromatin immunoprecipitation, Hos2 was reported to deacetylate multiple lysine residues on histones H3 and H4 with no noticeable preference to the different lysine residues (Wang et al. 2002). This is in contrast to deacetylases such as Rpd3, which primarily deacetylates H4K5 and H4K12 (Rundlett et al. 1996).

Figure 4-1. Molecular cartoon depicting regions of homology between the five class I and II histone deacetylases in *S. cerevisiae.* Schematic alignment of Rpd3, Hos2, Hda1, Hos1, and Hos3. Solid boxes show regions of highest conservation. Dashed lines represent gaps in alignment. Modified from (Suka et al. 1998).

Class I and II histone deacetylases in *S. cerevisiae*
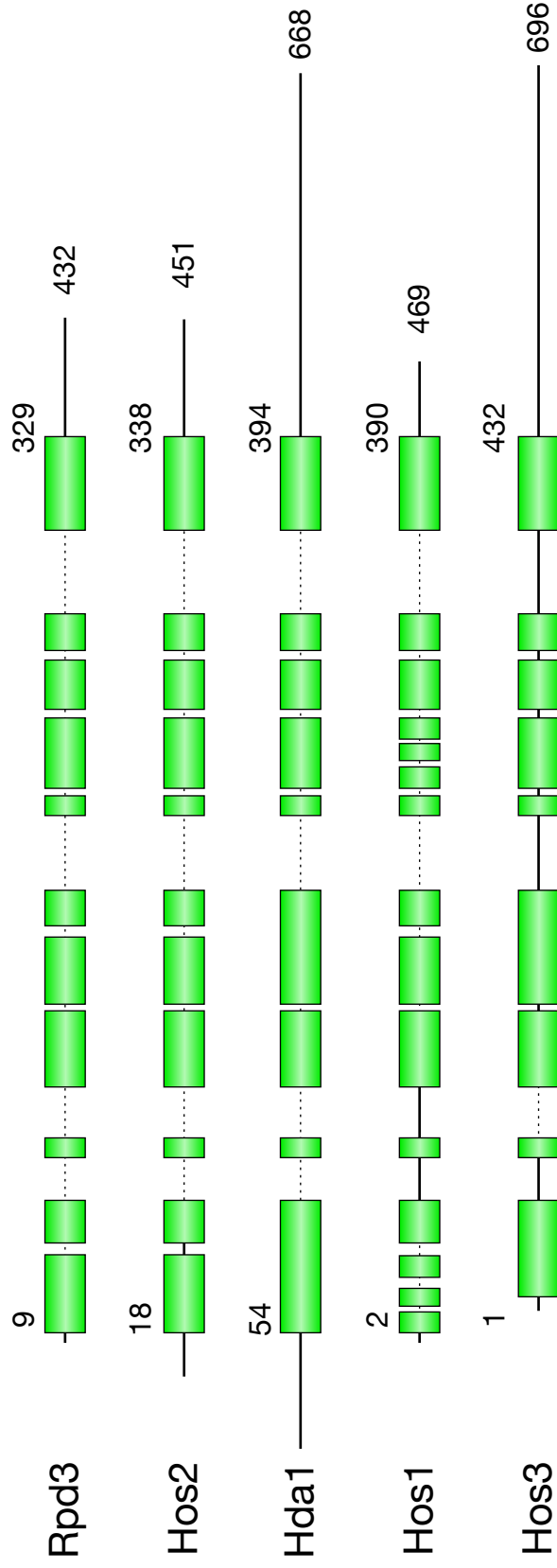
Similar to Rpd3, Hos2 has been found to function both in transcriptional activation and repression of genes. A genome-wide survey of Hos2 localization by chromatin immunoprecipitation found Hos2 binding to correlate with RNA polymerase II binding, indicating that Hos2 is present at the coding regions of actively transcribed genes (Wang et al. 2002). This study also defined Hos2 as an important transcriptional activator of the normally repressed *GAL* genes and *INO1*, under growth conditions that induce their transcription (Wang et al. 2002). Another genome-wide survey of Hos2 function identified regions of increased acetylation in the coding regions of several ribosomal protein genes in a *hos2Δ* strain, implying that Hos2 deacetylates histones at these highly transcribed genes (Robyr et al. 2002). However, it has not yet been established if deacetylation at these loci promotes transcriptional activation or repression.

Hos2's role in transcriptional repression was discovered through its identification as a subunit of the Set3 complex (Set3C) (Pijnappel et al. 2001). Set3C is named after its founding subunit, Set3, which contains a SET domain and a PHD domain. Both domains are conserved motifs found in many proteins involved in chromatin regulation and transcription. Set3C contains two deacetylases, Hos2 and the class III NAD^+-dependent deacetylase Hst1. Whereas Hst1 is present in two different complexes, Hos2 has, to date, been found only in Set3C. Hos2, as part of Set3C, represses mid-sporulation genes during the early transcriptional changes that occur to trigger sporulation, although it does not affect transcription of these genes during vegetative growth (Pijnappel et al. 2001). Set3C has also been shown to play a role in the secretory stress response through the Mpk1 MAP kinase cascade (Cohen et al. 2008). However, the direct involvement of Hos2 at sporulation and stress response genes is unclear.

In the ongoing analysis reported here, deletion of *HOS2* is shown to rescue *esa1*'s sensitivity to the DNA damaging agents camptothecin and hydroxyurea. This suppression is observed for several *esa1* conditional alleles, although deletion of *HOS2* has distinct allele-specific affects on the growth of different *esa1* mutants.

RESULTS

Deletion of *HOS2* suppresses *esa1*'s sensitivity to DNA damaging agents camptothecin and hydroxyurea. In evaluating the specificity of the interaction between the acetyltransferase Esa1 and the deacetylase Rpd3 (Chapter 3), a number of other histone deacetylase mutants were tested to determine if they could suppress *esa1-414*'s temperature-sensitivity (Figure 3-1). None except deletion of *RPD3* could suppress the *esa1* growth defect at elevated temperature. When tested for growth on the DNA damaging agent camptothecin, these deacetylase mutants revealed a number of different phenotypes. First, deletion of *HOS1* or *HDA1* resulted in a moderate sensitivity to camptothecin (Figure 4-2), indicating that Hos1 and Hda1 may function in the DNA damage response. At the same time, deletion of *HOS1* or *HDA1* in combination with *esa1* did not create any difference in camptothecin sensitivity of the *esa1* mutant (Figure 4-2). However, deletion of only one of these HDACs, *HOS2*, suppressed *esa1-414*'s sensitivity to the DNA damaging agent camptothecin (Figure 4-2). Suppression of *esa1-414*'s DNA damage was not observed with deletion of *RPD3* (Figure 3-7), suggesting that different HDACs and their complexes partner with Esa1 to mediate its diverse functions.

Camptothecin causes DNA damage by inhibition of topoisomerase I, which results in the accumulation of double-strand breaks that lead to cell death if not efficiently

125

Figure 4-2. Deletion of *HOS2*, but not *HOS1* or *HDA1*, suppresses *esa1-414*'s sensitivity to the DNA damage drug camptothecin. Serial dilutions of WT (LPY5), *esa1-414* (LPY4774), *esa1-414 hos1* (LPY13712), *esa1-414 hos2* (LPY13585), *esa1-414 hda1* (LPY13472), *hos1* (LPY13706), *hos2* (LPY13583), and *hda1* (LPY13472) were tested for growth on plates containing DMSO (control) and 20 μg/ml camptothecin at 30˚.

control   DNA damage

WT
esa1-414
esa1-414 hos1
esa1-414 hos2
esa1-414 hda1
hos1
hos2
hda1

DMSO   camptothecin
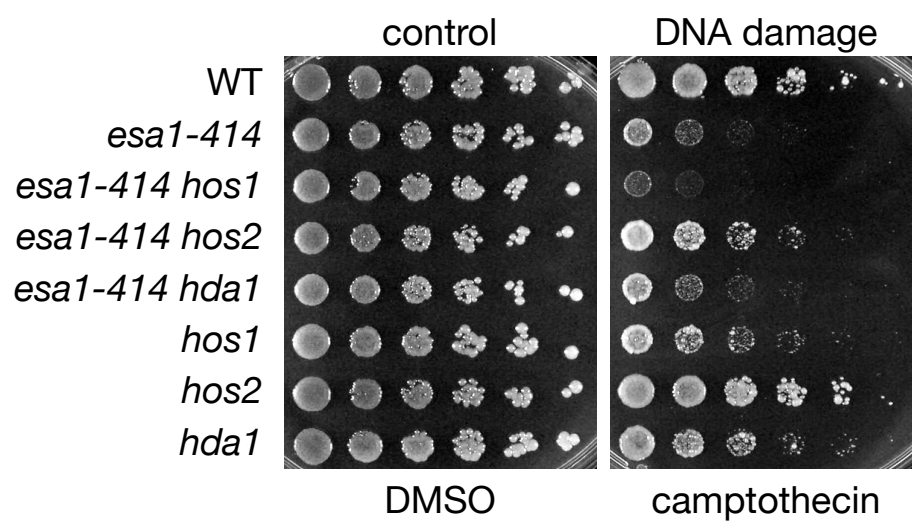
repaired (Hsiang et al. 1985). Hydroxyurea inhibits the biosynthetic enzyme

ribonucleotide reductase, which in turn depletes dNTP pools (Hampsey 1997).

Hydroxyurea creates DNA damage in cells by stalling replication forks, thereby allowing

replication-induced errors to accumulate. If not repaired, these too can lead to cell death

(Davies et al. 2009). Whereas camptothecin works through a more direct mechanism to

induce damage, hydroxyurea involves more of a cellular stress response. To determine if

HOS2 deletion suppressed multiple forms of DNA damage in an *esa1-414* mutant, *esa1-414 hos2* double mutants were tested for suppression in response to hydroxyurea. The

esa1-414 hos2 double mutant displayed improved growth on hydroxyurea compared to

esa1-414 alone (Figure 4-3), indicating that *hos2* may function as a general suppressor of

esa1-414 in DNA damage.

Deletion of *HOS2* creates a synthetic sick phenotype in integrated *esa1*

mutants. As reported in Chapter 3, deletion of *HOS2* in an *esa1-414* mutant exacerbated

the temperature-sensitive phenotype of *esa1-414* (Figure 3-1, Figure 4-4A). However, a

genome-wide survey of HAT and HDAC interactions found *HOS2* deletion to have an

opposite, suppressive effect on the growth of a distinct *esa1* mutant allele (Lin et al.

2008). The two major differences between the strains used in our studies and Lin et al.

are different strain backgrounds and *esa1* mutant alleles. Our strains are in the W303

background (Thomas and Rothstein 1989) and theirs are in BY4741 (Brachmann et al.

1998). Nucleotide variation between these two genetic backgrounds has been reported

(Winzeler et al. 2003; Schacherer et al. 2007), and may be the cause of the differences in

results. In addition, the specific *esa1* allele used in Lin et al., was a plasmid-borne allele

Figure 4-3. Deletion of the histone deacetylase gene *HOS2* suppresses DNA damage phenotypes of *esa1-414*. A) Deletion of *HOS2* suppressed *esa1-414*'s sensitivity to camptothecin. Serial dilutions of WT (LPY5), *esa1-414* (LPY4774), *esa1-414 hos2* (LPY13585), and *hos2* (LPY13583) strains were tested for growth on plates containing DMSO (control) and 20 μg/ml camptothecin at 30˚. B) Deletion of *HOS2* suppressed *esa1-414*'s sensitivity to hydroxyurea. Serial dilutions of the same strains as in A) were tested for growth on YPD plates at 30˚ with and without 100 mM hydroxyurea.

A
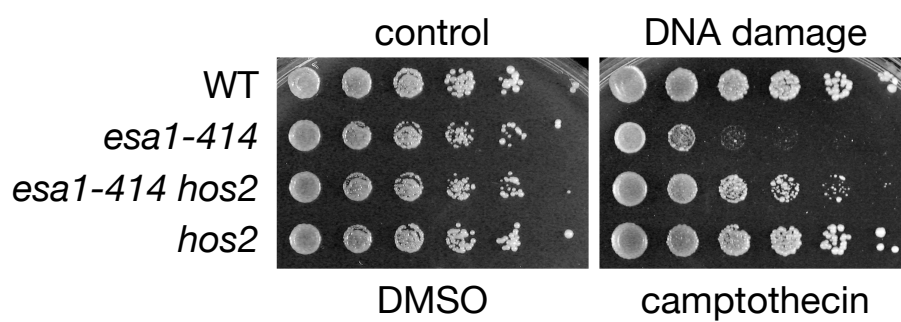
B
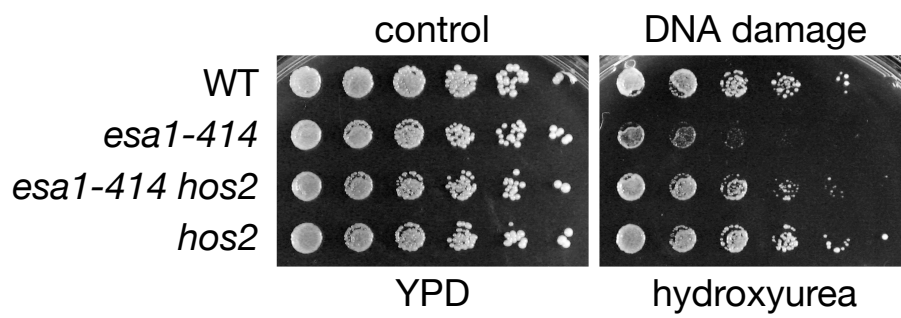
Figure 4-4. Deletion of *HOS2* exacerbates temperature-sensitivity of integrated *esa1-L254P* and *esa1-414*. A) Deletion of *HOS2* worsens the growth defect of *esa1-414* at non-permissive temperature. Serial dilutions of WT (LPY5), *esa1-414* (LPY4774), *esa1-414 hos2* (LPY13585), and *hos2* (LPY13583) were plated at permissive (30˚) and elevated (35˚) temperatures to assay growth. B) Deletion of *HOS2* worsens the growth defect of *esa1-L254P* at non-permissive temperature. Serial dilutions of WT (LPY5), *esa1-L254P* (LPY12160), *esa1-L254P hos2* (LPY14604), and *hos2* (LPY13583) were plated at permissive (30˚) and elevated (35˚) temperatures to assay growth.
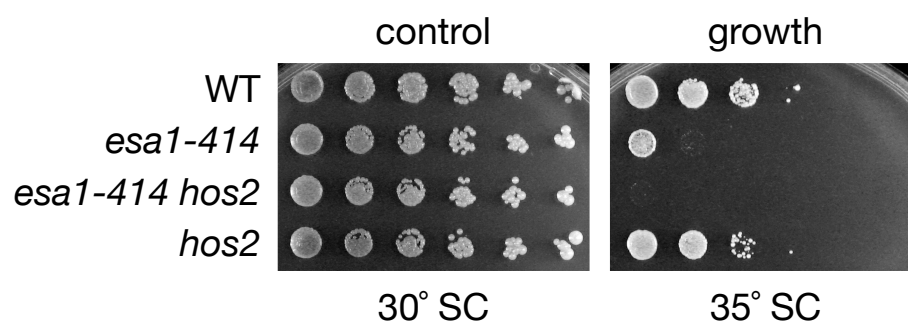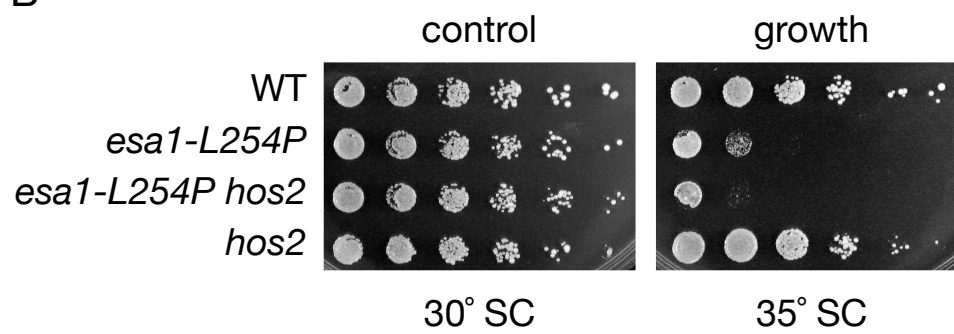
that contains substitutions at amino acid L254P and L346F. The data presented in Figures 4-2 and 4-3 are of integrated *esa1-414* mutant alleles at the chromosomal *ESA1* position.

To elucidate the differences in growth of the various *esa1 hos2* double mutants, *esa1-L254P hos2* (W303) integrated double mutants were tested for growth at elevated temperature. Since the *esa1-531* allele is a compound mutation of L254P and L346F, using the single L254P point mutant might separate the effects of the two mutations in *esa1-531* (see Figure 4-5 for map of *esa1* alleles). The *esa1-L254P hos2* double mutants grew more poorly compared to *esa1-L254P* (Figure 4-4B), similar to our previously reported results with *esa1-414 hos2*. Therefore, the suppressive effects of *hos2* on *esa1-531* do not appear to be due to the L254P substitution in Esa1. Actually, the growth suppression reported in the *esa1-531 hos2* double mutant (Lin et al. 2008) results from the use of plasmid-borne *esa1* alleles and is addressed in the following section.

Deletion of *HOS2* suppresses the growth defect of multiple *esa1* plasmid-borne mutant alleles. To compare directly the effect of *HOS2* deletion on the three different *esa1* alleles, *esa1Δ* and *esa1Δ hos2* strains were constructed carrying one of each of the three *esa1* mutants (*esa1-414*, *esa1-L254P*, and *esa1-531*) on a low-copy centromeric (CEN) plasmid. These strains were then assayed for growth at elevated temperature to test for suppression of *esa1* temperature-sensitivity. In this case, the *HOS2* deletion suppressed the growth defect of all three *esa1* mutant alleles (Figure 4-6) including *esa1-414* and *esa1-L254P*, in contrast to our previous results using the integrated version of these alleles (Figure 4-4). Thus, it appears that *hos2*'s differential effect on *esa1* growth is due to differences between integrated and plasmid-borne mutant alleles of *esa1*. This is likely due to gene dosage effects caused by using centromeric

Figure 4-5. Esa1 map with mutant alleles. Cartoon depicting location of *esa1* mutant

alleles. The *esa1-414* allele is a single nucleotide delete at amino acid position 414 that

causes a frameshift mutation and introduces an early stop codon. This results in six amino

acid substitutions and an early truncation lacking the last 22 amino acids of Esa1.

Mutated amino acids are shown in red. The *esa1-L254P* allele is a single point mutation

at L254P. The *esa1-531* allele is a compound allele resulting in substitutions of L254P

and L346F. These are shown on the map relative to the chromodomain (in gray) and the

conserved MYST domain (in purple).

135
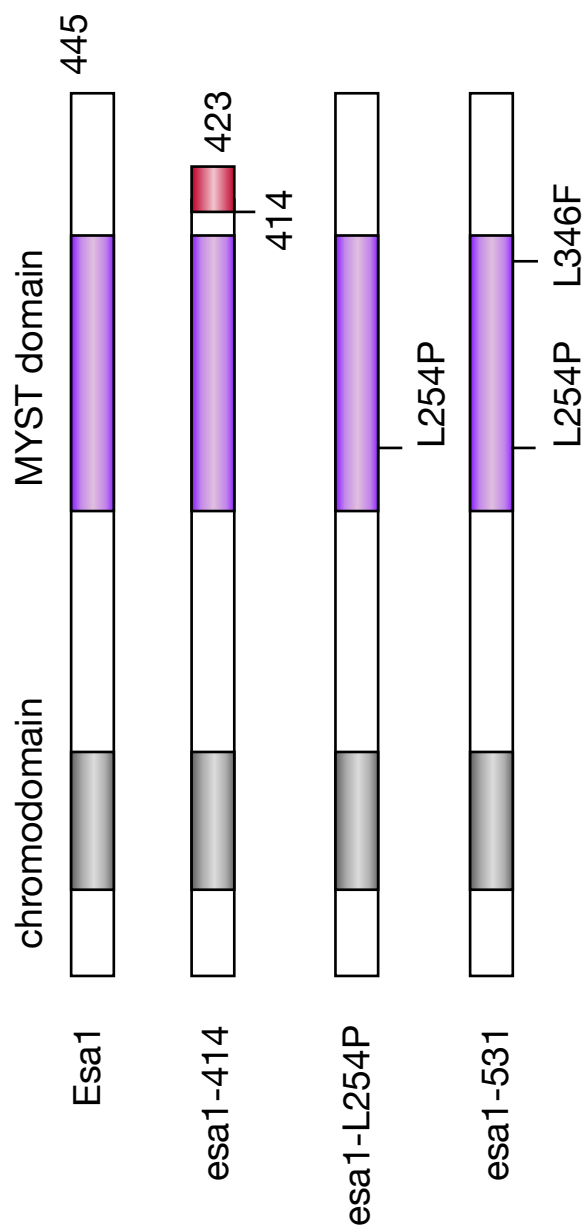
Figure 4-6. Deletion of *HOS2* suppresses the temperature-sensitivity of *esa1* mutant alleles when expressed on plasmids. A) Serial dilutions of *esa1Δ* (LPY14988) and *esa1Δ hos2* (LPY14989) strains carrying one of three different *esa1* mutant alleles on *TRP1* centromeric plasmids were assayed on YPD for growth at permissive (30˚) and non-permissive (33˚) temperature. The three different alleles are *esa1-414* (pLP863), *esa1-L254P* (pLP780), and *esa1-531* (pLP2374). B) same as in A) except strains were plated on SC-Trp.

136

A

strain	plasmid	control	growth
esa1Δ	*esa1-414*		
esa1Δ hos2Δ	*esa1-414*		
esa1Δ	*esa1-L254P*		
esa1Δ hos2Δ	*esa1-L254P*		
esa1Δ	*esa1-531*		
esa1Δ hos2Δ	*esa1-531*		
esa1Δ hos2Δ	*esa1-531*		
esa1Δ hos2Δ	*esa1-L254P*		

30° YPD   33° YPD

B

strain	plasmid	control	growth
esa1Δ	*esa1-414*		
esa1Δ hos2Δ	*esa1-414*		
esa1Δ	*esa1-L254P*		
esa1Δ hos2Δ	*esa1-L254P*		
esa1Δ	*esa1-531*		
esa1Δ hos2Δ	*esa1-531*		
esa1Δ hos2Δ	*esa1-531*		
esa1Δ hos2Δ	*esa1-L254P*		

30° SC-Trp   33° SC-Trp

plasmids for the *esa1* alleles. Although these plasmids should limit *esa1* to be expressed at a single copy, variations in copy number can exist and some cells may be expressing up to three or five copies (Futcher and Carbon 1986).

Deletion of *HOS2* suppresses DNA damage phenotypes of multiple *esa1* plasmid-borne mutant alleles. To determine whether deletion of *HOS2* promotes general or allele-specific suppression of *esa1* in response to DNA damage, three *esa1* mutants (*esa1-414, esa1-L254P,* and *esa1-531*), each on a centromeric plasmid, in combination with *hos2*Δ were directly compared for response to DNA damaging agents. The *esa1 hos2* double mutants were all more resistant than their corresponding *esa1* single mutants to camptothecin and hydroxyurea (Figure 4-7), confirming that deletion of *HOS2* acts as a general suppressor of *esa1* in response to DNA damage.

DISCUSSION

This chapter reports the finding that deletion of the histone deacetylase gene *HOS2* specifically suppresses the sensitivity of *esa1* mutants to two types of induced DNA damage. The suppression is observed with multiple alleles of *esa1* that have a reported loss of either *in vitro* or *in vivo* acetyltransferase activity. Thus, *hos2* appears to be a general suppressor of *esa1*'s defective response to DNA damage (summarized in Table 4-1) (Figure 4-8). Further investigation will establish a clearer molecular understanding of the functional interactions between *HOS2* and *ESA1*.

For example, to understand the mechanism of the suppression, it would be useful to construct an integrated *esa1-531* (L254P, L346F) allele, as well as the *esa1-L346F* single point mutant. These should then be individually tested for DNA damage

138

Figure 4-7. Deletion of *HOS2* suppresses DNA damage phenotypes of different plasmid-borne *esa1* mutant alleles. A) The *esa1Δ* and *esa1 hos2Δ* mutants carrying either *esa1-414, esa1-L254P*, or *esa1-531* on *TRP1* centromeric plasmids (same strains as in Figure 4-6) were tested for growth on plates containing DMSO (control) and 20 μg/ml camptothecin at 30˚. B) same as in A) except strains were plated on YPD and 100 mM hydroxyurea.

A

strain	plasmid	control	DNA damage
esa1Δ	esa1-414		
esa1Δ hos2Δ	esa1-414		
esa1Δ	esa1-L254P		
esa1Δ hos2Δ	esa1-L254P		
esa1Δ	esa1-531		
esa1Δ hos2Δ	esa1-531		
esa1Δ hos2Δ	esa1-531		
esa1Δ hos2Δ	esa1-L254P		
		DMSO	camptothecin

B

strain	plasmid	control	DNA damage
esa1Δ	esa1-414		
esa1Δ hos2Δ	esa1-414		
esa1Δ	esa1-L254P		
esa1Δ hos2Δ	esa1-L254P		
esa1Δ	esa1-531		
esa1Δ hos2Δ	esa1-531		
esa1Δ hos2Δ	esa1-531		
esa1Δ hos2Δ	esa1-L254P		
		YPD	hydroxyurea

Figure 4-8. Esa1 partners with the histone deacetylase Hos2 in response to DNA damage. A) Esa1 and Hos2 control histone acetylation and deacetylation at sites of DNA damage. B) Esa1 and Hos2 control histone acetylation and deacetylation for regulation of a transcriptional response at DNA damage-inducible genes.

at sites of DNA damage

transcriptional response
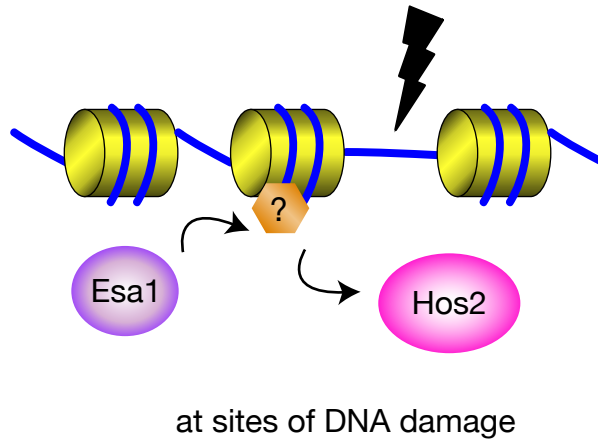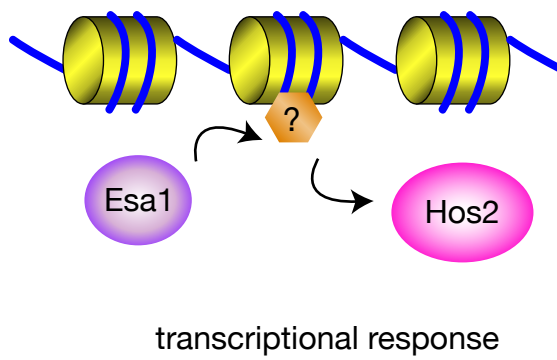
phenotypes and for the ability of *hos2* to suppress the phenotypes. Another important experiment will be to test if suppression by *hos2* is dependent on its histone deacetylase activity. Two histidines (H195, H196) in a conserved region of Hos2 have been identified by homology to Rpd3 as critical residues for catalysis (Wang et al. 2002), and these could be mutated to create a catalytically inactive *hos2* mutant to test suppression of *esa1*'s sensitivity to camptothecin and hydroxyurea. Furthermore, the specificity of the suppression between *esa1* and *hos2* has not yet been tested. Mutants of *GCN5*, a gene that encodes another yeast HAT, have also been reported to display sensitivity to campothecin (Choy and Kron 2002). Therefore, it will be interesting to test if suppression by deletion of *HOS2* applies to multiple HATs or is specific to Esa1's role in response to DNA damage.

To define the mechanism of *hos2* suppression of *esa1* in DNA damage, there are several other aspects to consider. In Chapter 3, H4K12 was identified as a critical residue for the growth suppression observed in the *esa1 rpd3* double mutant (Figure 3-11). Specifically, suppression was not observed only when H4K12 was mutated to an unacetylatable alanine. This same approach should be used to determine if acetylation and deacetylation of a single histone lysine residue is responsible for the suppression of DNA damage phenotypes observed in *esa1 hos2*. To do this, a collection of histone point mutants comprised of lysine to alanine substitutions (described in detail in Appendix B) will be used. Single lysine point mutants in combination with *esa1 hos2* will be tested to examine if they compromise the *hos2* rescue of *esa1*'s sensitivity to camptothecin or hydroxyurea. For example, if deletion of *HOS2* no longer suppresses *esa1*'s sensitivity to DNA damaging agents when H4K8 is mutated to an alanine, this would suggest a

specific role for acetylation and deacetylation of H4K8 in relation to Esa1, Hos2, and response to DNA damage. It is possible that the sensitivities to camptothecin and hydroxyurea will depend on different lysine residues. This may suggest the interesting possibility that Esa1's response to the two different drugs is mediated through different mechanisms. It is also possible that no single lysine residue will be responsible, but rather that a combination of multiple lysines, and that general acetylation of H4, but not acetylation of specific residues, is the key role for Esa1 in response to DNA damage.

As mentioned before, histone deacetylation may serve multiple functions in responses to DNA damage. It might be that Hos2-mediated deacetylation is required for transcriptional control of genes important for DNA repair (Figure 4-8B), or that Hos2 histone deacetylation at the double-strand breaks serves as a signal for repair enzymes (Figure 4-8A). Esa1 and Hos2 both contribute to activation of the damage-inducible genes *HUG1* and *RNR3* (Sharma et al. 2007). Therefore, it will be important to examine the transcriptional status of these genes in the *esa1 hos2* double mutant in response to camptothecin and hydroxyurea to determine if the suppression is mediated through this transcriptional program. In addition, analysis of checkpoint proteins that are hallmarks of DNA damage in *esa1 hos2* would define Esa1's role with Hos2 in ensuring a cellular response to damage.

It is possible that Hos2 participates with Esa1 to control the histone acetylation status directly at sites of double-strand breaks for repair. Esa1 has been shown to bind at break sites followed by a local increase in H4 acetylation (Downs et al. 2004; Tamburini and Tyler 2005), but it is not known if Hos2 is also recruited to double-strand break sites.

Hos2 localization can be tested by chromatin immunoprecipitation at specific sites of double-strand breaks.

Finally, although *esa1* mutants in combination with *rpd3* do not suppress reported *rpd3* phenotypes (Figure 3-8), it is possible that *esa1* may suppress *hos2* mutant phenotypes, uncovering new cellular roles for Esa1. Deletion of *HOS2* causes sensitivity to a number of different drugs that can be tested. Some of these include brefeldin A (Muren et al. 2001), which affects intracellular transport, the secretory stress drug tunicamycin (Cohen et al. 2008), and the DNA damaging agent MMS (Hanway et al. 2002). If these *hos2* phenotypes are suppressed in *esa1 hos2* double mutants, it will provide further evidence of Esa1 and Hos2 functioning together in a broader context, not just in response to DNA damage.

MATERIALS AND METHODS

Yeast strains and plasmids. Strains and plasmids used in this study are listed in Tables 4-2 and 4-3. The construction of *esa1*, *hda1*, *hos1*, and *hos2* single mutants is described in Chapter 3. All double mutants were introduced through standard genetic crosses. The strains in Figure 4-4 and 4-5 using *esa1* mutant alleles on centromeric *TRP1* plasmids were made by transforming the relevant *esa1*/*TRP1* plasmid into *esa1*Δ strains carrying an *ESA1*/*URA3* covering plasmid followed by counterselection on 5-FOA (0.1%). The pLP2374 (*esa1-531*/*TRP1*/CEN) was constructed by subcloning from pLP2354 (*esa1-531/URA3*/CEN) (Lin et al. 2008) into pLP863 with restriction enzymes NcoI and NdeI to release a 750 bp fragment from pLP2354 and a 6.2 kb fragment from

pLP863 used for ligation. Plasmids with correct *esa1-531* mutations were verified with DNA sequencing using oLP910 (5' CATAGCTTACCAGGCAAAGC 3').

Dilution assays for growth and drug sensitivity. Dilution assays represent five-fold serial dilutions, starting from an A_{600} of 1.0 after growth to saturation in a 3 ml liquid culture. Plates were incubated at 30˚ unless otherwise noted, and images were captured after 2-4 days of growth. Camptothecin (CPT) sensitivity was assayed using CPT dissolved in DMSO added to plates buffered with 100 mM potassium phosphate (pH7.5) for maximal drug activity (Nitiss and Wang 1988). Growth control plates contained equal concentrations of DMSO and phosphate buffer as CPT plates. Hydroxyurea sensitivity was assayed on YPD plates with 100 mM hydroxyurea.

Table 4-1. Effect of *HOS2* deletion on phenotypes of different *esa1* mutants

A) Effect of *HOS2* deletion on phenotypes of different *esa1* mutants (integrated alleles)

	esa1-414 hos2	*esa1-L254P hos2*	*esa1-531 hos2*
DNA damage	+	?	?
growth	–	–	?

B) Effect of *HOS2* deletion on phenotypes of different *esa1* mutants (plasmid-borne alleles)

	esa1-414 hos2	*esa1-L254P hos2*	*esa1-531 hos2*
DNA damage	+	+	+
growth	+	+	+

\+ indicates suppression of *esa1* defect
– indicates exacerbation of *esa1* defect
? indicates defect not yet tested

Suppression of DNA damage was assayed as growth on camptothecin and hydroxyurea.

Table 4-2. Yeast strains used in Chapter 4

Strain	Genotype	Source/ Reference
LPY5 (W303-1a)	*MAT*a *ade2-1 can1-100 his3-11,15 leu2-3,112 trp1-1 ura3-1*	Thomas and Rothstein 1989
LPY4774	W303 *MAT*a *esa1-414*	
LPY12160	W303 *MAT*a *esa1-L254P*	
LPY13472	W303 *MAT*a *hda1::kanMX*	
LPY13478	W303 *MAT*a *esa1-414 hda1::kanMX*	
LPY13583	W303 *MAT*a *hos2::kanMX*	
LPY13585	W303 *MAT*a *esa1-414 hos2::kanMX*	
LPY13706	W303 *MAT*a *hos1::kanMX*	
LPY13712	W303 *MAT*a *esa1-414 hos1::kanMX*	
LPY14604	W303 *MAT*a *esa1-L254P hos2::kanMX*	
LPY14988	W303 *MAT*a *esa1Δ::HIS3* + pLP796	
LPY14989	W303 *MAT*a *esa1Δ::HIS3 hos2::kanMX* + pLP796	

Unless otherwise noted, strains were constructed during the course of this study or are part of the standard lab collection.

Table 4-3. Plasmids used in Chapter 4

Plasmid	Description	Source/Reference
pLP863	*esa1-414 TRP1* CEN	A. Clarke
pLP780	*esa1-L254P TRP1* CEN	A. Clarke
pLP796	*ESA1 URA3* 2μ	A. Clarke
pLP2354	*esa1-531 URA3* CEN	J. Boeke
pLP2374	*esa1-531 TRP1* CEN	

Unless otherwise noted, plasmids were constructed during the course of this study or are part of the standard lab collection.

Chapter 5.

Future Directions

The main goal of my thesis project was to further the understanding of how Esa1, an essential histone acetyltransferase in yeast, functions together with other proteins in its diverse nuclear processes. Using suppression analysis, three genes were determined to functionally interact with *ESA1*. In the case presented in Chapter 2, Nab3, a protein that directs RNA 3'-end processing, showed strong functional links to Esa1. Chapters 3 and 4 defined partnerships between Esa1 and two different histone deacetylases, Rpd3 and Hos2, indicating that Esa1 has different partners to facilitate its distinct nuclear roles. Genetic suppression has provided an effective platform for identifying and characterizing these interactions. Further exploration of the molecular mechanism behind the relationship of these players should be of priority in the future.

Much of the work presented in this thesis has focused on a specific protein (Nab3, Rpd3, or Hos2) and its connections to Esa1. It is important to recognize that many proteins function as part of one or more multiprotein complexes. Therefore, one theme in the following suggestions addresses the involvement of other members of these nuclear complexes. These as well as additional experiments to extend the studies are discussed below.

RNA processing and histone acetyltransferase activity. Chapter 2 described mutant phenotypes of *esa1* that were suppressed by increased dosage of *NAB3*, a gene that encodes an RNA binding protein. In addition, new functions for Nab3 were discovered in rDNA silencing and DNA damage.

One possible explanation proposed in Chapter 2 for the observed suppression is that Nab3 is a substrate for Esa1 acetyltransferase activity, and that this modification influences eithers Nab3's abundance, stability, or function. In human cell lines, it has been reported that acetylation of the 3'-end mRNA processing factor CFIm25 alters its physical association with other RNA processing factors (Shimazu et al. 2007). Another motivation for proposing that Esa1 might acetylate Nab3 stemmed from an unvalidated report from a yeast proteome array that Nab3 is an *in vitro* substrate of Esa1 (Lin et al. 2009). Computational analysis using a program developed to predict protein acetylation sites (Basu et al. 2009) also identified that lysines in Nab3 may be acetylated.

Immunoprecipitation of Nab3 followed by an immunoblot with anti-acetyl lysine did not show any detectable form of acetylated Nab3 (Figure 2-7). However, several potential problems exist for detecting Nab3 acetylation *in vivo*. First, acetylation is a highly dynamic modification and only a very small proportion of Nab3 may be acetylated, making it difficult to capture the modified form *in vivo*. Second, detection is limited by the reactivity of the available antibodies against acetylated-lysines. Although the antibodies used in Figure 2-7 have been successfully used to detect a pool of acetylated proteins, it is unknown what percentage of all acetylated proteins this may represent.

In light of these issues, some additional experimental approaches could be taken to further test the idea of Nab3 acetylation by Esa1. Performing *in vitro* Esa1 HAT assays on Nab3 as the sole substrate could be useful in many ways. A positive result would confirm the readout from the proteome array (Lin et al. 2009). If the *in vitro* reaction can produce acetylated-Nab3, this particular modification could be detected by isotope

incorporation from radioactive acetyl-CoA, and also tested for reactivity with the acetyl-lysine antibodies. This would provide an answer to the question of whether the antibody is suitable for use in *in vivo* studies. A genetic approach could be to mutate the lysines on Nab3 that are predicted computationally to be acetylated. If these mutations result in a loss of phenotypic suppression, then it is possible they are targets of Esa1.

Nab3 functions in a complex with Nrd1 and Sen1 and this complex is referred to as the Nrd1 complex (Figure 5-1A) (Steinmetz and Brow 1996; Conrad et al. 2000). Both Nrd1 and Nab3 bind specific RNA sequences that serve to recruit the complex, and Sen1 is a helicase that is proposed to unwind DNA/RNA duplexes. To determine if suppression of *esa1* was unique to increased dosage of *NAB3* or shared with its other partners, some preliminary studies with *NRD1* overexpression were executed, and are presented in Appendix C. Many of these results indicate that Nrd1 also shares close ties to Esa1. Testing if *SEN1* overexpression can suppress *esa1* phenotypes would determine if initial RNA binding by Nab3 or Nrd1 is more critical for suppression or if it is the more downstream processing events that promote suppression. Along these same lines, suppression of *esa1* phenotypes by *NAB3* overexpression should be tested in *nrd1* and *sen1* mutants. Although Nab3 has not been reported to act outside of the Nrd1 complex, it is possible that *NAB3* mediates suppression independent of its known complex.

The experimental focus in Chapter 2 was to study Nab3's involvement with known Esa1 functions. One set of future experiments would be to address Esa1's role in known Nab3 functions. For example, are *esa1* mutants defective in 3'-end formation of non-polyadenylated transcripts? Is the *ESA1* transcript itself processed by the Nrd1 complex? There were no apparent changes in the *ESA1* transcript in the *nab3* mutant

152

Figure 5-1. The Nab3 and Hos2 complexes. A) Nab3 is one of three subunits in the

heterotrimeric Nrd1 complex that directs 3'-end processing of non-polyadenylated

transcripts (Steinmetz and Brow 1996; Conrad et al. 2000). Nab3 and Nrd1 both contain

RRM domains that bind specific RNA sequences. Sen1 is a putative DNA/RNA helicase.

B) Hos2 and Hst1 function in three different complexes. The full Set3 complex is made

up of seven members, and displays both NAD^+-independent and NAD^+-dependent

activities from Hos2 and Hst1. A subset of the Set3 complex functions independently of

Hst1. Hst1 is also physically associated with Sum1 and Rfm1 in a smaller complex

(Pijnappel et al. 2001).

A
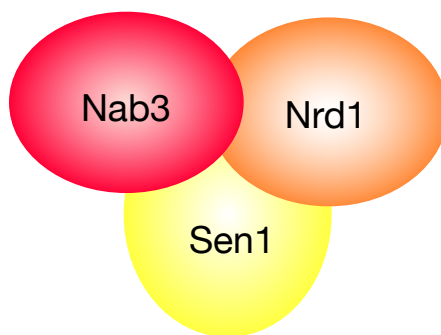
Nrd1 complex

B
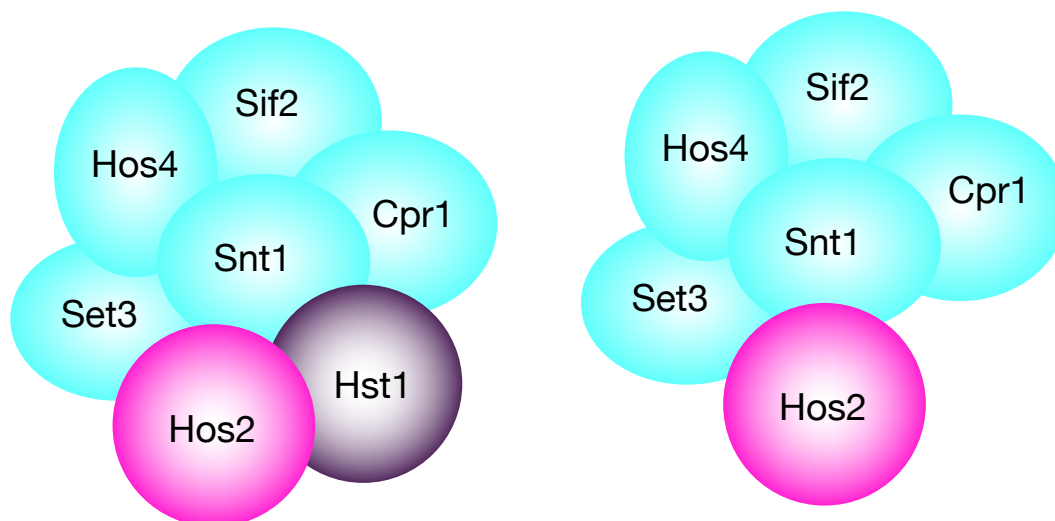
Set3 complex

Set3 complex
(no Hst1)
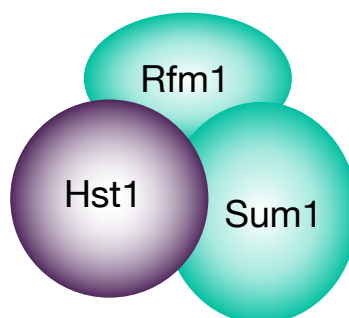
Hst1-Sum1 complex

(Figure 2-5), but this possibility has not yet been fully explored. Answers to these questions will reveal more about how the cell coordinates the diverse nuclear processes of acetylation and 3'-end processing (Figure 5-2A).

Esa1 and Rpd3 coordinate dynamic acetylation for cell viability. Chapter 3 established the idea that Esa1 and the HDAC Rpd3 contribute to cell viability via H4K12 acetylation and deacetylation (Figure 5-2B). Deletion of *RPD3* suppressed the growth defect of multiple temperature-sensitive *esa1* mutant alleles that display a loss of both *in vitro* and *in vivo* HAT activity. However, *RPD3* deletion did not restore viability to the inviable *esa1Δ* (Figure 3-2). Recent data suggests that the essential nature of Esa1 may not be due to its catalytic activity (Decker et al. 2008), raising questions about the non-catalytic functions of Esa1 and the non-catalytic members of its complexes, NuA4 and piccolo.

Several NuA4 and piccolo subunits are essential (Figure 1-1). Some of these subunits participate in other cellular functions in addition to their role in NuA4 or piccolo. For example, the essential *ACT1* gene encodes the actin protein needed for cytoskeletal structure (Gallwitz and Seidel 1980). Epl1, on the other hand, thus far has only been reported to function in NuA4 and piccolo (Boudreault et al. 2003). Examining the effect of Rpd3L disruption on *epl1* mutants (both conditional and null alleles) might reveal non-catalytic functions of NuA4 or piccolo. Some of these non-catalytic subunits may be critical for targeting the complexes to the proper genomic locus, or for bridging interactions of the complex with other proteins.

In addition, analysis of specific transcripts that change in response to Esa1 and Rpd3 would enrich the understanding of the coordination of H4K12 acetylation by these

Figure 5-2. Three suppressors of *esa1*. Suppression analysis of *esa1* mutants reveals

links between the histone acetyltransferase Esa1 to three proteins in different processes.

A) Connections between the acetyltransferase Esa1 and the 3'-end RNA processing

factor Nab3. B) Esa1 and the deacetylase Rpd3 control H4K12 acetylation for cell

viability. C) Esa1 and the deacetylase Hos2 coordinate response to DNA damage.

A   Esa1 and Nab3: histone acetylation and RNA processing
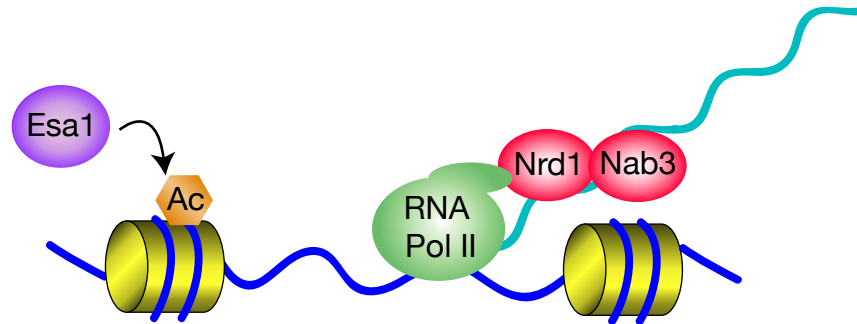
B   Esa1 and Rpd3: cell viability
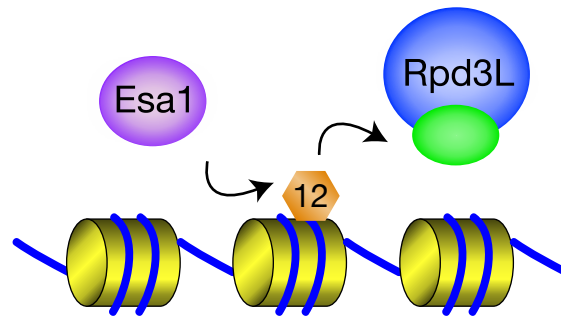
C   Esa1 and Hos2: DNA damage
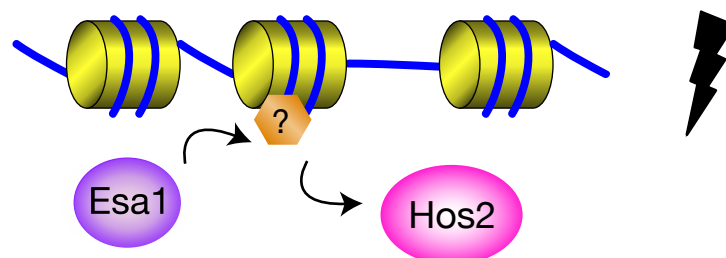
two enzymes. Preliminary attempts were reported in Appendix A (Figure A-5, Table A-1) using a candidate transcript approach. These did not identify any true targets of Esa1 and Rpd3. A more direct global analysis using genome-wide approaches may prove more fruitful. The development of yeast tiling arrays and ChIP-sequencing technology provide higher genomic resolution than the previous studies, and are likely to provide the necessary tools for identifying Esa1 and Rpd3 shared targets. Comparison of expression profiles between an *esa1* single mutant and *esa1 rpd3* could identify transcripts whose expression changes allow for the suppression. These could be complemented with genome-wide binding profiles to examine overlap of Esa1, Rpd3, and H4K12 acetylation enrichment to identify genomic loci that would test the model presented in Figure 3-16.

Esa1 and Hos2 participate in DNA repair. In Chapter 4, a different HDAC, Hos2, was discovered to function with Esa1 in response to DNA damage (Figure 5-2C). Deletion of *HOS2*, and but not other related HDAC genes, suppressed *esa1*'s sensitivity to the DNA damaging agents camptothecin and hydroxyurea. These results provide a contrast to the studies in Chapter 3 with Rpd3, where deletion of *RPD3* suppressed *esa1*'s growth defect, but not its camptothecin sensitivity. To further define the partnership between Esa1 and Hos2, experiments paralleling those done with Rpd3 were proposed and discussed in Chapter 4. First, catalytic activity of Hos2 should be tested for its role in the suppression. Then, it should be determined if acetylation of a particular histone lysine or set of lysines is critical for the suppression.

Further refining these interactions, it would be useful to focus attention on the multiprotein complexes in which Hos2 and Esa1 function. NuA4 and piccolo components have been described above and in Chapter 1 (Figure 1-1). The Set3 complex (Set3C) is

unique from NuA4 and piccolo in that it contains two catalytic subunits, Hos2 and the class III NAD^+-dependent HDAC Hst1, along with five other non-catalytic subunits (Figure 5-1B) (Pijnappel et al. 2001). These two HDACs make up three different complexes (Figure 5-1B). Set3C exists in two forms, with and without Hst1. Hst1 also forms a complex with Sum1 and Rfm1 (Pijnappel et al. 2001; Rusche and Rine 2001).

First, deletion of *HST1* should be tested for suppression of *esa1*'s sensitivity to camptothecin or hydroxyurea. This will determine if general HDAC activity, of Set3C or Hos2, specifically participates with Esa1 in response to DNA damage. Deletions of different subunits in these three complexes should be constructed in combination with *esa1* to test for suppression of *esa1*'s DNA damage phenotypes. It is feasible that disruption of one or all three of these complexes will suppress *esa1*'s DNA damage phenotype. Genetic analysis of the different components should allow for dissection of complexes involved in repair with Esa1.

In addition to refining the suppression in relation to the complexes, Esa1 and Hos2's influence on the molecular signals in DNA repair could be examined. There are many well-established hallmarks of repair pathways such as phosphorylation of the checkpoint protein Rad53 or transcriptional activation of a set of damage-inducible genes. Two candidate genes to test are *HUG1* and *RNR3*, which have previously been shown to require Esa1 and Hos2 for activation (Sharma et al. 2007). Esa1 localizes to double-strand breaks to acetylate histones (Bird et al. 2002). It is possible that Hos2 deacetylates histones at double-strand breaks, and that this deacetylation by Hos2 recruits Esa1. All of these hallmarks of repair could be examined in the *esa1 hos2* double mutant to determine the involvement of Esa1 and Hos2 at each step.

Although much remains to be done to fully dissect Esa1's multiple cellular

functions, the work presented in this thesis, identifying specific interacting partners for

Esa1 in different processes, contributes to this understanding (Figure 5-2). Because the

MYST family of HATs and the complexes in which they function in are deeply

conserved, studies such as this one may guide the further understanding of the Esa1

homolog Tip60 in vertebrates.

Appendix A.

Further functional and molecular analysis of Esa1 and Rpd3

Collaboration between the histone acetyltransferase Esa1 and the histone deacetylase Rpd3 was established in Chapter 3. A more comprehensive study than that described in Chapter 3 was undertaken and those results are presented and described in this Appendix. Some of these experiments evaluate the *esa1 rpd3* double mutants for cell cycle defects, changes in transcription of candidate genes, and sensitivity to drugs used in silencing assays. Whereas Chapter 3 highlights the coordination between Esa1 and Rpd3, many of the results in this Appendix indicate processes in which Esa1 and Rpd3 functions may be distinct.

RESULTS

Deletion of *RPD3* does not suppress the G2/M cell cycle block of e*sa1* mutants. Mutants of *ESA1* have a G2/M cell cycle defect that is dependent on the checkpoint protein Rad9 (Clarke et al. 1999). To determine whether deletion of *RPD3* in the *esa1* mutant rescues this cell cycle block, cell cycle profiles were observed by propidium iodide staining followed by flow cytometry. Flow cytometry is useful to distinguish cellular DNA content before (1C) and after (2C) replication. The cell cycle profile of the *esa1 rpd3* double mutant resembled the G2/M block of the *esa1* single mutant, visualized by a decrease in the 1C peak and an accumulation of cells at the 2C peak (Figure A-1). Thus, *rpd3* suppression of *esa1* phenotypes is not mediated by progression of the cell cycle of *esa1* mutants through G2/M.

161

Figure A-1. Deletion of *RPD3* does not suppress *esa1*'s G2/M cell cycle block. Cells were fixed and stained with propidium iodide and analyzed for cell cycle profiles by flow cytometry. X-axis represents fluorescence; Y-axis represents number of cells. Strains are: wild-type (LPY5), *esa1* (LPY4774), *rpd3* (LPY12154), and *esa1 rpd3* (LPY12156).

esa1 rpd3

rpd3

esa1

WT

30°

esa1 rpd3

rpd3

esa1

WT

36°
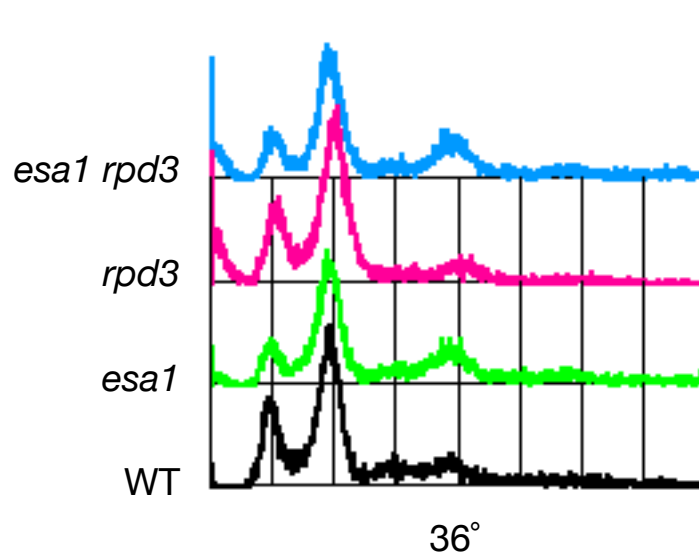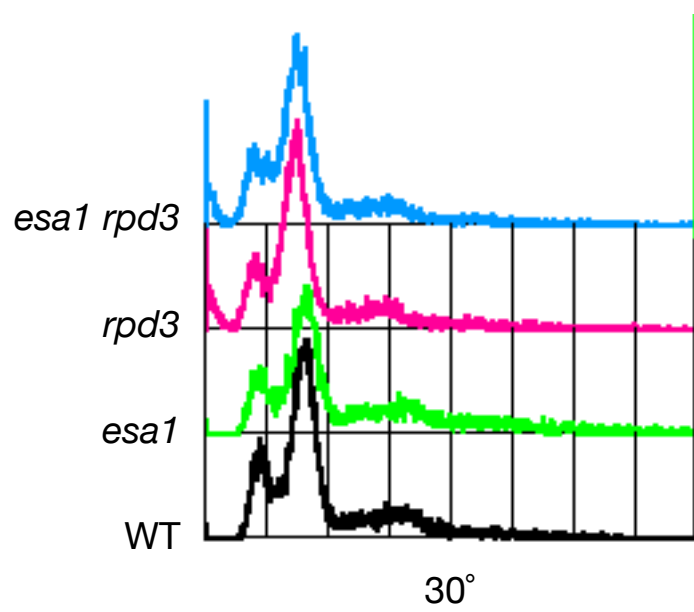
The *esa1* and *rpd3* mutants are not sensitive to drugs used in silencing assays.

To ensure that a decrease or increase in growth on canavanine and 5-FOA plates

presented in Chapter 3 (Figure 3-4, 3-5) truly represents silencing defects and not

sensitivity or resistance to the drugs used in the assays, *esa1* and *rpd3* strains without the

silencing reporters (rDNA*::ADE2-CAN1*, TELVR*::URA3*) were tested for sensitivity to

canavanine and 5-FOA. At the concentrations used in the rDNA and telomeric silencing

assays, all *esa1*, *rpd3*, or Rpd3L-specific mutants and double mutants showed no defect

in growth on canavanine or 5-FOA (Figure A-2). These results indicate that the effects

seen in Chapter 3 using the rDNA*::ADE2-CAN1* and TELVR*::URA3* reporters are

representative of genuine silencing defects and not non-specific drug sensitivities.

Histone H3 acetylation and methylation remains unchanged in *esa1 rpd3*

mutants. Esa1 and Rpd3 target lysines on histone H4, although there is evidence that

both also acetylate residues on histone H3 (Rundlett et al. 1996; Clarke et al. 1999). Since

restoration of global H4K5 and H4K12 acetylation defects were observed in the *esa1*

mutant by deletion of *RPD3* (Figure 3-9), *esa1* and *rpd3* mutants were also analyzed for

changes in global levels of acetylation at H3K9 and H3K14. As seen in Figure A-3, no

changes were observed for *esa1*, *rpd3*, and the Rpd3L-specific mutants and double

mutants, confirming that the enzymatic activities of Esa1 and Rpd3 primarily affect H4.

In addition, crosstalk between different modifications on histones is known to

occur. For example, methylation of H3R2 is known to prevent methylation of H3K4 from

occuring (Kirmizis et al. 2007). To test the possibility that H4 acetylation influences H3

methylation, the *esa1 rpd3* mutants were examined for changes in H3 methylation. No

global changes were observed for this modification (Figure A-3), although this does not

164

Figure A-2. The *esa1 rpd3* **mutants are not generally sensitive to drugs used in**

silencing assays. A) Mutants are not sensitive to canavanine at the concentrations used in

rDNA silencing assays with the rDNA::*ADE2-CAN1* reporter. Strains without the

reporter were tested for sensitivity to 16 μg/ml canavanine on SC-Arg plates. Same

results were observed for 32 μg/ml canavanine (data not shown). B) Mutants are not

sensitive to 5-FOA used in telomeric silencing assays with TELVR*::URA3* reporter.

Strains without the reporter were serially diluted and plated on 5-FOA to test for

sensitivity. Strains in both A) and B) are wild-type (LPY5), *esa1* (LPY4774), *esa1 rpd3*

(LPY12156), *rpd3* (LPY12154), *esa1 sds3* (LPY12956), *sds3* (LPY12958), *esa1 pho23*

(LPY12729), and *pho23* (LPY12732).

A
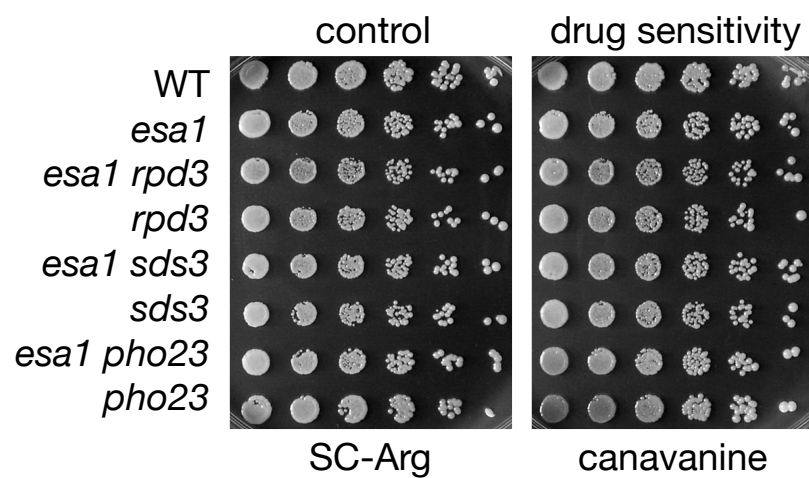
B
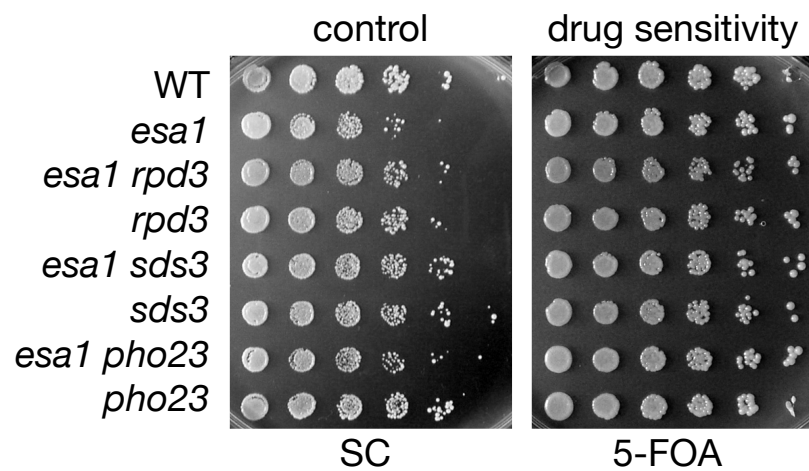
Figure A-3. H3 acetylation and methylation status remains unchanged in *esa1 rpd3*

mutants. A) Bulk histone H3 acetylation levels were analyzed in wild-type (LPY5), *esa1*

(LPY4774), *esa1 rpd3* (LPY12156), *rpd3* (LPY12154), *esa1 sds3* (LPY12956), *sds3*

(LPY12958), *esa1 pho23* (LPY12729), *pho23* (LPY12732), *esa1 rco1* (LPY12652), and

rco1 (LPY12645). Whole cell protein extracts were prepared and immunoblotted with

antisera specific to acetyl-H3K9, K14. B) Bulk histone H3 methylation levels were

analyzed in the same method as A), using antisera specific to dimethyl-H3K4.
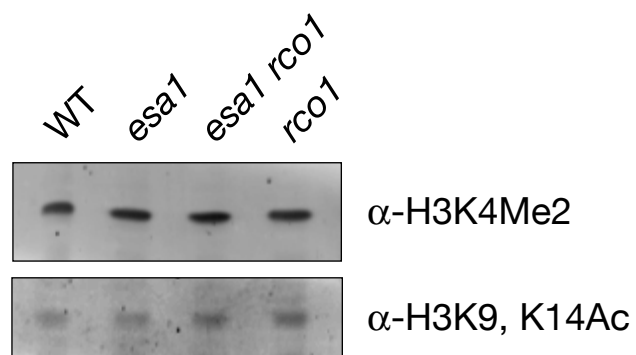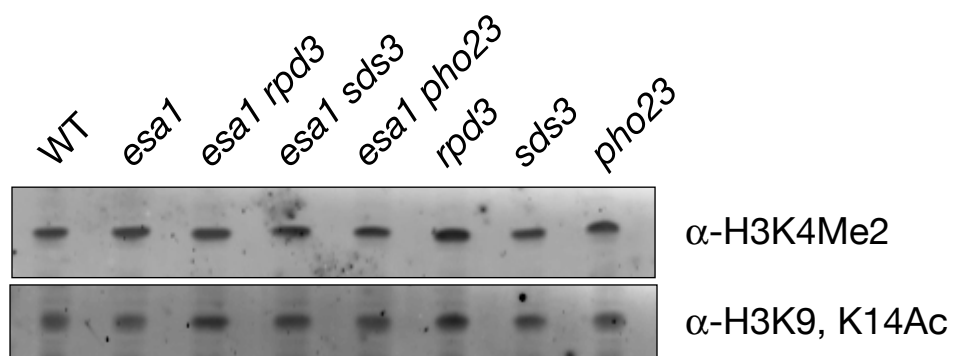
rule out the possibility that crosstalk between these two modifications occurs at localized regions in the genome.

Role of the histone acetyltransferase Hat1 in *esa1 rpd3* mutants. Several histone acetyltransferases share common lysine acetylation targets. One enzyme with targets overlapping those of Esa1 is Hat1. The Hat1 histone acetyltransferase primarily acetylates H4K5 and H4K12 (Kleff et al. 1995; Parthun et al. 1996), two residues that are shared targets of Esa1. To examine the possibility that Hat1 compensates for the absence of Esa1 in collaboration with Rpd3, *HAT1* was deleted in the *esa1 rpd3* double mutant. Growth of *esa1* was evaluated in the triple mutant. The suppression observed in the *esa1 rpd3* double mutant was independent of *HAT1*, shown by the same degree of suppression between *esa1 rpd3* and *hat1 esa1 rpd3* (Figure A-4A). Thus, *HAT1* does not appear to contribute to viability in the absence of Esa1 activity.

Global histone acetylation levels of H4K5Ac and H4K12Ac were also tested in a *hat1Δ* background to determine if Hat1 contributes to acetylation in the absence of Esa1 function. These results were similar to the growth suppression tests, showing that deletion of *RPD3* in the *esa1* mutant still restored global acetylation even in the absence of *HAT1* (Figure A-4B). Therefore, *HAT1* acts independently of *ESA1* and *RPD3*.

Transcript analysis of potential Esa1 and Rpd3 targets. The model presented in Chapter 3 proposes that Esa1 and Rpd3 function together to regulate transcripts required for growth through acetylation and deacetylation of H4K12. In attempts to evaluate candidate transcripts, several approaches were taken. First, efforts were made to confirm transcripts that were shown previously to change in either *esa1* or *rpd3* single

169

Figure A-4. Suppression in *esa1 rpd3* is *HAT1*-independent. A) Deletion of *RPD3*
suppressed the growth defect of *esa1* in a *hat1*Δ background. Serial dilutions of wild-type
(LPY5), *esa1* (LPY4774), *esa1 rpd3* (LPY12156), *rpd3* (LPY12154), *hat1* (LPY13862),
esa1 hat1 (LPY13866), *esa1 hat1 rpd3* (LPY13871), and *hat1 rpd3* (LPY13869) were
plated on SC at permissive (30˚) and restrictive (35˚) temperature to assay for growth. B)
Global acetylation changes in *esa1 rpd3* double mutants at H4K5 and H4K12 are *HAT1*-
independent. Whole cell protein extracts were prepared from the same strains as in A)
and immunoblotted with antisera specific to acetyl-H4K5 and acetyl-H4K12.

A
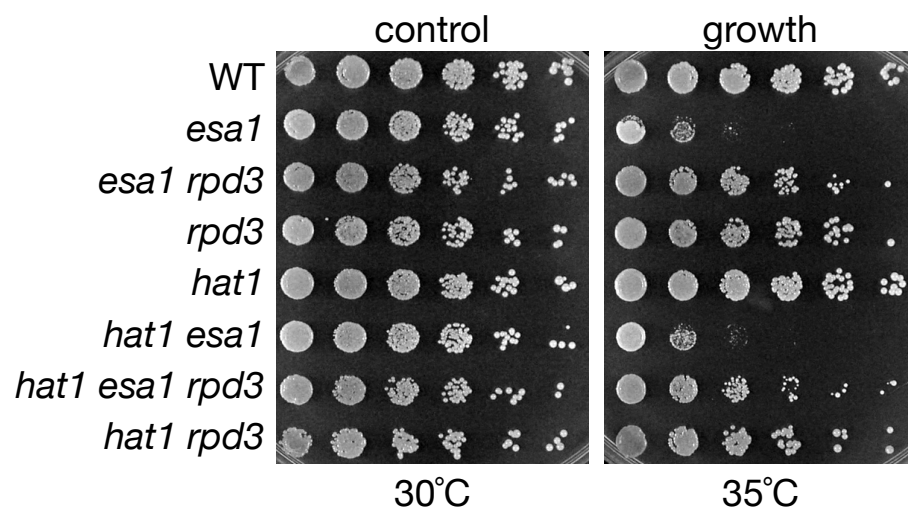
B
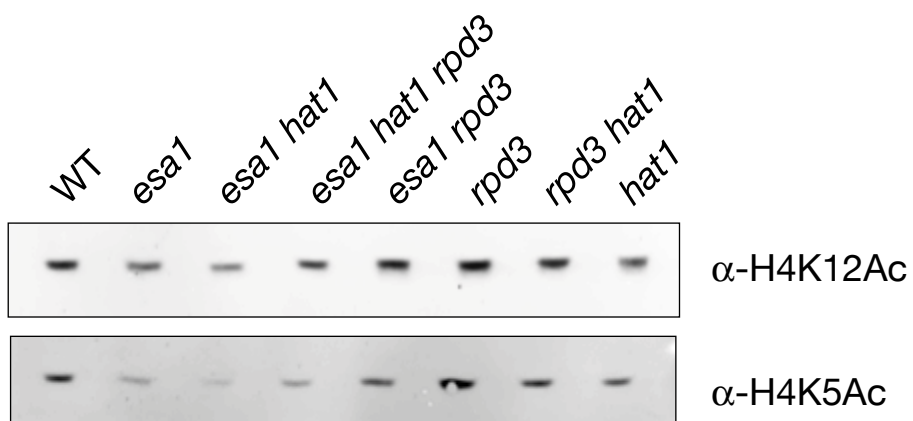
mutants. Second, genome-wide transcription profiles of *esa1* and *rpd3* single mutants were analyzed to identify candidate transcripts that might change in both mutants.

Although several genome-wide datasets have been generated to identify Esa1 binding sites, and to discover genes whose transcription depends on Esa1 (Reid et al. 2000; Durant and Pugh 2006), very few genes have been characterized as true Esa1-regulated transcripts. In contrast, several transcripts have been validated as responsive to Rpd3 (Rundlett et al. 1998).

A number of candidate transcripts were chosen to evaluate Esa1-dependent changes in expression. These are summarized in Table A-1. RNA was prepared and analyzed by quantitative RT-PCR from *esa1 rpd3* and *esa1* Rpd3L complex-specific double mutants for changes in expression of these genes. None of the genes predicted to change in *esa1* mutants were confirmed to be Esa1-dependent (Table A-1).

For the *RPD3* targets, *INO1* but not *ERG10* was significantly upregulated in *rpd3* mutants compared to either wild-type or *esa1* (Figure A-5). The upregulation was maintained in all the double mutants, although to a lesser extent in *pho23*, a noncatalytic subunit mutant. Because this particular transcript appears independent of *ESA1* status (compare WT and *esa1*, Figure A-5, bottom), *INO1* is not a gene at which both Esa1 and Rpd3 regulate its transcription. As discussed in Chapter 3 and Chapter 5, extended transcript analysis of genes regulated by both Esa1 and Rpd3 will be important for further understanding of their coordinated activities towards H4K12.

Rpd3 protein levels remain constant in Rpd3 complex-specific deletion strains. In the case that one or both of the Rpd3 complexes might contribute to regulation of Rpd3 expression, changes in Rpd3 levels were tested in strains deleted for *RCO1*

Figure A-5. Changes in *INO1* expression in Rpd3L-specific mutants. RNA was extracted from cells grown in YPD at 30˚ and analyzed by quantitative RT-PCR for changes in *INO1* expression. All values are normalized to *scR1* levels and represent fold increase over wild-type. *scR1* is a non-coding RNA subunit of the signal recognition particle and is used as an internal control locus. Strains are as follows: wild-type (LPY5), *esa1* (LPY4774), *esa1 rpd3* (LPY12156), *rpd3* (LPY12154), *esa1 sds3* (LPY12956), *sds3* (LPY12958), *esa1 pho23* (LPY12729), *pho23* (LPY12732), *esa1 rco1* (LPY12652), and *rco1* (LPY12645).

A
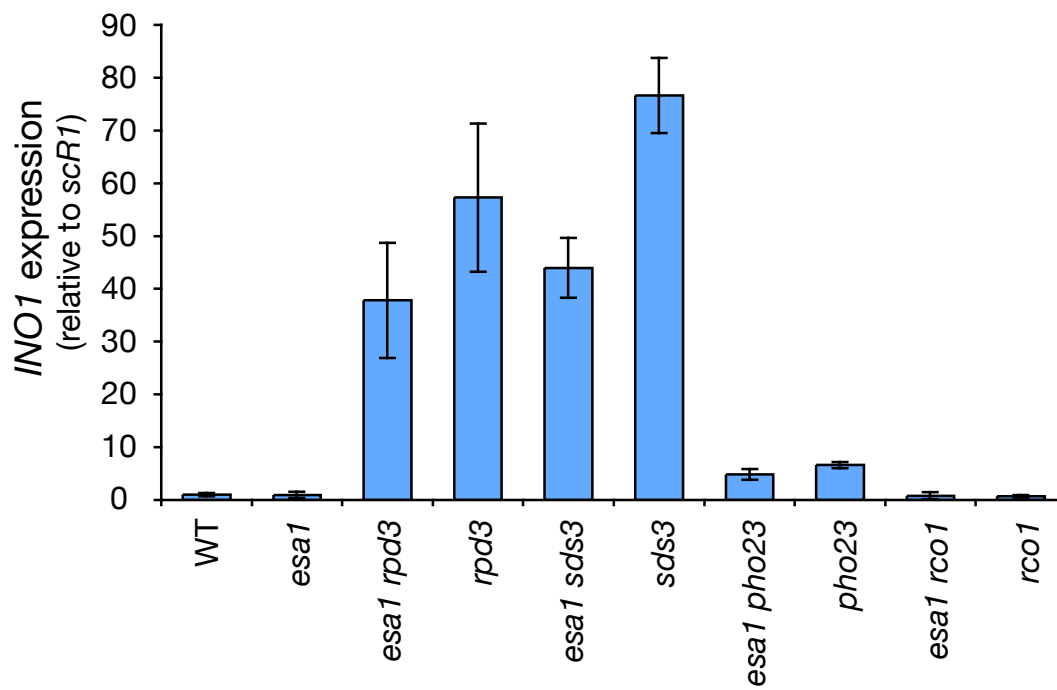
B
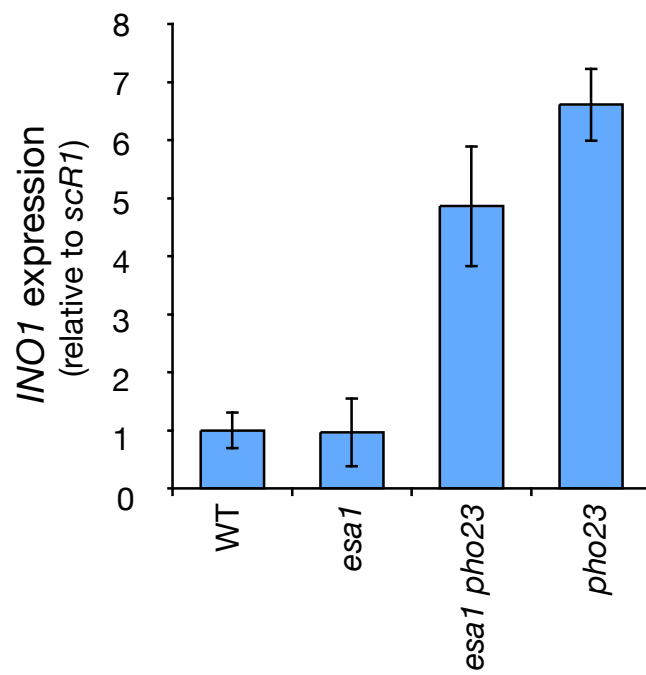
which encodes an Rpd3S-specific component, and *PHO23* and *SDS3* which each encode subunits specific to Rpd3L, and in combination with *esa1*. Protein extracts were made and analyzed for Rpd3 levels by immunoblot and found to be equivalent in all, regardless of the absence of Rpd3L- or Rpd3-specific complex members (Figure A-6).

Suppression in *esa1 rpd3 sds3* and *esa1 pho23 rpd3* triple mutants is equivalent to suppression in *esa1 rpd3*. The degree of suppression in the *esa1 pho23* and *esa1 sds3* Rpd3L-specific double mutants was moderately stronger than the *esa1 rpd3* double mutant (Chapter 3 and Figure A-7). Because these catalytic and non-catalytic subunits of the Rpd3L complex had individual functional interactions with Esa1, it is possible that there might be additive effects on the *esa1* from their combined deletion. To test this idea, *PHO23* and *SDS3* were individually deleted in the *esa1 rpd3* double mutants to create *esa1 pho23 rpd3* and *esa1 rpd3 sds3* triple mutants. Suppression of *esa1* by deletion of the Rpd3L-specific subunits was *RPD3*-dependent (Figure A-7). For example, the level of suppression observed in *esa1 pho23 rpd3* was equivalent to that of *esa1 rpd3*. This confirms that the genetic interaction observed between *ESA1* and *SDS3* or *PHO23* is mediated by *RPD3*, and not some other function of Sds3 or Pho23 that might be distinct from Rpd3 activity.

CONCLUSIONS AND FUTURE DIRECTIONS

As a companion to Chapter 3, this Appendix defines specific aspects of Esa1 and Rpd3 functions. In addition, it includes data that further confirm the validity of the observations presented in Chapter 3.

Figure A-6. Rpd3 protein levels are constant in *esa1* and Rpd3 complex-specific

mutants. Whole cell protein extracts were prepared from wild-type (LPY5), *esa1*

(LPY4774), *pho23* (LPY12732), *sds3* (LPY12958), *rco1* (LPY12645), *rpd3*

(LPY12154), *esa1 pho23* (LPY12729), *esa1 sds3* (LPY12956), and *esa1 rco1*

(LPY12652), separated on an 8% SDS-acrylamide gel and immunoblotted with antisera

specific to Rpd3 (top) and PGK (bottom) as a loading control. Arrow indicates band

corresponding to Rpd3.
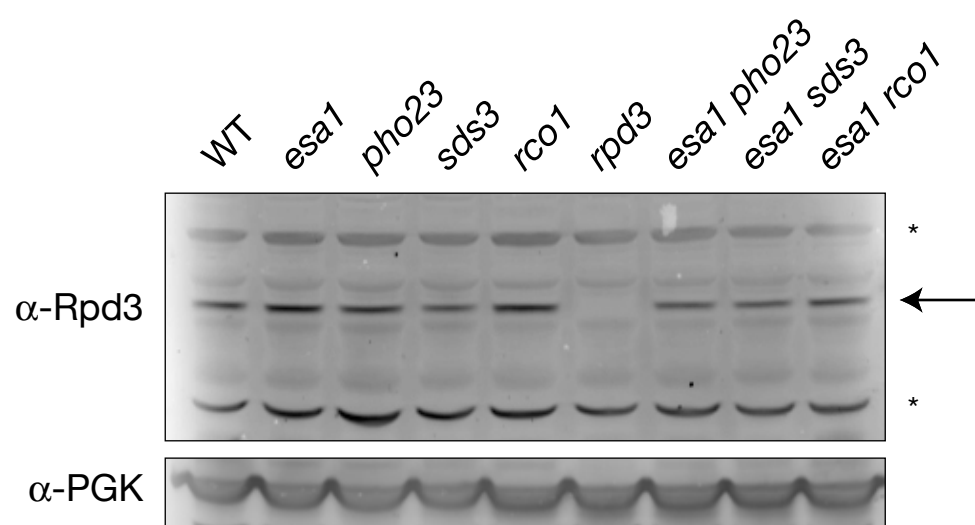
Figure A-7. Suppression in *esa1 rpd3 pho23* and *esa1 rpd3 sds3* triple mutants is equivalent to suppression in the *esa1 rpd3* double mutant. A) Serial dilutions of wild-type (LPY5), *esa1* (LPY4774), *esa1 rpd3* (LPY12156), *esa1 pho23* (LPY12729), *esa1 pho23 rpd3* (LPY14034), *pho23 rpd3* (LPY14030), *pho23* (LPY12732), and *rpd3* (LPY12154) were plated on SC at permissive (30˚) and restrictive (35˚) temperatures to assay for growth. B) Same strains as part A) with addition of *esa1 sds3* (LPY12956), *esa1 rpd3 sds3* (LPY14041), *rpd3 sds3* (LPY14050), and *sds3* (LPY12958) were plated on SC at permissive (30˚) and restrictive (35˚) temperatures to assay for growth.

A

control   growth

WT
esa1
esa1 rpd3
esa1 pho23
esa1 pho23 rpd3
pho23 rpd3
pho23
rpd3

30° SC   35° SC

B

control   growth

WT
esa1
esa1 rpd3
esa1 sds3
esa1 rpd3 sds3
rpd3 sds3
sds3
rpd3

30° SC   35° SC
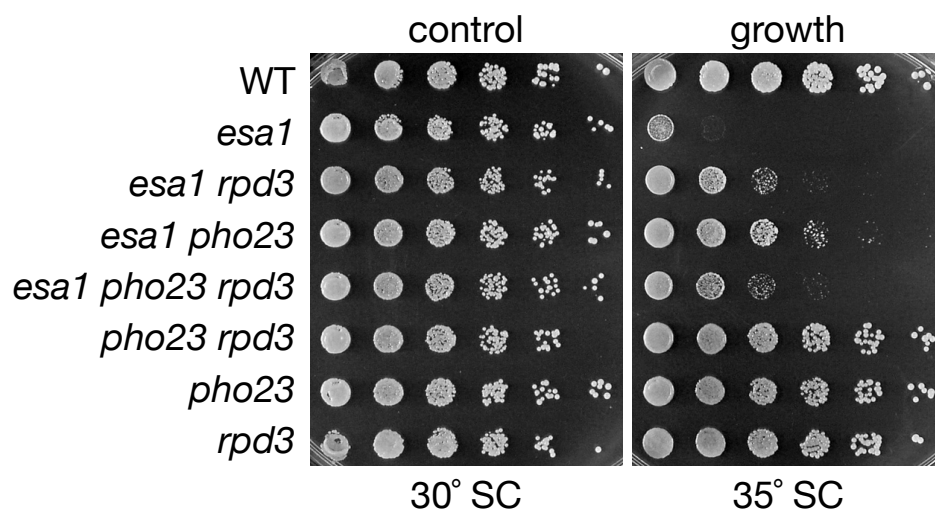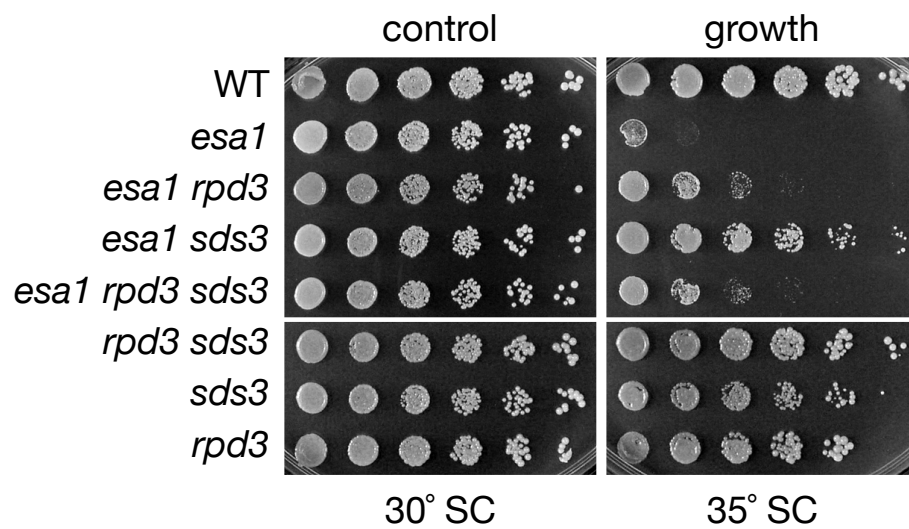
In Chapter 3, Esa1 and Rpd3 were established as coordinating dynamic acetylation and deacetylation of H4K12 for cell growth. One explanation for Esa1's contribution to cell growth could be its participation in cell cycle progression. However, the cell cycle profiles analyzed in Figure A-1 show that the suppression of *esa1*'s growth defect mediated by *rpd3Δ* does not overcome this cell cycle block. Therefore, a more likely hypothesis is that deletion of *RPD3* in the *esa1* mutant allows for a change in transcription of genes that promote viability.

One powerful tool to identify gene targets for which Esa1 and Rpd3 partner would be the ability to examine localized changes in H4K12 acetylation by chromatin immunoprecipitation (ChIP), since H4K12 was established as the critical lysine in the suppression. Unfortunately, although the commercially available antibodies for H4K12Ac are suitable for immunoblots, they yield high non-specific binding when used for ChIP (data not shown). Pilot experiments were performed to evaluate H4K12 acetylation changes at genomic loci where acetylation is thought to be affected by Esa1 or Rpd3 activity. The results of these experiments showed the same level of H4K12Ac in a wild-type strain as the H4K12A negative control strain. The development of more specific antibodies or immunoprecipitation conditions to confidently detect H4K12 acetylation by ChIP would greatly aid efforts to determine regions of the genome where H4K12 acetylation and deacetylation by Esa1 and Rpd3 contribute to cell viability.

MATERIALS AND METHODS

Yeast strains and plasmids. All strains used in this study are listed in Table A-2.

The *hat1Δ::kanMX* (LPY13862) mutant was constructed by amplification (oligonucleotide sequences listed in Table A-3) of the *kanMX* cassettes from *Saccharomyces* Genome Deletion Project strains, transformed into W303-1a (LPY5) and backcrossed prior to use. The *esa1 rpd3 sds3* and *esa1 pho23 rpd3* triple mutants were constructed by standard genetic crosses. When unable to infer genotype by single markers, strains were molecularly genotyped as outlined in Table A-4. The *rpd3*, *sds3*, and *pho23* mutants were also confirmed by a reduced mating efficiency defect.

Cell cycle profiles. Cell cycle profiles were obtained by flow cytometry of cells stained with propidium iodide on a FACScaliber machine (Becton Dickinson). Cells were harvested at an A_{600} of 0.6-1 after a six hour shift to 36˚ and fixed in 70% ethanol overnight before staining with propidium iodide. Each plot represents 100,000 cell counts.

Growth dilution assays and silencing assays. Unless otherwise noted, all dilution assays represent five-fold serial dilutions, starting from an A_{600} of 1.0 after growth to saturation in 3 ml of liquid synthetic complete (SC) medium grown at 30˚. Suppression of *esa1*'s growth defect on SC plates was assayed at the restrictive temperature of 35˚. All images were captured after 2-4 days of growth.

Protein immunoblots. Whole cell extracts were prepared from cells grown to A_{600} of 0.6-1.0 at 30˚. Extracts were prepared by bead-beating as described previously (Clarke et al. 1999). Briefly, cells were resuspended in phosphate buffered saline with protease inhibitors and lysed by vortexing with glass beads. Whole cell extracts were then denatured by boiling in sample loading buffer and separated from the insoluble pellet by centrifugation. For histone immunoblots, proteins were separated on 18% SDS-

polyacrylamide gels and transferred to nitrocellulose (0.2μm). Primary antisera used were anti-H4K5Ac (1:5000 dilution, Serotec), anti-H4K12Ac (1:2500 dilution, Serotec), anti-H3K4Me$_2$ (1:10,000 dilution, Upstate), and anti-H3K9,K14Ac (1:10,000 dilution, Upstate). For Rpd3 and PGK detection, same as above except 8% SDS-polyacrylamide gels were used. Anti-Rpd3 was generously provided by Michael Grunstein (Rundlett et al. 1996). Goat anti-rabbit or goat anti-mouse conjugated to horseradish peroxidase (Promega) was used as a secondary antibody, and signal was detected with Western Lightning® Chemiluminescence Reagent (Perkin Elmer) on Kodak™ X-Omat™ film.

RNA transcript analysis. RNA was isolated using hot acid-phenol from yeast grown to an A$_{600}$ of 0.6-1. Cells were grown at 30˚ in YPD for *INO1* analysis. All other transcripts (Table A-1) were analyzed in cells grown at 36˚ for six hours in SC. RNA was DNase-treated with TURBO DNA-*free*™ (Applied Biosystems), and reverse transcription was performed using TaqMan® Reverse Transcription Reagents (Applied Biosystems) with random hexamer priming. cDNA was analyzed using real-time PCR on a DNA Engine Opticon 2 (MJ Research). Oligonucleotide sequences are listed in Table A-5. Data shown is representative of at least two experiments that were analyzed in triplicate.

Acknowledgements. Michael Grunstein provided the Rpd3 antibody.

Table A-1. Candidate transcripts analyzed by quantitative RT-PCR analysis

Transcript	Predicted change in transcript level	Reference[a]	Description[b]
RPL9A	decrease in *esa1*	Reid et al. 2000	Ribosomal protein
RPS11B	decrease in *esa1*	Reid et al. 2000	Ribosomal protein
CDC33	decrease in *esa1*	Combined microarray	Translation initiation factor eIF4E
NOP1	decrease in *esa1*	Combined microarray	Nucleolar protein required for processing of pre-18S rRNA
PHO85	decrease in *esa1*	Combined microarray	Cyclin-dependent kinase involved in cellular response to nutrients
SPT15	decrease in *esa1*	Combined microarray	TATA-binding protein; essential for viability
ARG3	increase in *esa1*	Combined microarray	Ornithine carbamoyltransferase, catalyzes step in arginine biosymthesis
GPD1	increase in *esa1*	Combined microarray	NAD^+-dependent glycerol-3-phosphate dehydrogenase; enzyme in glycerol synthesis
RNR2	increase in *esa1*	Combined microarray	Ribonucleotide-diphosphate reductase, small subunit
INO1	increase in *rpd3*[c]	Rundlett et al. 1998	Inositol 1-phosphate synthase
ERG10	increase in *rpd3*	Rundlett et al. 1998	Acetyl-CoA C-acetyltransferase
scR1	Control locus		RNA subunit of the Signal Recognition Peptide

[a] Combined microarray reflects analysis of two datasets: A. Clarke and S. Berger (unpublished) and Durant and Pugh 2006.

[b] Summary from *Saccharomyces* Genome Database (http://yeastgenome.org)

[c] Of the tested candidates in Table A-1, only *INO1* expression changed as predicted in either *esa1* or *rpd3*.

Table A-2. Yeast strains used in Appendix A

Strain	Genotype	Source/ Reference
LPY5 (W303-1a)	*MAT*a *ade2-1 can1-100 his3-11,15 leu2-3,112 trp1-1 ura3-1*	Thomas and Rothstein 1989
LPY4774	W303 *MAT*a *esa1-414*	
LPY12154	W303 *MAT*a *rpd3::kanMX*	
LPY12156	W303 *MAT*a *esa1-414 rpd3::kanMX*	
LPY12645	W303 *MAT*a *rco1Δ::kanMX*	
LPY12652	W303 *MAT*a *esa1-414 rco1Δ::kanMX*	
LPY12729	W303 *MAT*a *esa1-414 pho23Δ::kanMX*	
LPY12732	W303 *MAT*a *pho23Δ::kanMX*	
LPY12956	W303 *MAT*a *esa1-414 sds3Δ::kanMX*	
LPY12958	W303 *MAT*a *sds3Δ::kanMX*	
LPY13862	W303 *MAT*a *hat1Δ::kanMX*	
LPY13866	W303 *MAT*a *esa1-414 hat1Δ::kanMX*	
LPY13871	W303 *MAT*a *esa1-414 hat1Δ::kanMX rpd3::kanMX*	
LPY13869	W303 *MAT*a *hat1Δ::kanMX rpd3::kanMX*	
LPY14034	W303 *MAT*a *esa1-414 pho23Δ::kanMX rpd3::kanMX*	
LPY14041	W303 *MAT*a *esa1-414 rpd3::kanMX sds3Δ::kanMX*	
LPY14030	W303 *MAT*a *pho23Δ::kanMX rpd3::kanMX*	
LPY14050	W303 *MAT*a *rpd3::kanMX sds3Δ::kanMX*	

Unless otherwise noted, strains were constructed during the course of this study or are part of the standard lab collection.

Table A-3. Oligonucleotide sequences used in Appendix A for strain construction

Oligo #	Name	Sequence (5'-3')
950	*PHO23* KO forward	CTTCGCCCAGCACATTGTCC
951	*PHO23* KO reverse	CGGCGATTAGACTGAGCTGC
974	*SDS3* KO forward	CACTCAAGCGATGATCGTTTCG
975	*SDS3* KO reverse	CTACAGTGGCATTAGTTGCAGC
1086	*HAT1* KO forward	GCGACCATTTCATCAAGAGC
1087	*HAT1* KO reverse	GCTACCATGGTGTGTCACTT
882	*kanMX* forward	ATTACGGCTCCTCGCTGCAG
883	*kanMX* reverse	CAGCCATTACGCTCGTCATC
1142	*LEU2* reverse	AATCTGGAGCAGAACCGTGG
236	*kanMX* forward	GATGACGAGCGTAATGGCTG

Table A-4. Molecular genotyping of deletion strains used in Appendix A

Gene	Oligo pair (oLP#)	Mutant product size	Wild-type product size
hat1Δ::kanMX	1086-1087	2.9 kb	2.4 kb
hat1Δ::kanMX	1086-883	1.8 kb	None
hat1Δ::kanMX	1087-882	1.7 kb	None
pho23Δ::kanMX	950-951	2.2 kb	1.7 kb
pho23Δ::kanMX	950-883	1.3 kb	None
pho23Δ::kanMX	951-882	1.5 kb	None
rpd3::leu2::kanMX	1142-236	600 bp	None
sds3Δ::kanMX	974-975	2.8 kb	2.2 kb
sds3Δ::kanMX	974-883	1.5 kb	None
sds3Δ::kanMX	975-882	1.9 kb	None

Table A-5. Oligonucleotide sequence pairs used in Appendix A for quantitative RT-PCR

Gene	Oligo pair (oLP#)	Sequence (5'-3')
RPL9A	1251-1252	Forward (F): GAGAACCGTCAAGTCTTTGG Reverse (R): CAGCAGCGTTTTGGGAAACG
RPS11B	1253-1254	(F): GTGACAGATTAACCAGAGCC (R): CCCAAGTCAATGTGTTCGTC
CDC33	1245-1246	(F): ATTCCTGAGCCACACGAACTAC (R): AATTCCAAATGCCCGTCATCGG
NOP1	1247-1248	(F): TGAACCACATAGACATGCCG (R): TGAATGGGTTCCATACACGG
PHO85	1249-1250	(F): CAGTGTACAAGGGACTGAAC (R): AGTTCTAGCCCTCTTGGTGT
SPT15	1255-1256	(F): GGGAAAATGGTTGTTACCGG (R): CAATTCTGGCTCATAGGAGG
ARG3	1257-1258	(F): CGAGAATTTCGACCGAAGGT (R): CACCAATCCATGCCATCTTC
GPD1	1259-1260	(F): CAATGTGGTGCTCTATCTGG (R): CGAATCTGATGATCTCACCC
RNR2	1261-1262	(F): GGTATGATGCCCGGTTTAAC (R): AAGCAACCAACAGTCTGTCG
INO1	1279-1280	(F): TGCTCATTGGGTTAGGTGGCAA (R): TTATTCGCCAATACCGAGGCCA
ERG10	1263-1264	(F): ACTGTTACTGCCGCTAACGCTT (R): TTCGGAAACCAAGATGACGGCT
scR1	1275-1276[a]	(F): CGCGGCTAGACACGGATT (R): GCACGGTGCGGAATAGAGAA

[a] oLP1275 (ALK402) and oLP1276 (oALK403) sequences are from Yang and Kirchmaier 2006.

Appendix B.

Initial analysis of histone H4 lysine point mutant phenotypes

Both *in vitro* and *in vivo* studies have identified lysine residues in the four core histones (H2A, H2B, H3, and H4) and the histone variant H2A.Z that are targeted for acetylation by the histone acetyltransferase Esa1 [reviewed in (Lafon et al. 2007)]. *In vitro*, Esa1 has been shown to target four lysines (K5, K8, K12, K16) on the N-terminal tail of H4 (Clarke et al. 1999). Chromatin immunoprecipitation studies done in *esa1* mutants to examine localized changes in acetylation at candidate genes revealed H4K16 as primarily an *in vitro* but not an *in vivo* target (Suka et al. 2001). A global decrease in acetylation in *esa1* mutants is most dramatic at H4K5 (Clarke et al. 1999), indicating that H4K5 is Esa1's primary *in vivo* target.

The data presented in this Appendix focus on the characterization of mutant phenotypes of the four N-terminal lysines of H4, and their function in relation to Esa1. Each lysine was individually mutated to alanine, glutamine, or arginine (Figure B-1) and tested for temperature-sensitivity and rDNA silencing defects in the presence and absence of wild-type *ESA1*. These residues were used to create the lysine substitution mutants because glutamine is thought to mimic acetylated lysine and arginine is considered to mimic an unacetylated lysine. The alanine substitution provides a small unacetylatable amino acid that is predicted to leave intact the structural integrity of the nucleosome.

188

Figure B-1. Strategy for mutation of H4 lysines to alanine, glutamine, and arginine.

A) Each lysine on the N-terminus of H4 (K5, K8, K12, and K16) was mutated to alanine, glutamine, and arginine, with the exception of the absence of the arginine mutation for H4K16. These substitutions were carried out on the *HHF2* gene on a CEN *TRP1* plasmid. B) These plasmids were individually transformed into a wild-type or *esa1* mutant yeast strain lacking all H3 and H4 chromosomal loci (*hht1-hhf1Δ*, *hht2-hhf2Δ*) carrying a CEN *URA3* covering plasmid with wild-type *HHT2-HHF2*. 5-FOA was then used to counterselect for strains that lost the wild-type *HHT2-HHF2 URA3* plasmid, leaving only the *hhf2* (H4) mutant plasmid.

189

A

B

1. Transform H4
mutant plasmid

2. 5-FOA
WT H4 on
URA3 plasmid
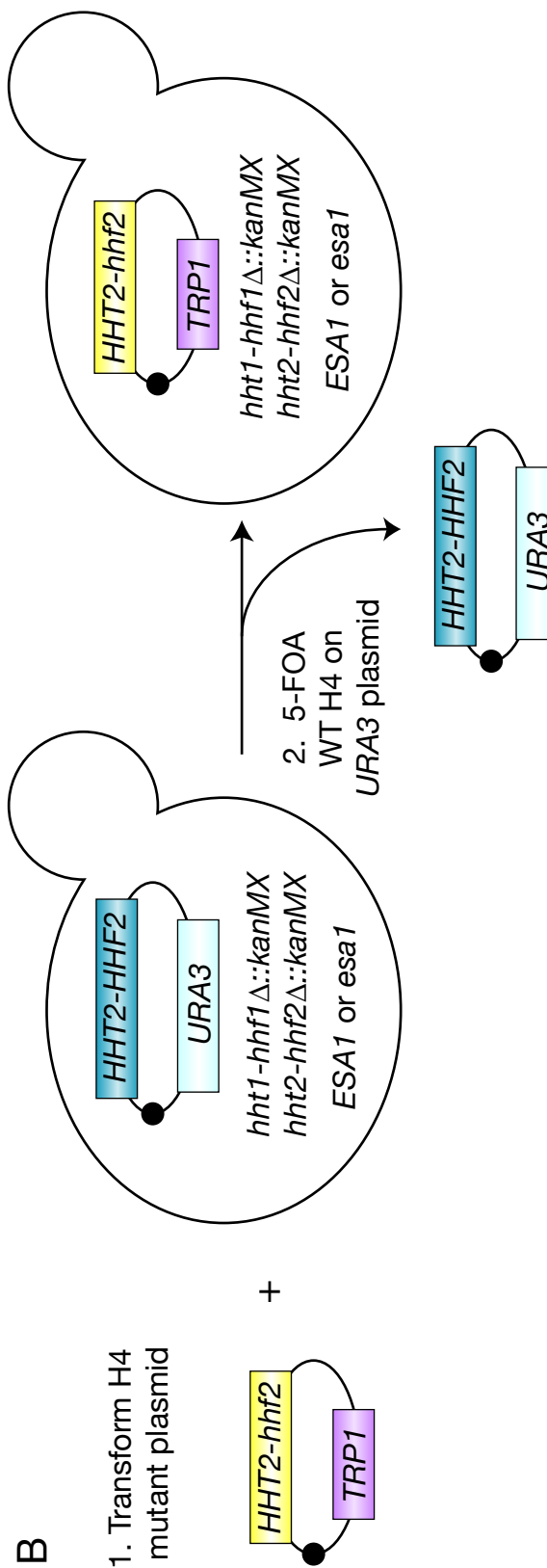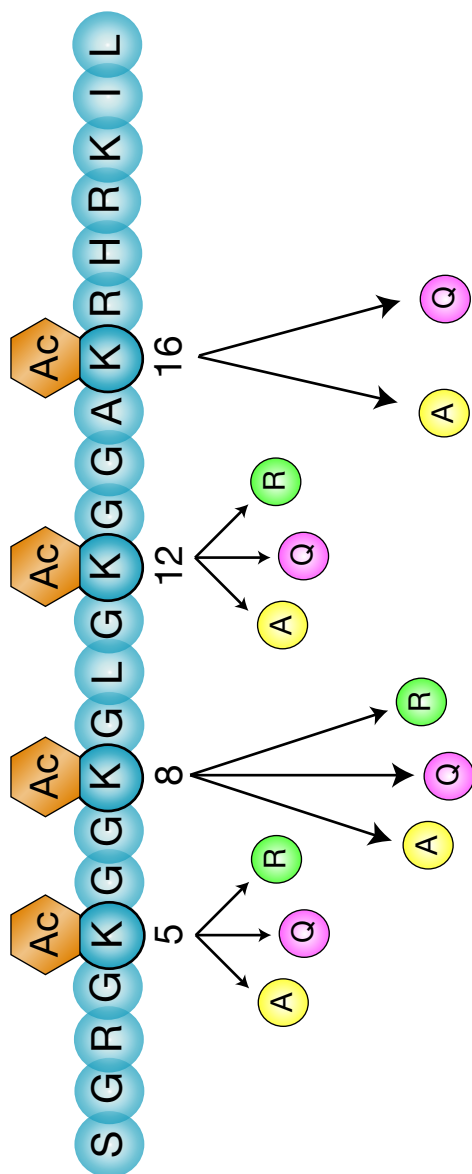
RESULTS

Temperature-sensitivity and synthetic sickness of H4 mutants with *esa1*.

Individual substitution of the H4 lysines (K5, K8, K12, and K16) resulted in viable,

healthy strains with no signs of any growth defect and no temperature-sensitive

phenotypes (Figures B-2, 3, 4, and 5). Thus, no single site mutation of these Esa1 targets

appears to phenocopy the temperature-sensitive *esa1* mutants. This result is not

unexpected, especially considering the large number of Esa1 targets. In combination with

a temperature-sensitive allele of *esa1*, mutation of K5, K8, or K12 (K16, not tested) did

not produce any additive defect or suppressive effect on growth of the *esa1* mutant at

elevated temperature (Figure B-2, 3, 4).

rDNA silencing phenotypes of H4 mutants. When examined for rDNA

silencing defects, the different amino acid substitutions (alanine, glutamine, and arginine)

did not always yield the same result. For example, the H4K5A single mutant is slightly

defective in rDNA silencing yet the H4K5Q and H4K5R mutants both appear to have

intact rDNA silencing (Figure B-6). Also, both the H4K5A and H4K5Q substitutions in

an *esa1* mutant showed moderate suppressive effects on the *esa1* rDNA silencing defect

(Figure B-6). One interpretation of the suppressive effect of the H4K5Q mutation is that

since glutamine mimics an acetylated lysine, it allows for proper rDNA silencing.

The H4K8 mutants had no effect on rDNA silencing and no additional effect in

the *esa1* mutant (Figure B-7). Similar to H4K5, only H4K12A seemed to have a slight

defect in rDNA silencing. However, no improved rDNA silencing was observed with the

H4K12 mutation in the *esa1* mutant (Figure B-8). Thus, H4K12 may function in

promoting silencing at the rDNA, possibly independent of acetylation by Esa1.

Figure B-2. H4K5 point mutants are not temperature-sensitive and are not synthetically sick with *esa1*. Plasmids bearing unacetylatable H4K5 mutants were transformed into WT and *esa1* strains to test for growth at elevated temperature (37˚) on SC. Strains are as follows: WT (LPY12383), H4K5A (LPY12385), H4K5R (LPY12386), H4K5Q (LPY12387), *esa1* (LPY12384), *esa1* H4K5A (LPY12388), *esa1* H4K5R (LPY12389), and *esa1* H4K5Q (LPY12390).

strain	plasmid	30°	37°
WT	WT		
WT	H4K5A		
WT	H4K5R		
WT	H4K5Q		
esa1	WT		
esa1	H4K5A		
esa1	H4K5R		
esa1	H4K5Q		
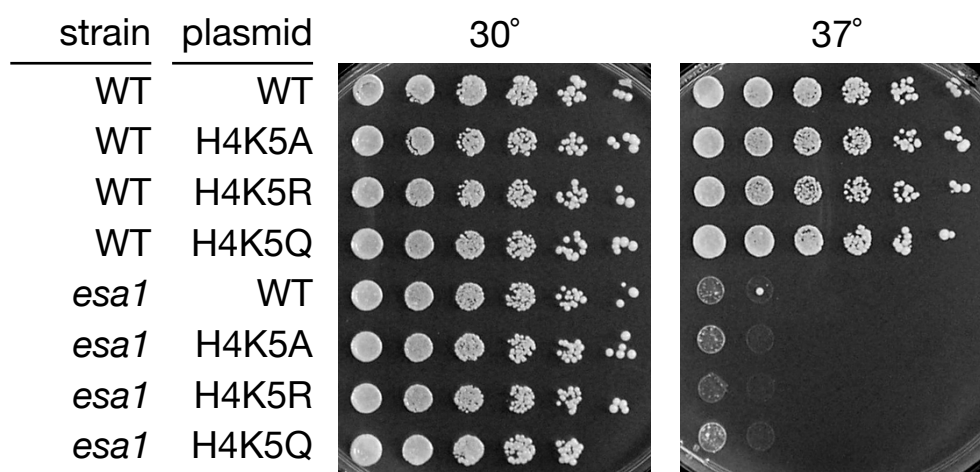
Figure B-3. H4K8 point mutants are not temperature-sensitive and are not synthetically sick with *esa1*. Plasmids bearing unacetylatable H4K8 mutants were transformed into WT and *esa1* strains to test for growth at elevated temperature (37˚) on SC. Strains are as follows: WT (LPY12383), H4K8A (LPY12391), H4K8R (LPY12392), H4K8Q (LPY12393), *esa1* (LPY12384), *esa1* H4K8A (LPY12069), *esa1* H4K8R (LPY11992), and *esa1* H4K8Q (LPY11849).

strain	plasmid	30°	37°
WT	WT		
WT	H4K8A		
WT	H4K8R		
WT	H4K8Q		
esa1	WT		
esa1	H4K8A		
esa1	H4K8R		
esa1	H4K8Q		
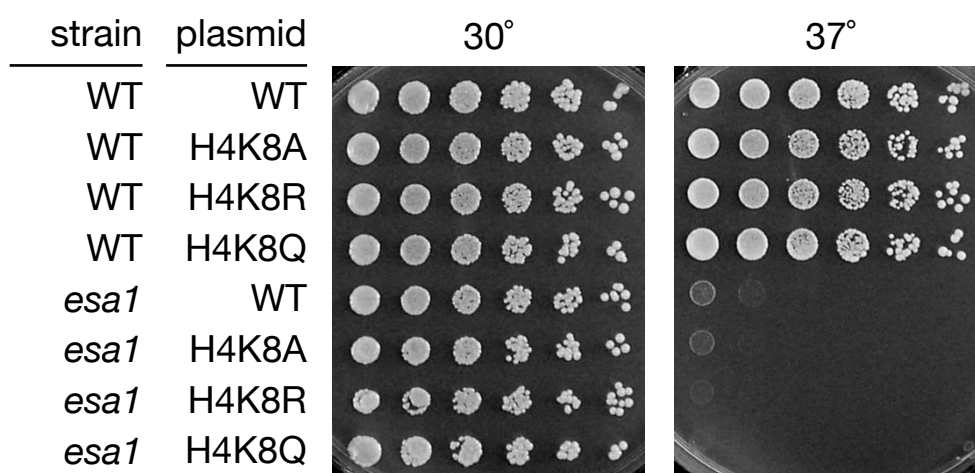
Figure B-4. H4K12 point mutants are not temperature-sensitive and are not synthetically sick with _esa1_. Plasmids bearing unacetylatable H4K12 mutants were transformed into WT and _esa1_ strains to test for growth at elevated temperature (37˚) on SC. Strains are as follows: WT (LPY12383), H4K12A (LPY12394), H4K12R (LPY12395), H4K12Q (LPY12396), _esa1_ (LPY12384), _esa1_ H4K12A (LPY12071), _esa1_ H4K12R (LPY12026), and _esa1_ H4K12Q (LPY11850).

strain	plasmid	30°	37°
WT	WT		
WT	H4K12A		
WT	H4K12R		
WT	H4K12Q		
esa1	WT		
esa1	H4K12A		
esa1	H4K12R		
esa1	H4K12Q		
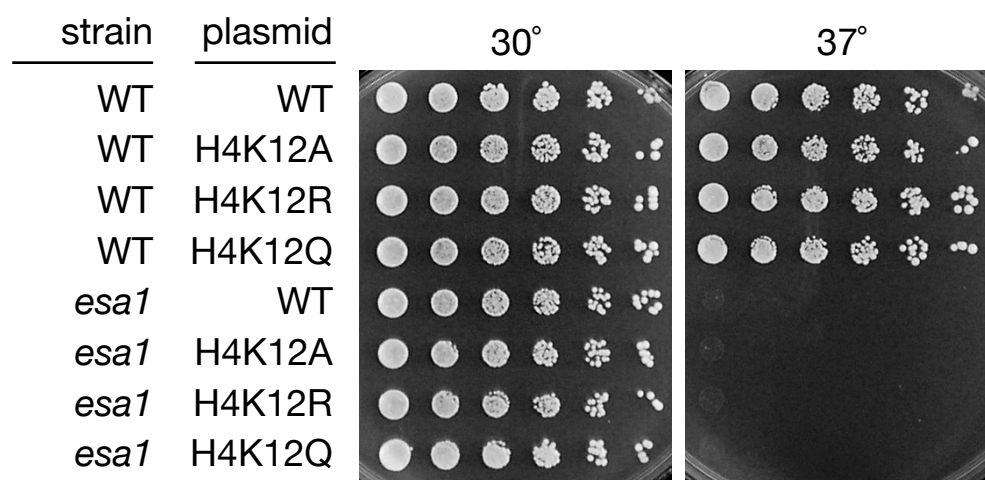
Figure B-5. H4K16 point mutants are not temperature-sensitive. Plasmids bearing

unacetylatable H4K16 mutants were transformed into a WT strain to test for growth at

elevated temperature (37˚) on SC. Strains are as follows: WT (LPY12383), H4K16A

(LPY12399), and H4K16Q (LPY12400). H4K16 mutants were not tested in combination

with *esa1*.

strain	plasmid	30°	37°
WT	WT		
WT	H416A		
WT	H416Q		
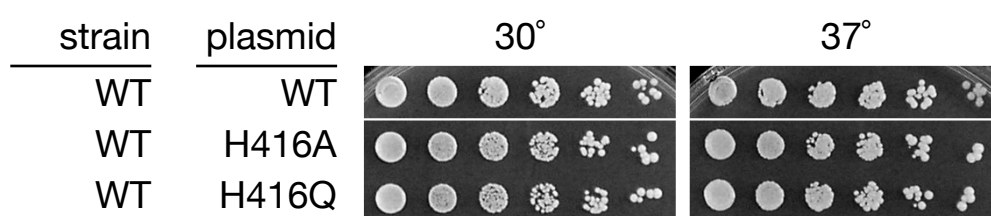
Figure B-6. H4K5 point mutants have distinct effects on rDNA silencing. Strains are as follows: WT (LPY12383), H4K5A (LPY12385), H4K5R (LPY12386), H4K5Q (LPY12387), *esa1* (LPY12384), *esa1* H4K5A (LPY12388), *esa1* H4K5R (LPY12389), and *esa1* H4K5Q (LPY12390). All strains have the rDNA*::ADE2-CAN1* reporter and were plated on SC-Ade-Arg with and without canavanine (32 μg/ml) at 30˚.

strain	plasmid	control	rDNA silencing
WT	WT		
WT	H4K5A		
WT	H4K5R		
WT	H4K5Q		
esa1	WT		
esa1	H4K5A		
esa1	H4K5R		
esa1	H4K5Q		
		SC-Ade-Arg	canavanine
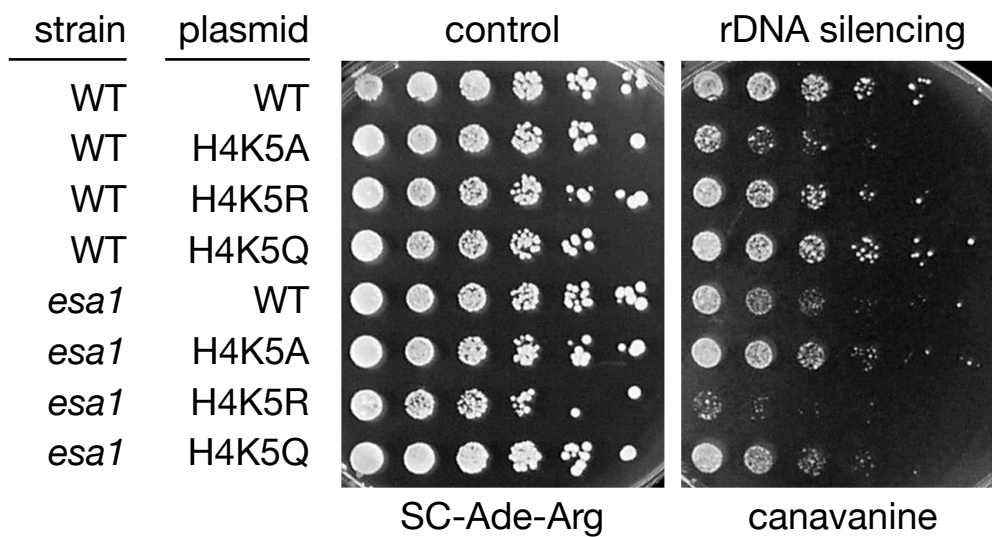
Figure B-7. H4K8 point mutants do not have rDNA silencing defects. Strains are as follows: WT (LPY12383), H4K8A (LPY12391), H4K8R (LPY12392), H4K8Q (LPY12393), *esa1* (LPY12384), *esa1* H4K8A (LPY12069), *esa1* H4K8R (LPY11992), and *esa1* H4K8Q (LPY11849). All strains have the rDNA*::ADE2-CAN1* reporter and were plated on SC-Ade-Arg with and without canavanine (32 µg/ml) at 30˚.

Chr XII ── rDNA ─ rDNA ─ *ADE2* ─ *CAN1* ─ rDNA ─ rDNA ──

strain	plasmid	control	rDNA silencing
WT	WT		
WT	H4K8A		
WT	H4K8R		
WT	H4K8Q		
esa1	WT		
esa1	H4K8A		
esa1	H4K8R		
esa1	H4K8Q		

SC-Ade-Arg   canavanine
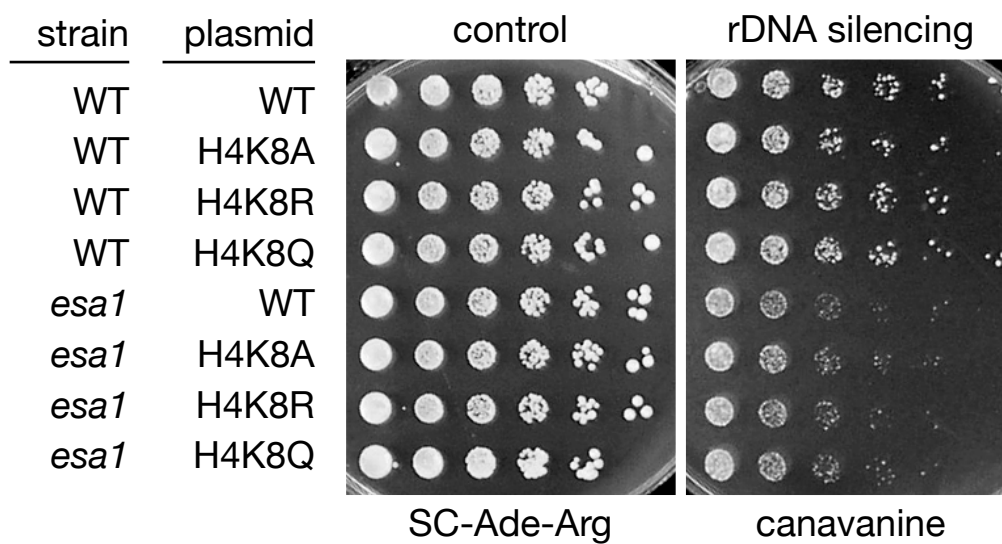
Figure B-8. H4K12 point mutants slightly interfere with rDNA silencing. Strains are as follows: WT (LPY12383), H4K12A (LPY12394), H4K12R (LPY12395), H4K12Q (LPY12396), *esa1* (LPY12384), *esa1* H4K12A (LPY12071), *esa1* H4K12R (LPY12026), and *esa1* H4K12Q (LPY11850). All strains have the rDNA*::ADE2-CAN1* reporter and were plated on SC-Ade-Arg with and without canavanine (32 μg/ml) at 30˚.

Chr XII — rDNA — rDNA — *ADE2* — *CAN1* — rDNA — rDNA —

strain	plasmid	control	rDNA silencing
WT	WT		
WT	H4K12A		
WT	H4K12R		
WT	H4K12Q		
esa1	WT		
esa1	H4K12A		
esa1	H4K12R		
esa1	H4K12Q		
		SC-Ade-Arg	canavanine
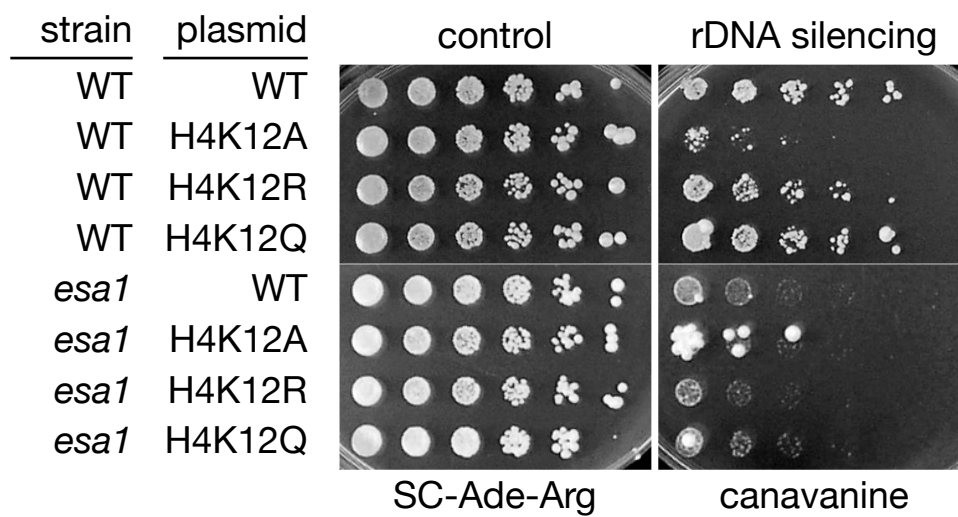
Neither the H4K16A nor H4K16Q mutants displayed any defect in rDNA silencing (Figure B-9), although H4K16 mutants are known to be defective in telomeric silencing (Meijsing and Ehrenhofer-Murray 2001). Sir2 deacetylates H4K16 to promote silent chromatin formation at the telomeres. However, Sir2's precise role in silencing at the rDNA locus is not as clear (Rusche et al. 2003), and based on these results it appears deacetylation by Sir2 of H4K16 may not be as critical in rDNA silencing as it is for telomeric silencing.

Specificity of isoform-specific antisera and crosstalk between neighboring modifications. Since detection of the acetylated lysines on H4 by antisera has been an important tool for all the chapters presented here, it was important to test their specificity. To do this, protein extracts were collected from all the histone mutants and used for immunoblotting with multiple acetyl-specific antisera. This also answered the question of whether mutation of neighboring residues affected the recognition of an acetyl-lysine, or if there was any crosstalk between modifications.

The H4K5Ac, H4K12Ac, and H4K16Ac antisera all performed as expected against protein extracts from the histone mutants (Figure B-10). However, there were two unexpected observations pertaining to H4K5 and H4K8. First, the H4K8Ac antisera displayed reduced but detectable reactivity for all three H4K8 mutants. Second, no reactivity was observed in the H4K5 mutants using anti-H4K8Ac. It is possible that the absence of H4K8 acetylation prevents H4K5 acetylation, although no crosstalk between these two modifications has been previously observed. Another explanation would be that the specificity for anti-H4K8Ac requires H4K5 acetylation.

Figure B-9. H4K16 point mutants do not have rDNA silencing defects. WT

(LPY12383), H4K16A (LPY12399), H4K16Q (LPY12400), *esa1* (LPY12384), *esa1*

H4K16A (LPY12411), and *esa1* H4K16Q (LPY12412), All strains have the

rDNA*::ADE2-CAN1* reporter and were plated on SC-Ade-Arg with and without

canavanine (32 μg/ml) at 30˚.

Chr XII — rDNA — rDNA — *ADE2* — *CAN1* — rDNA — rDNA

strain	plasmid	control	rDNA silencing
WT	WT		
WT	H4K16A		
WT	H4K8Q		
esa1	WT		
esa1	H4K16A		
esa1	H4K8Q		
		SC-Ade-Arg	canavanine

208

Figure B-10. Immunoblots examining specificity and potential crosstalk interference of acetyl-specific antisera. A) Protein extracts were made from WT (LPY12383), H4K5A (LPY12385), H4K5R (LPY12386), H4K5Q (LPY12387), H4K8A (LPY12391), H4K8R (LPY12392), H4K8Q (LPY12393), H4K16A (LPY12399), and H4K16Q (LPY12400), separated on 18% SDS-acrylamide gels, and immunoblotted with anti-H4K5Ac, anti-H4K8Ac, anti-H4K12Ac, or anti-H4K16Ac. H4K5 point mutants are not recognized by anti-H4K5Ac and anti-H4K8Ac. H4K8 mutants are recognized by all three antisera and have reduced signal in anti-H4K8Ac. anti-H4K12Ac recognizes H4K5, H4K8, and H4K16 point mutants. H4K16 mutants are recognized by all three antisera except for anti-H4K16Ac (* denotes that top band is a non-specific band). B) Protein extracts were made from WT (LPY12383), H4K12A (LPY12394), H4K12R (LPY12395), and H4K12Q (LPY12396), separated on an 18% SDS-acrylamide gel, and immunoblotted with anti-H4K12Ac and anti-H4K5Ac. H4K12 mutants are not recognized by anti-H4K12Ac.

A

α-H4K5Ac

α-H4K8Ac

α-H4K12Ac

α-H4K16Ac

WT H4K5A H4K5R H4K5Q H4K8A H4K8R H4K8Q H4K16A H4K16Q

*

B

α-H4K12Ac

α-H4K5Ac

WT H4K12A H4K12R H4K12Q
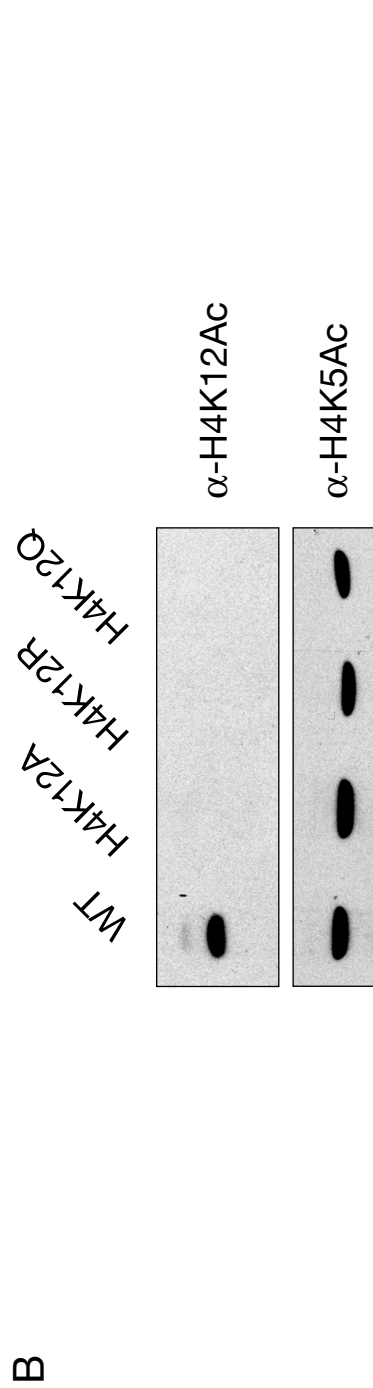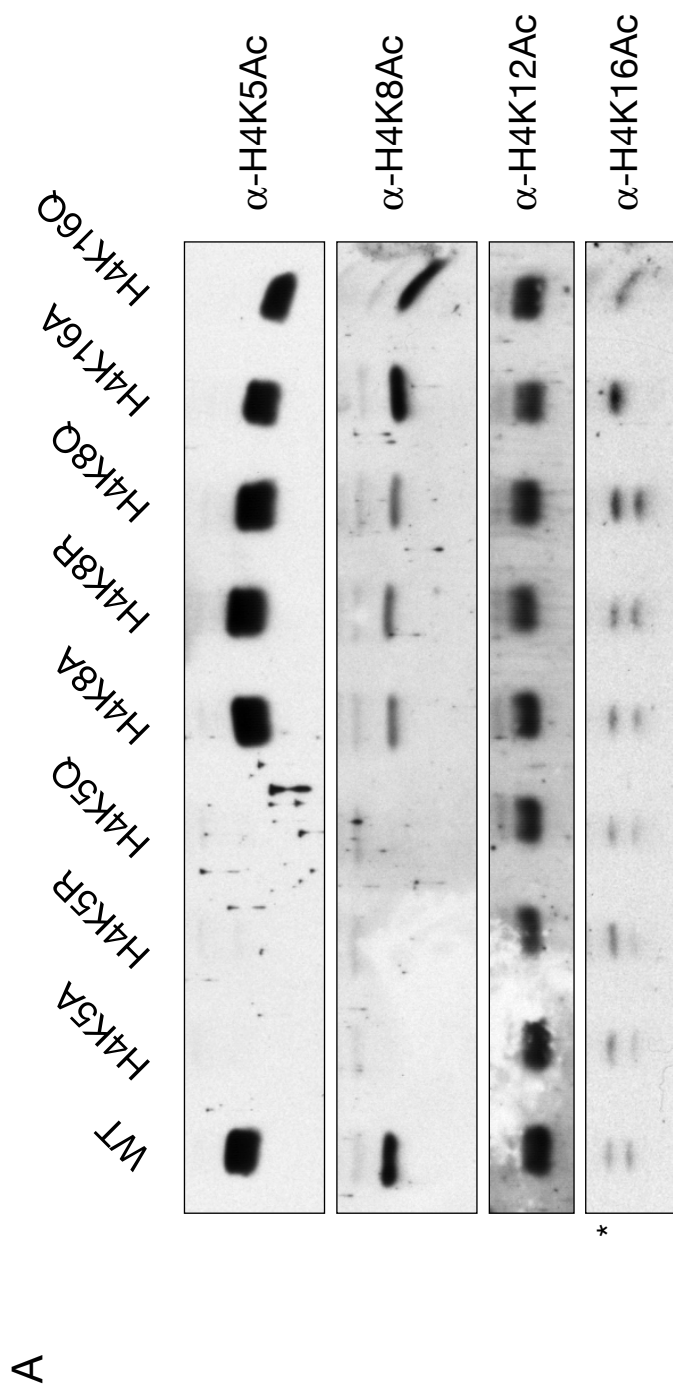
CONCLUSIONS AND FUTURE DIRECTIONS

In this Appendix, a brief survey of phenotypes for H4 lysine mutants was undertaken. For the most part, the results yielded few conclusive phenotypes for these mutants. One general observation is that the lysine to arginine substitutions resulted in strains with less robust growth. Although arginine mimics an unacetylated-lysine by charge, it is also larger in size than lysine, which may be more disruptive to protein structure and stability.

In contrast to H4K16 and its critical role in establishing silencing at the telomeres, H4K5 and H4K12 appear to be the most important for rDNA silencing. This might be expected since both Esa1 and the deacetylase Rpd3 have an *in vivo* global preference to these residues, and both chromatin modifiers are known to function in rDNA silencing, as discussed in Chapter 3.

It is notable that none of the single histone mutants tested here definitively mimics the inviable *esa1Δ*. Therefore, the essential nature of Esa1 can not be attributed solely to acetylation of a specific residue on H4. It is likely that since Esa1 has so many *in vivo* targets, it is required for cell viability because it is needed for acetylation of these multiple lysines.

Since these studies were performed, several resources have become available to the yeast community for studying histone mutants. Two reports have identified specific point mutants that appear to be sensitive to genotoxic agents, as well as residues in the histone core domains that are essential for viability (Huang et al. 2009) (Matsubara et al. 2007). Another group has constructed a comprehensive library containing individual plasmids with each histone residue mutated to alanine (Nakanishi et al. 2008), allowing

for powerful high-throughput genetic screens for mutant phenotypes. These all should be of great use for furthering the preliminary studies presented in this Appendix.

MATERIALS AND METHODS

Construction of histone mutant strains. All strains used in this study are listed in Table B-1. Histone mutant strains, derived from MSY1905 (a generous gift from M. M. Smith) (Ruault and Pillus 2006) are chromosomally deleted for both *HHF-HHT* loci, and initially contained wild-type histones on the plasmid pJH33 (*CEN URA3 HTA1 HTB1 HHF2 HHT2*) (Ahn et al. 2005). For mutant construction, strains were transformed with a *TRP1* plasmid containing the relevant H4 (*HHF2*) mutation, and then subjected to a plasmid shuffle by counterselection on 5-FOA to recover cells bearing only the newly mutated or control plasmid (Figure B-1). All plasmids used in this study are listed in Table B-2. Histone mutant plasmids were constructed by site-directed mutagenesis using rolling-circle amplification with oligonucleotide sequences listed in Table B-3. Plasmids were confirmed to contain only the indicated mutation by DNA sequencing.

Acknowledgements. All experiments in this Appendix were performed in collaboration with Erin Scott. Mitch Smith provided the original histone mutant background strain. DNA Sequencing was performed by the Moores UCSD Cancer Core Sequencing Facility.

Table B-1. Yeast strains used in Appendix B

Strain	Genotype	Reference
LPY5 (W303-1a)	*MAT*a *ade2-1 can1-100 his3-11,15 leu2-3,112 trp1-1 ura3-1*	Thomas and Rothstein 1989
LPY11816	W303 *MATα hht1-hhf1Δ::kanMX hht2-hhf2Δ::kanMX hta2-htb2Δ::HPH* rDNA*::ADE2-CAN1* + pJH33	
LPY11817	W303 *MATα esa1-414 hht1-hhf1Δ::kanMX hht2-hhf2Δ::kanMX hta2-htb2Δ::HPH* rDNA*::ADE2-CAN1* + pJH33	
LPY12383	LPY11816 + pLP1775 (no pJH33)	
LPY12385	LPY11816 + pLP2181 (no pJH33)	
LPY12386	LPY11816 + pLP2185 (no pJH33)	
LPY12387	LPY11816 + pLP2184 (no pJH33)	
LPY12391	LPY11816 + pLP2145 (no pJH33)	
LPY12392	LPY11816 + pLP2138 (no pJH33)	
LPY12393	LPY11816 + pLP2121 (no pJH33)	
LPY12394	LPY11816 + pLP2146 (no pJH33)	
LPY12395	LPY11816 + pLP2142 (no pJH33)	
LPY12396	LPY11816 + pLP2125 (no pJH33)	
LPY12399	LPY11816 + pLP1990 (no pJH33)	
LPY12400	LPY11816 + pLP1972 (no pJH33)	
LPY12384	LPY11817 + pLP1775 (no pJH33)	
LPY12384	LPY11817 + pLP1775 (no pJH33)	
LPY12388	LPY11817 + pLP2181 (no pJH33)	
LPY12389	LPY11817 + pLP2185 (no pJH33)	
LPY12390	LPY11817 + pLP2184 (no pJH33)	
LPY12069	LPY11817 + pLP2145 (no pJH33)	
LPY11992	LPY11817 + pLP2138 (no pJH33)	
LPY11849	LPY11817 + pLP2121 (no pJH33)	
LPY12071	LPY11817 + pLP2146 (no pJH33)	
LPY12026	LPY11817 + pLP2142 (no pJH33)	
LPY11850	LPY11817 + pLP2125 (no pJH33)	
LPY12411	LPY11817 + pLP1990 (no pJH33)	
LPY12412	LPY11817 + pLP1972 (no pJH33)	

Table B-2. Plasmids used in Appendix B

Plasmid (alias)	Description	Source/Reference
pJH33	*HTA1 HTB1 HHF2 HHT2 URA3*	Ahn et al. 2005
pLP1775	*HHF2 HHT2 TRP1* CEN	S. L. Berger
pLP2181	*hhf2-K5A HHT2 TRP1* CEN	
pLP2185	*hhf2-K5R HHT2 TRP1* CEN	
pLP2184	*hhf2-K5Q HHT2 TRP1* CEN	
pLP2145	*hhf2-K8A HHT2 TRP1* CEN	
pLP2138	*hhf2-K8R HHT2 TRP1* CEN	
pLP2121	*hhf2-K8Q HHT2 TRP1* CEN	
pLP2146	*hhf2-K12A HHT2 TRP1* CEN	
pLP2142	*hhf2-K12R HHT2 TRP1* CEN	
pLP2125	*hhf2-K12Q HHT2 TRP1* CEN	
pLP1990	*hhf2-K16A HHT2 TRP1* CEN	
pLP1972	*hhf2-K16Q HHT2 TRP1* CEN	

Unless otherwise noted, plasmids were constructed during the course of this study or are part of the standard lab collection.

Table B-3. Oligonucleotide sequences used in Appendix B

Oligo #	Name	Sequence (5'-3')
921	H4K5A sense	TCCGGTAGAGGT**GC**AGGTGGTAAAGG
922	H4K5A antisense	CCTTTACCACCT**GC**ACCTCTACCGGA
873	H4K5R sense	TCCGGTAGAGGT**G**CAGGTGGTAAAGG
874	H4K5R antisense	CCTTTACCACCT**G**CACCTCTACCGGA
858	H4K5Q sense	TCCGGTAGAGGT**C**AAGGTGGTAAAGG
859	H4K5Q antisense	CCTTTACCACCTT**G**ACCTCTACCGGA
898	H4K8A sense	GTAAAGGTGGT**GC**AGGTCTAGGAAAAGG
899	H4K8A antisense	CCTTTTCCTAGACCT**GC**ACCACCTTTAC
886	H4K8R sense	GTAAAGGTGGT**CG**AGGTCTAGGAAAAGG
887	H4K8R antisense	CCTTTTCCTAGACCT**CG**ACCACCTTTAC
860	H4K8Q sense	GTAAAGGTGGT**C**AAGGTCTAGGAAAAGG
861	H4K8Q antisense	CCTTTTCCTAGACCTT**G**ACCACCTTTAC
900	H4K12A sense	AAGGTCTAGGA**GC**AGGTGGTGCCAAGC
901	H4K12A antisense	GCTTGGCACCACCT**GC**TCCTAGACCTT
888	H4K12R sense	AAGGTCTAGGA**CG**AGGTGGTGCCAAGC
889	H4K12R antisense	GCTTGGCACCACCT**CG**TCCTAGACCTT
864	H4K12Q sense	AAGGTCTAGGA**C**AAGGTGGTGCCAAGC
865	H4K12Q antisense	GCTTGGCACCACCTT**G**TCCTAGACCTT
788	H4K16A sense	GGAAAAGGTGGTGCC**GC**GCGTCACAGAA AGATT
789	H4K16A antisense	AATCTTTCTGTGACGC**GC**GGCACCACCTT TTCC
772	H4K16Q sense	GGAAAAGGTGGTGCC**C**AGCGTCACAGAA AGATTC
773	H4K16Q antisense	GAATCTTTCTGTGACGCT**G**GGCACCACCT TTCC

Nucleotides in **bold underline** in the above sequences are mutagenic, compared to the wild-type sequence.

Appendix C.

Analysis of *NRD1* in chromatin functions

   NRD1 (<u>n</u>uclear pre-m<u>R</u>NA <u>d</u>own-regulation) is an essential gene that encodes an

RNA binding protein with tightly linked functions to *NAB3*. Nrd1 and Nab3 function

together to process 3' end termination of specific classes of transcripts. These transcripts

are primarily non-polyadenylated RNAs that include snRNAs, snoRNAs, and CUTs

(cryptic untstable transciprts) [reviewed in (Lykke-Andersen and Jensen 2007)]. Because

of the connections identified in Chapter 2 between Nab3 and the histone acetyltransferase

Esa1, and the known similarities between Nab3 and Nrd1, Nrd1 was chosen for further

examination of possible links to Esa1.

RESULTS

   Overexpression of *NRD1* suppresses *esa1* mutant phenotypes. Although *NRD1*

was not identified as a high-copy suppressor of *esa1* in the screen described in Chapter 2,

the many known connections between *NRD1* and *NAB3* hinted that *NRD1* might also

function as a high-copy suppressor of *esa1*. Indeed, *NRD1* overexpression had similar

effects to *NAB3* overexpression in *esa1* strains. *NRD1*, when overexpressed from a 2-

micron high-copy plasmid was able to suppress the temperature sensitive phenotype of

esa1 (Figure C-1), and increased dosage of *NRD1* also suppressed rDNA silencing

defects in *esa1* (Figure C-1). Both of these results are consistent with *NAB3*

overexpression although *NRD1* overexpression often resulted in a lesser degree of

suppression than *NAB3* (Figure C-1).

Figure C-1. *NRD1* is also a high-copy suppressor of *esa1-414*.

A) 2-micron overexpression of *NRD1* weakly suppresses the temperature-sensitivity of *esa1-414*. LPY3291 (*esa1Δ::HIS3* + pLP863 - *esa1-414*/*TRP1*/CEN) was transformed with 2-micron plasmids containing high-copy suppressor *NAB3* (pLP2018), *NRD1* (pLP2054), or vector (pLP362). Serial dilutions of multiple isolates from the transformations were plated on SC-Ura-Trp at permissive (30˚) and restrictive temperatures (34˚ and 35˚) to test for suppression of temperature-sensitivity. Weak but reproducible suppression was observed. B) Overexpression of *NRD1* suppresses *esa1*'s rDNA silencing defect. WT (LPY4909) and *esa1-414* (LPY4911) have the rDNA*::ADE2-CAN1* silencing marker. Both strains were transformed with 2-micron overexpression plasmids containing vector (pLP362), *NAB3* (pLP2018), or *NRD1* (pLP2054) and plated on SC-Ade-Arg-Ura at 33˚ with and without canavanine (8 μg/ml and 16 μg/ml) to test for silencing.

A

	30°	34°	35°

esa1-414: vector, vector, NAB3, NAB3, NAB3, NRD1, NRD1, NRD1

SC-Ura-Trp

B

Chr XII — rDNA – rDNA – *ADE2* – *CAN1* – rDNA – rDNA

strain	plasmid	control	rDNA silencing	rDNA silencing
WT	vector			
WT	NAB3			
WT	NRD1			
esa1	vector			
esa1	NAB3			
esa1	NAB3			
esa1	NRD1			
esa1	ESA1			

SC-Ade-Arg-Ura | cananvanine 8 µg/ml | canavanine 16 µg/ml
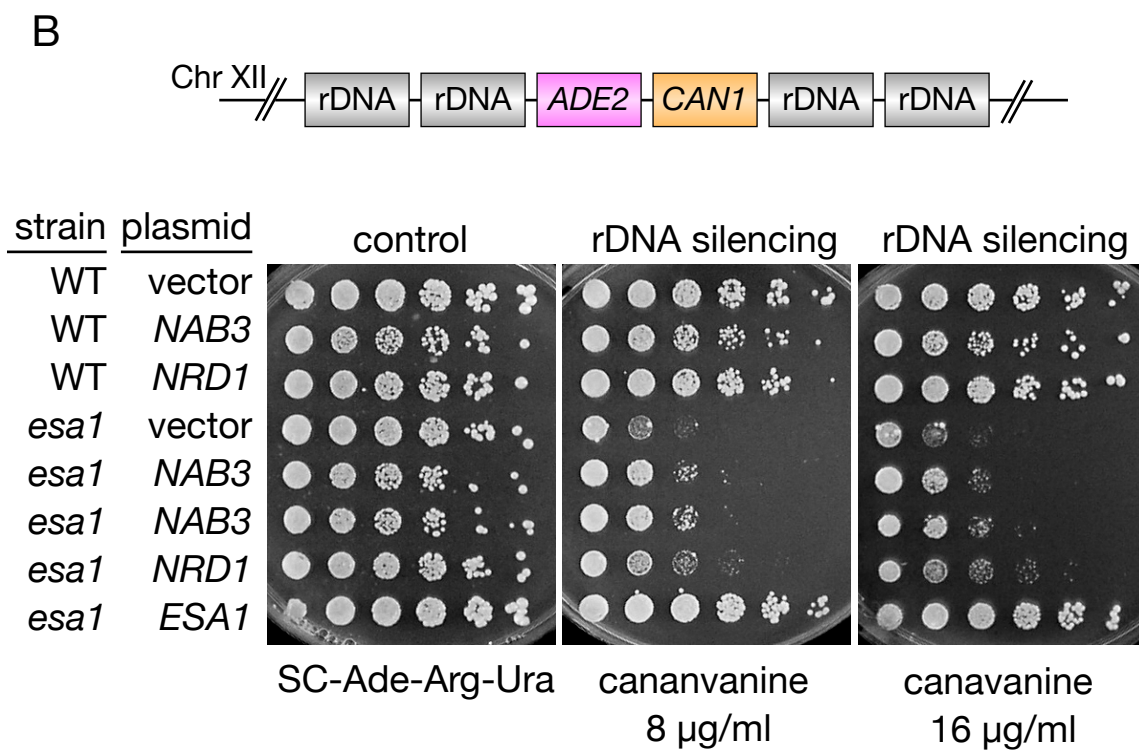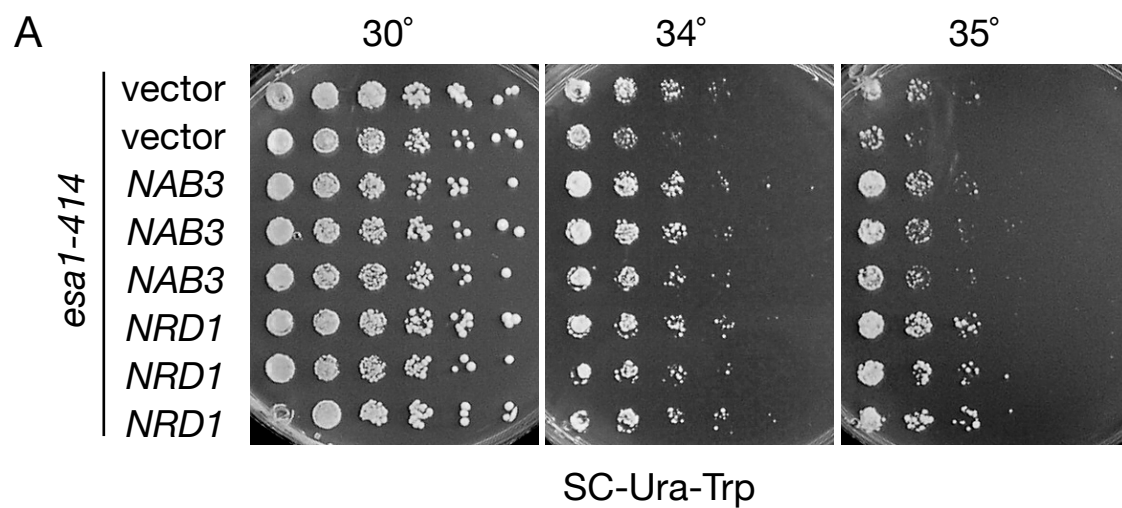
Evaluation of *nrd1* mutant phenotypes. Because *NRD1* is essential for viability, over the years many *nrd1* conditional alleles have been constructed and characterized (Steinmetz and Brow 1996; Conrad et al. 2000). To determine whether *NRD1* function was required for the specific nuclear processes that were discovered in Chapter 2 to require *NAB3*, *nrd1* mutants were tested for defects in transcriptional silencing and sensitivity to DNA damage. Nrd1 contains four defined regions (Figure C-2). Two of these are motifs rich in specific amino acids that are found in other RNA-binding proteins: an arginine/glutamate, arginine/serine region and a proline/glutamine region. Nrd1 also has an RNA-recognition motif (RRM) similar to those found in RNA-binding proteins, and a region at the N-terminus that interacts with the CTD of RNA polymerase II (CID) (Steinmetz and Brow 1996).

The *nrd1-3*, *nrd1-5*, *nrd1-101*, and *nrd1-102* alleles were chosen for an initial test of phenotypes. Both *nrd1-5* and *nrd1-102* contain point mutations within the RRM. The *nrd1-3* allele contains a point mutation that results in an early truncation, and *nrd1-101* is a point mutant in the CID (Steinmetz and Brow 1996; Conrad et al. 2000)(Figure C-2). These alleles were obtained on low-copy centromeric plasmids and used in *nrd1Δ* strains. The data presented below are preliminary studies of phenotypes for the various *nrd1* mutants, and therefore not all *nrd1* alleles have been tested for all the phenotypes.

First, *nrd1-3* and *nrd1-5* mutants were tested for sensitivity to DNA damage. As described in Chapter 2, *nab3* mutants are sensitive to the DNA damaging agent camptothecin. However, *nrd1-3* displayed no sensitivity, whereas *nrd1-5* displayed a slight resistance to camptothecin (Figure C-3). The *nrd1-101* and *nrd1-102* mutants were next tested for rDNA silencing defects using the rDNA::*ADE2-CAN1* reporter. These two

Figure C-2. Nrd1 protein domain map and location of mutant alleles. Nrd1 has four

defined features. The N-terminal domain of Nrd1, or the CTD-interacting domain (CID)

interacts with the C-terminal domain (CTD) of RNA polymerase II. Nrd1 also has a short

stretch of residues with a high density of alternating arginine/glutamate (RE) and

arginine/serine (R/S) pairs and an RNA-recognition motif (RRM) often found in RNA

binding proteins. At the C-terminus, there is another stretch of residues rich in glutamine

and proline (P/Q) (Steinmetz and Brow 1996). The mutant proteins nrd1-3 and nrd1-5 are

illustrated below wild-type Nrd1. The second set of mutants, nrd1-101 and nrd1-102,

includes a double-HA tag at the C-terminus.
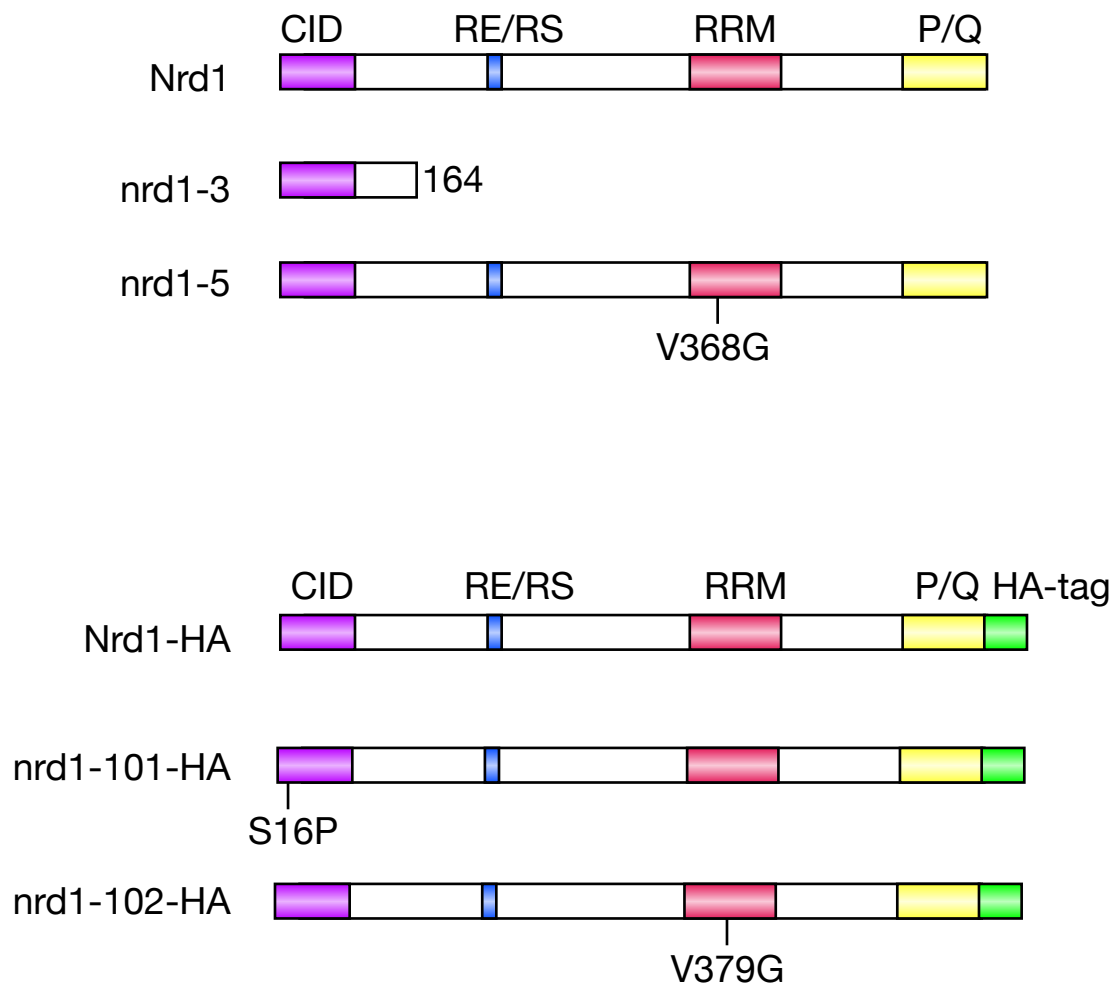
Figure C-3. The *nrd1-5* mutant is temperature-sensitive and slightly resistant to the DNA damaging agent camptothecin. A) *nrd1Δ* strains carrying plasmids with either wild-type *NRD1* (LPY11715), *nrd1-3* (LPY11719), or *nrd1-5* (LPY11723) were plated at permissive (30˚) and elevated (34˚) temperature on SC-Ura to confirm temperature-sensitivity. B) The same strains as above were plated on SC-Ura control (DMSO) and camptothecin (25 μg/ml) to test for response to camptothecin at 30˚.

A
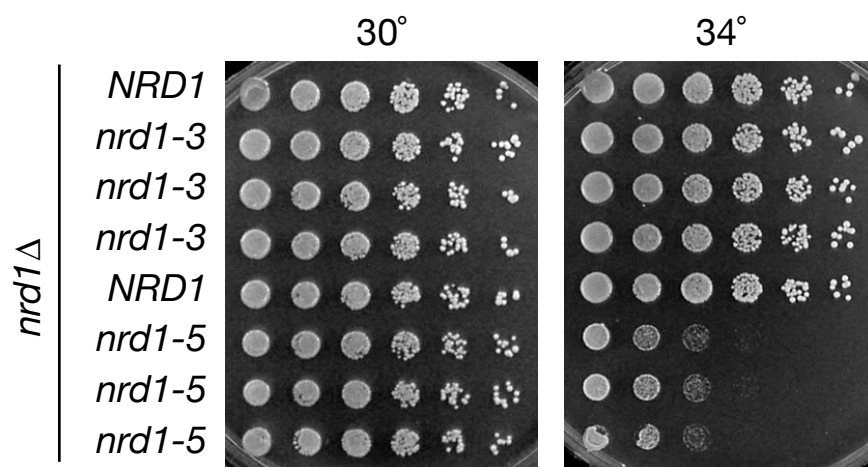
B
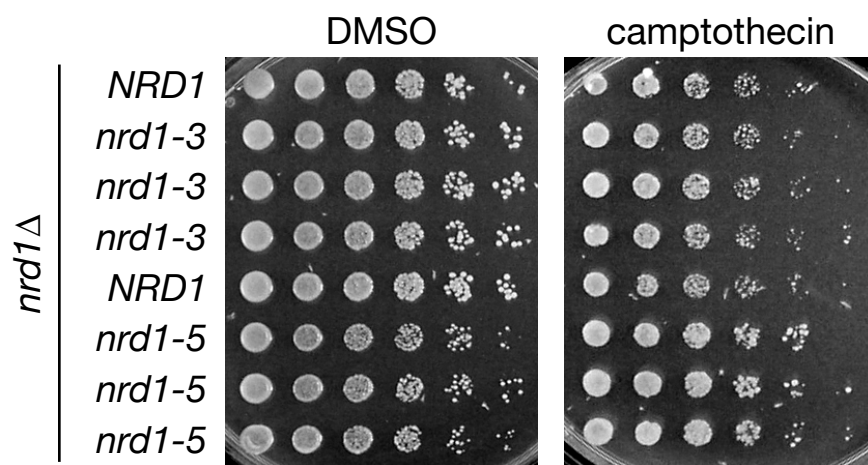
alleles contain point mutations in different critical regions of *NRD1* (Figure C-2). From Chapter 2, it was found that *nab3* mutants are defective in rDNA silencing and overexpression of *NAB3* was found to rescue the silencing defect of *esa1* mutants. The *nrd1-102* RRM mutant, but not the *nrd1-101* CID mutant, showed a defect in rDNA silencing (Figure C-4). Therefore, Nrd1 is needed to maintain proper rDNA silencing, and this role relies on its ability to bind RNA but not its interactions with RNA polymerase II. Several double mutants were constructed of *nrd1* with *esa1*, and of these tested no additional silencing defects were observed (Figure C-4).

CONCLUSIONS AND FUTURE DIRECTIONS

As a continuation of the story presented in Chapter 2, which defined new roles in connection to the histone acetyltransferase Esa1 for the RNA binding protein Nab3, this Appendix reports explore a beginning of new roles for Nrd1, a closely-related RNA binding protein. Similar to *NAB3*, *NRD1* overexpression was found to suppress the temperature-sensitivity and rDNA silencing defect of an *esa1* mutant. In addition, some *nrd1* mutants displayed rDNA silencing and DNA damage phenotypes.

Integration of *nrd1* mutant alleles. To further study the *nrd1-101* and *nrd1-102* mutants, plasmids were obtained (Conrad et al. 2000) (J. Corden) to construct chromosomally integrated alleles. These alleles also have a double-HA tag at the C-terminus. The wild-type *NRD1* with the HA-tag was successfully integrated using the strategy diagrammed in Figure C-5. However, integration of *nrd1-101* and *nrd1-102* alleles were attempted but resulted in only incorrect integrants. Since gene dosage on centromeric plasmids can vary from cell to cell, construction of *nrd1* integrated alleles

224

Figure C-4. The *nrd1-102* allele, which has a RRM domain mutation is defective in rDNA silencing. A) *nrd1-101* and *nrd1-102* mutants were tested for rDNA silencing phenotypes using the rDNA::*ADE2-CAN1* reporter. The *nrd1Δ* strains carrying plasmids with either wild-type *NRD1* (LPY11872), *nrd1-101* (LPY11873), or *nrd1-102* (LPY11874) were plated at 25˚ and 30˚ on SC-Ade-Arg-Leu with and without canavanine (32 μg/ml) to test for rDNA silencing defects in comparison to *esa1-414* (LPY11875). The modest *nrd1-102* rDNA silencing defect is visible at 25˚ (bolded). The *nrd1-102* allele is inviable at 30˚ as seen below in part B). B) *esa1 nrd1* double mutants display rDNA silencing defects similar to each single mutant. Top: *esa1-414 nrd1Δ* strains carrying plasmids with either wild-type *NRD1* (LPY11875), *nrd1-101* (LPY11876), or *nrd1-102* (LPY11877) all have the rDNA::*ADE2-CAN1* reporter and were plated at 25˚ on SC-Ade-Arg-Leu with and without canvanine (32 μg /ml) to test for rDNA silencing defects. Bottom: same as above except strains were plated at 30˚ on SC-Ade-Arg-Leu with and without canavanine (16 μg/ml). The equivalent silencing defect in *esa1*, *esa1 nrd1-102*, and *nrd1-102* can be seen in the bolded rows.

Chr XII rDNA — rDNA — *ADE2* — *CAN1* — rDNA — rDNA

A

strain	plasmid	control	rDNA silencing	
nrd1Δ	*NRD1*			
nrd1Δ	*NRD1*			
esa1 nrd1Δ	*NRD1*			
esa1 nrd1Δ	*NRD1*			25°
nrd1Δ	*nrd1-101*			
nrd1Δ	*nrd1-101*			
nrd1Δ	**nrd1-102**			
nrd1Δ	**nrd1-102**			
nrd1Δ	*NRD1*			
nrd1Δ	*NRD1*			
esa1 nrd1Δ	*esa1-414*			
esa1 nrd1Δ	*esa1-414*			30°
nrd1Δ	*nrd1-101*			
nrd1Δ	*nrd1-101*			

SC-Ade-Arg-Leu   canavanine

B

strain	plasmid	control	rDNA silencing	
nrd1Δ	*NRD1*			
esa1 nrd1Δ	**NRD1**			
nrd1Δ	*nrd1-101*			
nrd1Δ	**nrd1-102**			25°
esa1 nrd1Δ	*nrd1-101*			
esa1 nrd1Δ	*nrd1-101*			
esa1 nrd1Δ	**nrd1-102**			
esa1 nrd1Δ	**nrd1-102**			
nrd1Δ	*NRD1*			
esa1 nrd1Δ	*NRD1*			
nrd1Δ	*nrd1-101*			30°
nrd1Δ	*nrd1-102*			
esa1 nrd1Δ	*nrd1-101*			

SC-Ade-Arg-Leu   canavanine

226

Figure C-5. *NRD1* **tagging strategy and confirmation of integration.** A) Successful

NRD1 HA-tagging at its chromosomal locus was performed using the *URA3* integrating

plasmid pJC743. First, pJC743 was digested with BsrGI and transformed into W303-1a.

Unsuccessful attempts were made using pJC744 (*nrd1-101*) and pJC745 (*nrd1-102*) with

BsrGI and SfoI, respectively. After selection on SC-Ura plates, transformants contain the

endogenous wild-type copy of *NRD1* followed by the *URA3* gene and the integrated

NRD1 allele. Excision of *URA3* with one of the *NRD1* copies was performed on 5-FOA

to yield either *NRD1* wild-type or *NRD1-HA$_2$*. B) Correct tagging was confirmed by

immunoblotting for anti-HA. Whole cell extracts were prepared from candidate strains

and resolved on an 8% SDS-polyacrylamide gel, transferred to nitrocellulose, and probed

with an anti-HA antibody. Lane 1-2: *NRD1-HA$_2$* (LPY11682 and LPY11683); Lane 3-6:

incorrect integrants; Lane 7: W303-1a; Lane 8: *HSL7-HA$_3$* (LPY9119). C) Molecular

genotyping was performed by amplification of the *NRD1* region using oligonucleotides

(oLP813 and oLP814) followed by digestion with BamHI. Correct integration introduces

a BamHI site at the 3' end of the HA-tag. Lane 1: *NRD1-HA$_2$* (LPY11682); Lane 2:

incorrect integrant; Lane 3: W303-1a.
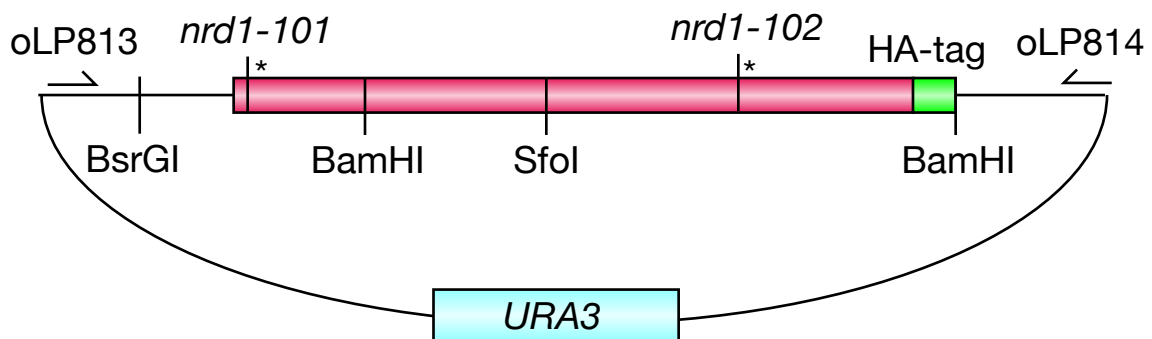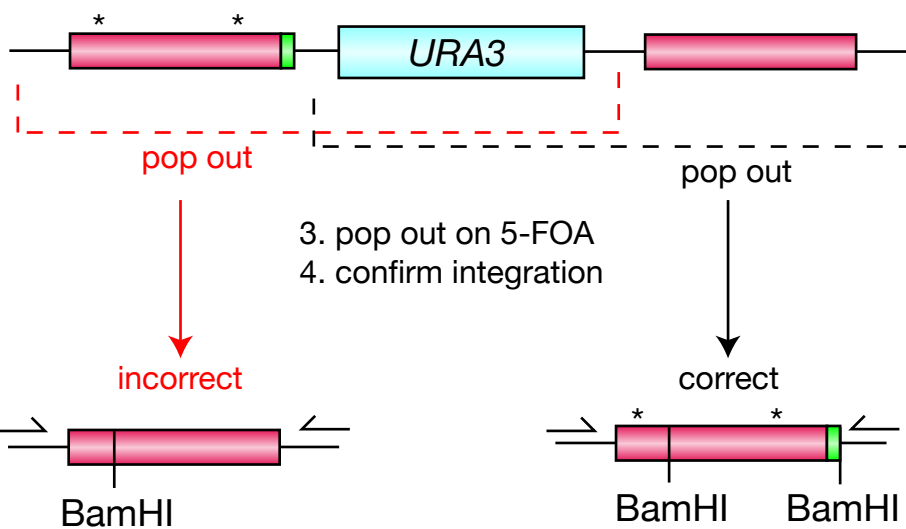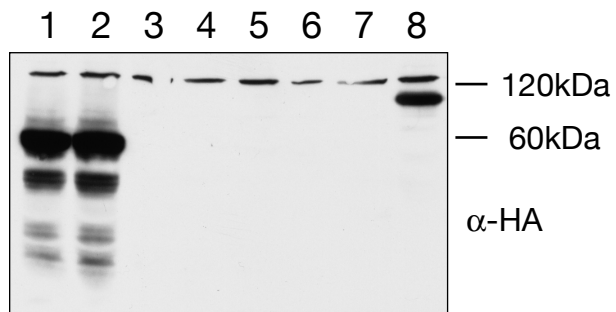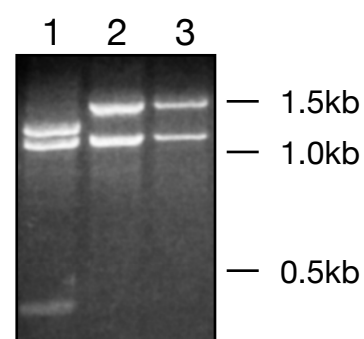
will be necessary for furthering the studies presented here of Nrd1 roles in rDNA silencing and the DNA damage response.

Nrd1 and DNA damage. Of the different processes examined for *NRD1* in this Appendix, most phenotypic analysis proved similar to results obtained in Chapter 2 for *NAB3*. Thus far, Nab3 and Nrd1 have been thought to function together [reviewed in (Lykke-Andersen and Jensen 2007)], and the two proteins have been purified as a heterodimer with a 1:1 ratio (Carroll et al. 2007). However, the observation that a particular *nrd1* mutant, *nrd1-5*, displayed modest resistance to the DNA damaging agent camptothecin (Figure C-3), in contrast to *nab3* mutants, which are sensitive to camptothecin (Figure 2-9). Since the effect was subtle, it would be useful to test the modest resistance observed for *nrd1-5* at higher concentrations of camptothecin. The *nab3* allele used in Chapter 2 was a *nab3-10* mutant that contained a single amino acid substitution in its RRM domain. The *nrd1* camptothecin resistant mutant allele, *nrd1-5*, is also a single amino acid substitution in its RRM domain. It would be useful to test the other *nrd1* RRM mutant, *nrd1-102*, to test if camptothecin resistance results as a general failure from Nrd1, but not Nab3, to bind to RNA. One distinguishing feature of Nrd1 is that its N-terminal CID domain physically contacts the CTD of RNAPII (Conrad et al. 2000) . Since *nrd1-101* is a point mutant in the CID domain, *nrd1-101* should also be tested for camptothecin resistance to find out if interaction with the CTD is important for Nrd1's role in DNA damage.

Although mutation or deletion of many genes results in sensitivity to camptothecin, few mutants have been identified that are resistant to camptothecin. One group of genes that has been identified encodes proteasome chaperones that aid in 20S

proteasome assembly (Le Tallec et al. 2007). One hypothesis to explain *nrd1* resistance to camptothecin would be that Nrd1 down-regulates some of these proteasome chaperone genes. Different sequence motifs have been identified for Nrd1 and Nab3 binding to RNA targets (Carroll et al. 2004). Many transcripts known to be regulated by the Nrd1/Nab3 complex contain multiple binding sites for both proteins. It is possible that specific transcripts that affect the transcriptional DNA damage response would contain sites for Nrd1 and not Nab3, implying that Nrd1 may function at these genes without Nab3. To determine if the resistance to DNA damage of *nrd1* mutants is a general property, response to other forms of DNA damage should be tested in *nrd1* mutants. These studies should further the understanding of Nrd1 function in termination of transcripts in response to DNA damage or reveal a new role for Nrd1 in addition to 3' end termination.

MATERIALS AND METHODS

Yeast strains and plasmids. All strains and plasmids used in this study are listed in Tables C-1 and C-2. All *nrd1Δ* strains originate from a *nrd1Δ::kanMX/NRD1* (LPY11620) heterozygous diploid constructed by amplification (oligonucleotides listed in Table C-3) of the *kanMX* cassette from *Saccharomyces* Genome Deletion Project strain, transformed into a W303 diploid (LPY1552). LPY11620 was transformed with a wild-type *NRD1* plasmid (pLP2054) and tetrads were dissected to yield *nrd1Δ* haploid strains carrying pLP2054. The *esa1 nrd1* double mutants and rDNA silencing marker (rDNA*::ADE2-CAN1*) (Fritze et al. 1997) were introduced through standard genetic crosses. The *nrd1-3* and *nrd1-5* strains (LPY11715, 11719, 11723) were constructed by a

series of plasmid shuffles in a heterozygous *nrd1Δ::kanMX*/*NRD1* diploid strain so that
only the relevant *NRD1* mutation on a *URA3* plasmid remained. Diploids were then
dissected to yield LPY11715, LPY11719, and LPY11723. The *nrd1-101* and *nrd1-102*
strains (LPY11872-11877) were constructed by transforming in the relevant mutation on
a *LEU2* plasmid into a haploid *nrd1Δ::kanMX* strain covered by pLP2054
(*NRD1*/2μ/*URA3*), and then subjected to a plasmid shuffle by counterselection on 5-FOA
for loss of pLP2054. *NRD1* was HA-tagged at its chromosomal locus using *URA3*
integrating plasmid pJC743 (J. Corden). pJC743 was digested with BsrGI, and
transformed into W303-1a. After selection for integration of the plasmid on SC-Ura
plates, excision of the wild-type allele was selected for on 5-FOA to yield *NRD1-HA$_2$*
(LPY11682 and LPY11683). Correct tagging was confirmed by anti-HA western and
molecular genotyping (see Figure C-5 for details). pLP2054 was constructed by
subcloning from pLP2009 (E. Steinmetz and D. Brow) into pRS426 using SalI and NotI
restriction sites. Digestion of pLP2009 with SalI and NotI yields a 3.6 kb insert that
contains *NRD1* sequence.

Table C-1. Yeast strains used in Appendix C

Strain	Genotype	Reference
LPY5 (W303-1a)	*MAT*a *ade2-1 can1-100 his3-11,15 leu2-3,112 trp1-1 ura3-1*	Thomas and Rothstein 1989
LPY1552	*MAT*a/*MAT*α *ade2-1 can1-100 his3-11,15 leu2-3,112 trp1-1 ura3-1*	
LPY3291	*MAT*a *his3Δ200 leu2-3,112 trp1Δ1 ura3-52 esa1Δ::HIS3* + pLP863	Clarke et al. 1999
LPY4909	W303 *MAT*α rDNA*::ADE2-CAN1*	Clarke et al. 2006
LPY4911	W303 *MAT*α *esa1-414* rDNA*::ADE2CAN1*	Clarke et al. 2006
LPY9119	W303 *MAT*a *HSL7-HA₃::kanMX*	M. Ruault
LPY11682	W303 *MAT*a *NRD1-HA₂*	
LPY11683	W303 *MAT*a *NRD1-HA₂*	
LPY11715	W303 *MAT*α *nrd1Δ::kanMX* + pLP2004	
LPY11719	W303 *MAT*α *nrd1Δ::kanMX* + pLP2007	
LPY11723	W303 *MAT*α *nrd1Δ::kanMX* + pLP2008	
LPY11872	W303 *MAT*a *nrd1Δ::kanMX* rDNA*::ADE2-CAN1* + pLP1995	
LPY11873	W303 *MAT*a *nrd1Δ::kanMX* rDNA*::ADE2-CAN1* + pLP1996	
LPY11874	W303 *MAT*a *nrd1Δ::kanMX* rDNA*::ADE2-CAN1* + pLP1997	
LPY11875	W303 *MAT*a *esa1-414 nrd1Δ::kanMX* rDNA*::ADE2-CAN1* + pLP1995	
LPY11876	W303 *MAT*a *esa1-414 nrd1Δ::kanMX* rDNA*::ADE2-CAN1* + pLP1996	
LPY11877	W303 *MAT*a *esa1-414 nrd1Δ::kanMX* rDNA*::ADE2-CAN1* + pLP1997	

Unless otherwise noted, strains were constructed during the course of this study or are part of the standard lab collection.

Table C-2. Plasmids used in Appendix C

Plasmid (alias)	Description	Source/Reference
pLP863	*esa1-414 TRP1* CEN	A. Clarke
pLP362 (pRS426)	vector *URA3* 2μ	Sikorski and Hieter 1989
pLP1402 (pRS202)	vector *URA3* 2μ	P. Hieter
pLP2018	*NAB3 URA3* 2μ	
pLP2054	*NRD1 URA3* 2μ	
pLP1995 (pJC580)	*NRD1-HA LEU2* CEN	Conrad et al. 2000
pLP1996 (pJC719)	*nrd1-101-HA LEU2* CEN	Conrad et al. 2000
pLP1997 (pJC720)	*nrd1-102-HA LEU2* CEN	Conrad et al. 2000
pLP1998 (pJC743)	*NRD1-HA$_2$ URA3* Integrating	J. Corden
pLP1999 (pJC744)	*nrd1-101-HA$_2$ URA3* Integrating	J. Corden
pLP2000 (pJC745)	*nrd1-102-HA$_2$ URA3* Integrating	J. Corden
pLP2004	*NRD1 URA3* CEN	Steinmetz and Brow 1996
pLP2007	*nrd1-3 URA3* CEN	Steinmetz and Brow 1996
pLP2008	*nrd1-5 URA3* CEN	Steinmetz and Brow 1996
pLP2009	*NRD1 TRP1* CEN	Steinmetz and Brow 1996

Unless otherwise noted, plasmids were constructed during the course of this study or are part of the standard lab collection.

Table C-3. Oligonucleotide sequences used in Appendix C

Oligo #	Name	Sequence (5'-3')
813	NRD1-F Sac1	TTATGGTCGAAATGAGCT**C**CTGCGCACG
814	NRD1-R XhoI	GGTACT**C**GAGAAGCGCTTATGATTACG
838	NRD1-rev_1kb	CACCTAGTTCTCAATGGCAG

Nucleotides in **bold underline** in the above sequences are mutagenic, compared to the wild-type sequence. For all the knockout pairs, PCR was performed on genomic DNA isolated from haploid deletion strains dissected from the heterozygous diploid collection from the *Saccharomyces* Genome Deletion Project.

REFERENCES

Ahn, S.H., Cheung, W.L., Hsu, J.Y., Diaz, R.L., Smith, M.M., and Allis, C.D. 2005. Sterile 20 kinase phosphorylates histone H2B at serine 10 during hydrogen peroxide-induced apoptosis in *S. cerevisiae*. *Cell* **120**(1): 25-36.

Alejandro-Osorio, A.L., Huebert, D.J., Porcaro, D.T., Sonntag, M.E., Nillasithanukroh, S., Will, J.L., and Gasch, A.P. 2009. The histone deacetylase Rpd3p is required for transient changes in genomic expression in response to stress. *Genome Biol* **10**(5): R57.

Allard, S., Utley, R.T., Savard, J., Clarke, A., Grant, P., Brandl, C.J., Pillus, L., Workman, J.L., and Côté, J. 1999. NuA4, an essential transcription adaptor/histone H4 acetyltransferase complex containing Esa1p and the ATM-related cofactor Tra1p. *EMBO J* **18**(18): 5108-5119.

Aparicio, J.G., Viggiani, C.J., Gibson, D.G., and Aparicio, O.M. 2004. The Rpd3-Sin3 histone deacetylase regulates replication timing and enables intra-S origin control in Saccharomyces cerevisiae. *Mol Cell Biol* **24**(11): 4769-4780.

Avvakumov, N. and Côté, J. 2007. The MYST family of histone acetyltransferases and their intimate links to cancer. *Oncogene* **26**(37): 5395-5407.

Babiarz, J.E., Halley, J.E., and Rine, J. 2006. Telomeric heterochromatin boundaries require NuA4-dependent acetylation of histone variant H2A.Z in *Saccharomyces cerevisiae*. *Genes Dev* **20**(6): 700-710.

Basu, A., Rose, K.L., Zhang, J., Beavis, R.C., Ueberheide, B., Garcia, B.A., Chait, B., Zhao, Y., Hunt, D.F., Segal, E., Allis, C.D., and Hake, S.B. 2009. Proteome-wide prediction of acetylation substrates. *Proc Natl Acad Sci USA* **106**(33): 13785-13790.

Bernstein, B.E., Tong, J.K., and Schreiber, S.L. 2000. Genomewide studies of histone deacetylase function in yeast. *Proc Natl Acad Sci USA* **97**(25): 13708-13713.

Bird, A.W., Yu, D.Y., Pray-Grant, M.G., Qiu, Q., Harmon, K.E., Megee, P.C., Grant, P.A., Smith, M.M., and Christman, M.F. 2002. Acetylation of histone H4 by Esa1 is required for DNA double-strand break repair. *Nature* **419**(6905): 411-415.

Bishop, D.K., Nikolski, Y., Oshiro, J., Chon, J., Shinohara, M., and Chen, X. 1999. High copy number suppression of the meiotic arrest caused by a *dmc1* mutation: *REC114* imposes an early recombination block and *RAD54* promotes a *DMC1*-independent DSB repair pathway. *Genes Cells* **4**(8): 425-444.

Biswas, D., Takahata, S., and Stillman, D.J. 2008. Different genetic functions for the Rpd3(L) and Rpd3(S) complexes suggest competition between NuA4 and Rpd3(S). *Mol Cell Biol* **28**(14): 4445-4458.

Blander, G. and Guarente, L. 2004. The Sir2 family of protein deacetylases. *Annu Rev Biochem* **73**: 417-435.

Boudreault, A.A., Cronier, D., Selleck, W., Lacoste, N., Utley, R.T., Allard, S., Savard, J., Lane, W.S., Tan, S., and Côté, J. 2003. Yeast enhancer of polycomb defines global Esa1-dependent acetylation of chromatin. *Genes Dev* **17**(11): 1415-1428.

Brachmann, C.B., Davies, A., Cost, G.J., Caputo, E., Li, J., Hieter, P., and Boeke, J.D. 1998. Designer deletion strains derived from *Saccharomyces cerevisiae* S288C: a useful set of strains and plasmids for PCR-mediated gene disruption and other applications. *Yeast* **14**(2): 115-132.

Brachmann, C.B., Sherman, J.M., Devine, S.E., Cameron, E.E., Pillus, L., and Boeke, J.D. 1995. The *SIR2* gene family, conserved from bacteria to humans, functions in silencing, cell cycle progression, and chromosome stability. *Genes Dev* **9**(23): 2888-2902.

Buszczak, M., Paterno, S., and Spradling, A.C. 2009. Drosophila stem cells share a common requirement for the histone H2B ubiquitin protease scrawny. *Science* **323**(5911): 248-251.

Carlson, M. 1997. Genetics of transcriptional regulation in yeast: connections to the RNA polymerase II CTD. *Annu Rev Cell Dev Biol* **13**: 1-23.

Carroll, K.L., Ghirlando, R., Ames, J.M., and Corden, J.L. 2007. Interaction of yeast RNA-binding proteins Nrd1 and Nab3 with RNA polymerase II terminator elements. *RNA* **13**(3): 361-373.

Carroll, K.L., Pradhan, D.A., Granek, J.A., Clarke, N.D., and Corden, J.L. 2004. Identification of cis elements directing termination of yeast nonpolyadenylated snoRNA transcripts. *Mol Cell Biol* **24**(14): 6241-6252.

Carrozza, M.J., Florens, L., Swanson, S.K., Shia, W.J., Anderson, S., Yates, J., Washburn, M.P., and Workman, J.L. 2005a. Stable incorporation of sequence specific repressors Ash1 and Ume6 into the Rpd3L complex. *Biochim Biophys Acta* **1731**(2): 77-87; discussion 75-76.

Carrozza, M.J., Li, B., Florens, L., Suganuma, T., Swanson, S.K., Lee, K.K., Shia, W.J., Anderson, S., Yates, J., Washburn, M.P., and Workman, J.L. 2005b. Histone H3 methylation by Set2 directs deacetylation of coding regions by Rpd3S to suppress spurious intragenic transcription. *Cell* **123**(4): 581-592.

Chang, C.S. and Pillus, L. 2009. Collaboration between the essential Esa1 acetyltransferase and the Rpd3 deacetylase is mediated by H4K12 histone acetylation in *Saccharomyces cerevisiae*. *Genetics* **183**(1): 149-160.

Choy, J.S. and Kron, S.J. 2002. NuA4 subunit Yng2 function in intra-S-phase DNA damage response. *Mol Cell Biol* **22**(23): 8215-8225.

Clarke, A. 2001. Genetic and biochemical characterization of *ESA1*: an essential histone acetyltransferase involved in cell cycle progression and transcriptional silencing. In *Molecular, Cellular and Developmental Biology*. University of Colorado, Boulder, Boulder, CO.

Clarke, A.S., Lowell, J.E., Jacobson, S.J., and Pillus, L. 1999. Esa1p is an essential histone acetyltransferase required for cell cycle progression. *Mol Cell Biol* **19**(4): 2515-2526.

Clarke, A.S., Samal, E., and Pillus, L. 2006. Distinct Roles for the Essential MYST Family HAT Esa1p in Transcriptional Silencing. *Mol Biol Cell* **17**(4): 1744-1757.

Cohen, T.J., Mallory, M.J., Strich, R., and Yao, T.P. 2008. Hos2p/Set3p deacetylase complex signals secretory stress through the Mpk1p cell integrity pathway. *Eukaryot Cell* **7**(7): 1191-1199.

Collins, S.R., Miller, K.M., Maas, N.L., Roguev, A., Fillingham, J., Chu, C.S., Schuldiner, M., Gebbia, M., Recht, J., Shales, M., Ding, H., Xu, H., Han, J., Ingvarsdottir, K., Cheng, B., Andrews, B., Boone, C., Berger, S.L., Hieter, P., Zhang, Z., Brown, G.W., Ingles, C.J., Emili, A., Allis, C.D., Toczyski, D.P., Weissman, J.S., Greenblatt, J.F., and Krogan, N.J. 2007. Functional dissection of protein complexes involved in yeast chromosome biology using a genetic interaction map. *Nature* **446**(7137): 806-810.

Conrad, N.K., Wilson, S.M., Steinmetz, E.J., Patturajan, M., Brow, D.A., Swanson, M.S., and Corden, J.L. 2000. A yeast heterogeneous nuclear ribonucleoprotein complex associated with RNA polymerase II. *Genetics* **154**(2): 557-571.

Costanzo, M., Baryshnikova, A., Bellay, J., Kim, Y., Spear, E.D., Sevier, C.S., Ding, H., Koh, J.L., Toufighi, K., Mostafavi, S., Prinz, J., St Onge, R.P., VanderSluis, B., Makhnevych, T., Vizeacoumar, F.J., Alizadeh, S., Bahr, S., Brost, R.L., Chen, Y., Cokol, M., Deshpande, R., Li, Z., Lin, Z.Y., Liang, W., Marback, M., Paw, J., San Luis, B.J., Shuteriqi, E., Tong, A.H., van Dyk, N., Wallace, I.M., Whitney, J.A., Weirauch, M.T., Zhong, G., Zhu, H., Houry, W.A., Brudno, M., Ragibizadeh, S., Papp, B., Pal, C., Roth, F.P., Giaever, G., Nislow, C., Troyanskaya, O.G., Bussey, H., Bader, G.D., Gingras, A.C., Morris, Q.D., Kim, P.M., Kaiser, C.A., Myers, C.L., Andrews, B.J., and Boone, C. 2010. The genetic landscape of a cell. *Science* **327**(5964): 425-431.

Dang, W., Steffen, K.K., Perry, R., Dorsey, J.A., Johnson, F.B., Shilatifard, A., Kaeberlein, M., Kennedy, B.K., and Berger, S.L. 2009. Histone H4 lysine 16 acetylation regulates cellular lifespan. *Nature* **459**(7248): 802-807.

Davies, B.W., Kohanski, M.A., Simmons, L.A., Winkler, J.A., Collins, J.J., and Walker, G.C. 2009. Hydroxyurea induces hydroxyl radical-mediated cell death in *Escherichia coli*. *Mol Cell* **36**(5): 845-860.

De Nadal, E., Zapater, M., Alepuz, P.M., Sumoy, L., Mas, G., and Posas, F. 2004. The MAPK Hog1 recruits Rpd3 histone deacetylase to activate osmoresponsive genes. *Nature* **427**(6972): 370-374.

De Rubertis, F., Kadosh, D., Henchoz, S., Pauli, D., Reuter, G., Struhl, K., and Spierer, P. 1996. The histone deacetylase RPD3 counteracts genomic silencing in Drosophila and yeast. *Nature* **384**(6609): 589-591.

Decker, P.V., Yu, D.Y., Iizuka, M., Qiu, Q., and Smith, M.M. 2008. Catalytic-site mutations in the MYST family histone acetyltransferase Esa1. *Genetics* **178**(3): 1209-1220.

Dion, M.F., Altschuler, S.J., Wu, L.F., and Rando, O.J. 2005. Genomic characterization reveals a simple histone H4 acetylation code. *Proc Natl Acad Sci USA* **102**(15): 5501-5506.

Downs, J.A., Allard, S., Jobin-Robitaille, O., Javaheri, A., Auger, A., Bouchard, N., Kron, S.J., Jackson, S.P., and Côté, J. 2004. Binding of chromatin-modifying activities to phosphorylated histone H2A at DNA damage sites. *Mol Cell* **16**(6): 979-990.

Doyon, Y. and Côté, J. 2004. The highly conserved and multifunctional NuA4 HAT complex. *Curr Opin Genet Dev* **14**(2): 147-154.

Durant, M. and Pugh, B.F. 2006. Genome-wide relationships between TAF1 and histone acetyltransferases in *Saccharomyces cerevisiae*. *Mol Cell Biol* **26**(7): 2791-2802.

Eisen, A., Utley, R.T., Nourani, A., Allard, S., Schmidt, P., Lane, W.S., Lucchesi, J.C., and Côté, J. 2001. The yeast NuA4 and Drosophila MSL complexes contain homologous subunits important for transcription regulation. *J Biol Chem* **276**(5): 3484-3491.

Fritze, C.E., Verschueren, K., Strich, R., and Easton Esposito, R. 1997. Direct evidence for *SIR2* modulation of chromatin structure in yeast rDNA. *EMBO J* **16**(21): 6495-6509.

Futcher, B. and Carbon, J. 1986. Toxic effects of excess cloned centromeres. *Mol Cell Biol* **6**(6): 2213-2222.

Galarneau, L., Nourani, A., Boudreault, A.A., Zhang, Y., Heliot, L., Allard, S., Savard, J., Lane, W.S., Stillman, D.J., and Côté, J. 2000. Multiple links between the NuA4 histone acetyltransferase complex and epigenetic control of transcription. *Mol Cell* **5**(6): 927-937.

Gallwitz, D. and Seidel, R. 1980. Molecular cloning of the actin gene from yeast Saccharomyces cerevisiae. *Nucleic Acids Res* **8**(5): 1043-1059.

Gershey, E.L., Vidali, G., and Allfrey, V.G. 1968. Chemical studies of histone acetylation. The occurrence of epsilon-N-acetyllysine in the f2a1 histone. *J Biol Chem* **243**(19): 5018-5022.

Gotta, M., Strahl-Bolsinger, S., Renauld, H., Laroche, T., Kennedy, B.K., Grunstein, M., and Gasser, S.M. 1997. Localization of Sir2p: the nucleolus as a compartment for silent information regulators. *EMBO J* **16**(11): 3243-3255.

Grant, P.A., Schieltz, D., Pray-Grant, M.G., Yates, J.R., 3rd, and Workman, J.L. 1998. The ATM-related cofactor Tra1 is a component of the purified SAGA complex. *Mol Cell* **2**(6): 863-867.

Hampsey, M. 1997. A review of phenotypes in *Saccharomyces cerevisiae. Yeast* **13**(12): 1099-1133.

Hanway, D., Chin, J.K., Xia, G., Oshiro, G., Winzeler, E.A., and Romesberg, F.E. 2002. Previously uncharacterized genes in the UV- and MMS-induced DNA damage response in yeast. *Proc Natl Acad Sci USA* **99**(16): 10605-10610.

Hawley, R.S. and Walker, M.Y. 2003. *Advanced genetic analysis : finding meaning in a genome*. Blackwell Pub., Malden, MA.

Henikoff, S. 2005. Histone modifications: combinatorial complexity or cumulative simplicity? *Proc Natl Acad Sci USA* **102**(15): 5308-5309.

Henry, S.A., Klig, L.S., and Loewy, B.S. 1984. The genetic regulation and coordination of biosynthetic pathways in yeast: amino acid and phospholipid synthesis. *Annu Rev Genet* **18**: 207-231.

Hsiang, Y.H., Hertzberg, R., Hecht, S., and Liu, L.F. 1985. Camptothecin induces protein-linked DNA breaks via mammalian DNA topoisomerase I. *J Biol Chem* **260**(27): 14873-14878.

Huang, H., Maertens, A.M., Hyland, E.M., Dai, J., Norris, A., Boeke, J.D., and Bader, J.S. 2009. HistoneHits: a database for histone mutations and their phenotypes. *Genome Res* **19**(4): 674-681.

Jacobson, S. and Pillus, L. 2009. The SAGA subunit Ada2 functions in transcriptional silencing. *Mol Cell Biol* **29**(22): 6033-6045.

Jazayeri, A., McAinsh, A.D., and Jackson, S.P. 2004. Saccharomyces cerevisiae Sin3p facilitates DNA double-strand break repair. *Proc Natl Acad Sci USA* **101**(6): 1644-1649.

Jenuwein, T. and Allis, C.D. 2001. Translating the histone code. *Science* **293**(5532): 1074-1080.

Kadosh, D. and Struhl, K. 1997. Repression by Ume6 involves recruitment of a complex containing Sin3 corepressor and Rpd3 histone deacetylase to target promoters. *Cell* **89**(3): 365-371.

Kadosh, D. and Struhl, K. 1998a. Histone deacetylase activity of Rpd3 is important for transcriptional repression in vivo. *Genes Dev* **12**(6): 797-805.

Kadosh, D. and Struhl, K. 1998b. Targeted recruitment of the Sin3-Rpd3 histone deacetylase complex generates a highly localized domain of repressed chromatin in vivo. *Mol Cell Biol* **18**(9): 5121-5127.

Kasten, M.M., Dorland, S., and Stillman, D.J. 1997. A large protein complex containing the yeast Sin3p and Rpd3p transcriptional regulators. *Mol Cell Biol* **17**(8): 4852-4858.

Keogh, M.C., Kurdistani, S.K., Morris, S.A., Ahn, S.H., Podolny, V., Collins, S.R., Schuldiner, M., Chin, K., Punna, T., Thompson, N.J., Boone, C., Emili, A., Weissman, J.S., Hughes, T.R., Strahl, B.D., Grunstein, M., Greenblatt, J.F., Buratowski, S., and Krogan, N.J. 2005. Cotranscriptional Set2 methylation of histone H3 lysine 36 recruits a repressive Rpd3 complex. *Cell* **123**(4): 593-605.

Keogh, M.C., Mennella, T.A., Sawa, C., Berthelet, S., Krogan, N.J., Wolek, A., Podolny, V., Carpenter, L.R., Greenblatt, J.F., Baetz, K., and Buratowski, S. 2006. The *Saccharomyces cerevisiae* histone H2A variant Htz1 is acetylated by NuA4. *Genes Dev* **20**(6): 660-665.

Kimura, A., Umehara, T., and Horikoshi, M. 2002. Chromosomal gradient of histone acetylation established by Sas2p and Sir2p functions as a shield against gene silencing. *Nat Genet* **32**(3): 370-377.

Kirmizis, A., Santos-Rosa, H., Penkett, C.J., Singer, M.A., Vermeulen, M., Mann, M., Bahler, J., Green, R.D., and Kouzarides, T. 2007. Arginine methylation at histone H3R2 controls deposition of H3K4 trimethylation. *Nature* **449**(7164): 928-932.

Kleff, S., Andrulis, E.D., Anderson, C.W., and Sternglanz, R. 1995. Identification of a gene encoding a yeast histone H4 acetyltransferase. *J Biol Chem* **270**(42): 24674-24677.

Knott, S.R., Viggiani, C.J., Tavare, S., and Aparicio, O.M. 2009. Genome-wide replication profiles indicate an expansive role for Rpd3L in regulating replication initiation timing or efficiency, and reveal genomic loci of Rpd3 function in *Saccharomyces cerevisiae*. *Genes Dev* **23**(9): 1077-1090.

Kornberg, R.D. and Lorch, Y. 1999. Twenty-five years of the nucleosome, fundamental particle of the eukaryote chromosome. *Cell* **98**(3): 285-294.

Krogan, N.J., Keogh, M.C., Datta, N., Sawa, C., Ryan, O.W., Ding, H., Haw, R.A., Pootoolal, J., Tong, A., Canadien, V., Richards, D.P., Wu, X., Emili, A., Hughes, T.R., Buratowski, S., and Greenblatt, J.F. 2003. A Snf2 family ATPase complex required for recruitment of the histone H2A variant Htz1. *Mol Cell* **12**(6): 1565-1576.

Kurdistani, S.K., Robyr, D., Tavazoie, S., and Grunstein, M. 2002. Genome-wide binding map of the histone deacetylase Rpd3 in yeast. *Nat Genet* **31**(3): 248-254.

Lafon, A., Chang, C.S., Scott, E.M., Jacobson, S.J., and Pillus, L. 2007. MYST opportunities for growth control: yeast genes illuminate human cancer gene functions. *Oncogene* **26**(37): 5373-5384.

Le Tallec, B., Barrault, M.B., Courbeyrette, R., Guerois, R., Marsolier-Kergoat, M.C., and Peyroche, A. 2007. 20S proteasome assembly is orchestrated by two distinct pairs of chaperones in yeast and in mammals. *Mol Cell* **27**(4): 660-674.

Lechner, T., Carrozza, M.J., Yu, Y., Grant, P.A., Eberharter, A., Vannier, D., Brosch, G., Stillman, D.J., Shore, D., and Workman, J.L. 2000. Sds3 (suppressor of defective silencing 3) is an integral component of the yeast Sin3·Rpd3 histone deacetylase complex and is required for histone deacetylase activity. *J Biol Chem* **275**(52): 40961-40966.

Lin, Y.Y., Lu, J.Y., Zhang, J., Walter, W., Dang, W., Wan, J., Tao, S.C., Qian, J., Zhao, Y., Boeke, J.D., Berger, S.L., and Zhu, H. 2009. Protein acetylation microarray reveals that NuA4 controls key metabolic target regulating gluconeogenesis. *Cell* **136**(6): 1073-1084.

Lin, Y.Y., Qi, Y., Lu, J.Y., Pan, X., Yuan, D.S., Zhao, Y., Bader, J.S., and Boeke, J.D. 2008. A comprehensive synthetic genetic interaction network governing yeast histone acetylation and deacetylation. *Genes Dev* **22**(15): 2062-2074.

Loewith, R., Meijer, M., Lees-Miller, S.P., Riabowol, K., and Young, D. 2000. Three yeast proteins related to the human candidate tumor suppressor p33(ING1) are associated with histone acetyltransferase activities. *Mol Cell Biol* **20**(11): 3807-3816.

Loewith, R., Smith, J.S., Meijer, M., Williams, T.J., Bachman, N., Boeke, J.D., and Young, D. 2001. Pho23 is associated with the Rpd3 histone deacetylase and is required for its normal function in regulation of gene expression and silencing in *Saccharomyces cerevisiae*. *J Biol Chem* **276**(26): 24068-24074.

Longtine, M.S., McKenzie, A., 3rd, Demarini, D.J., Shah, N.G., Wach, A., Brachat, A., Philippsen, P., and Pringle, J.R. 1998. Additional modules for versatile and economical PCR-based gene deletion and modification in Saccharomyces cerevisiae. *Yeast* **14**(10): 953-961.

Lykke-Andersen, S. and Jensen, T.H. 2007. Overlapping pathways dictate termination of RNA polymerase II transcription. *Biochimie* **89**(10): 1177-1182.

Matsubara, K., Sano, N., Umehara, T., and Horikoshi, M. 2007. Global analysis of functional surfaces of core histones with comprehensive point mutants. *Genes Cells* **12**(1): 13-33.

Megee, P.C., Morgan, B.A., and Smith, M.M. 1995. Histone H4 and the maintenance of genome integrity. *Genes Dev* **9**(14): 1716-1727.

Meijsing, S.H. and Ehrenhofer-Murray, A.E. 2001. The silencing complex SAS-I links histone acetylation to the assembly of repressed chromatin by CAF-I and Asf1 in Saccharomyces cerevisiae. *Genes Dev* **15**(23): 3169-3182.

Millar, C.B., Xu, F., Zhang, K., and Grunstein, M. 2006. Acetylation of H2AZ Lys 14 is associated with genome-wide gene activity in yeast. *Genes Dev* **20**(6): 711-722.

Mitchell, L., Lambert, J.P., Gerdes, M., Al-Madhoun, A.S., Skerjanc, I.S., Figeys, D., and Baetz, K. 2008. Functional dissection of the NuA4 histone acetyltransferase reveals its role as a genetic hub and that Eaf1 is essential for complex integrity. *Mol Cell Biol* **28**(7): 2244-2256.

Mizuguchi, G., Shen, X., Landry, J., Wu, W.H., Sen, S., and Wu, C. 2004. ATP-driven exchange of histone H2AZ variant catalyzed by SWR1 chromatin remodeling complex. *Science* **303**(5656): 343-348.

Mizzen, C.A., Yang, X.J., Kokubo, T., Brownell, J.E., Bannister, A.J., Owen-Hughes, T., Workman, J., Wang, L., Berger, S.L., Kouzarides, T., Nakatani, Y., and Allis, C.D. 1996. The TAF(II)250 subunit of TFIID has histone acetyltransferase activity. *Cell* **87**(7): 1261-1270.

Mnaimneh, S., Davierwala, A.P., Haynes, J., Moffat, J., Peng, W.T., Zhang, W., Yang, X., Pootoolal, J., Chua, G., Lopez, A., Trochesset, M., Morse, D., Krogan, N.J., Hiley, S.L., Li, Z., Morris, Q., Grigull, J., Mitsakakis, N., Roberts, C.J., Greenblatt, J.F., Boone, C., Kaiser, C.A., Andrews, B.J., and Hughes, T.R. 2004. Exploration of essential gene functions via titratable promoter alleles. *Cell* **118**(1): 31-44.

Muren, E., Oyen, M., Barmark, G., and Ronne, H. 2001. Identification of yeast deletion strains that are hypersensitive to brefeldin A or monensin, two drugs that affect intracellular transport. *Yeast* **18**(2): 163-172.

Nakanishi, S., Sanderson, B.W., Delventhal, K.M., Bradford, W.D., Staehling-Hampton, K., and Shilatifard, A. 2008. A comprehensive library of histone mutants identifies nucleosomal residues required for H3K4 methylation. *Nat Struct Mol Biol* **15**(8): 881-888.

Nitiss, J. and Wang, J.C. 1988. DNA topoisomerase-targeting antitumor drugs can be studied in yeast. *Proc Natl Acad Sci USA* **85**(20): 7501-7505.

Nonet, M.L. and Young, R.A. 1989. Intragenic and extragenic suppressors of mutations in the heptapeptide repeat domain of *Saccharomyces cerevisiae* RNA polymerase II. *Genetics* **123**(4): 715-724.

Norris, K.L., Lee, J.Y., and Yao, T.P. 2009. Acetylation goes global: the emergence of acetylation biology. *Sci Signal* **2**(97): pe76.

Nourani, A., Howe, L., Pray-Grant, M.G., Workman, J.L., Grant, P.A., and Côté, J. 2003. Opposite role of yeast ING family members in p53-dependent transcriptional activation. *J Biol Chem* **278**(21): 19171-19175.

Papamichos-Chronakis, M., Petrakis, T., Ktistaki, E., Topalidou, I., and Tzamarias, D. 2002. Cti6, a PHD domain protein, bridges the Cyc8-Tup1 corepressor and the SAGA coactivator to overcome repression at *GAL1*. *Mol Cell* **9**(6): 1297-1305.

Parthun, M.R., Widom, J., and Gottschling, D.E. 1996. The major cytoplasmic histone acetyltransferase in yeast: links to chromatin replication and histone metabolism. *Cell* **87**(1): 85-94.

Pijnappel, W.W., Schaft, D., Roguev, A., Shevchenko, A., Tekotte, H., Wilm, M., Rigaut, G., Seraphin, B., Aasland, R., and Stewart, A.F. 2001. The *S. cerevisiae* SET3 complex includes two histone deacetylases, Hos2 and Hst1, and is a meiotic-specific repressor of the sporulation gene program. *Genes Dev* **15**(22): 2991-3004.

Prelich, G. 1999. Suppression mechanisms: themes from variations. *Trends Genet* **15**(7): 261-266.

Raisner, R.M. and Madhani, H.D. 2008. Genomewide screen for negative regulators of sirtuin activity in *Saccharomyces cerevisiae* reveals 40 loci and links to metabolism. *Genetics* **179**(4): 1933-1944.

Ramos, F., Verhasselt, P., Feller, A., Peeters, P., Wach, A., Dubois, E., and Volckaert, G. 1996. Identification of a gene encoding a homocitrate synthase isoenzyme of *Saccharomyces cerevisiae*. *Yeast* **12**(13): 1315-1320.

Reid, J.L., Iyer, V.R., Brown, P.O., and Struhl, K. 2000. Coordinate regulation of yeast ribosomal protein genes is associated with targeted recruitment of Esa1 histone acetylase. *Mol Cell* **6**(6): 1297-1307.

Renauld, H., Aparicio, O.M., Zierath, P.D., Billington, B.L., Chhablani, S.K., and Gottschling, D.E. 1993. Silent domains are assembled continuously from the telomere and are defined by promoter distance and strength, and by *SIR3* dosage. *Genes Dev* **7**(7A): 1133-1145.

Rine, J. 1991. Gene overexpression in studies of *Saccharomyces cerevisiae*. *Methods Enzymol* **194**: 239-251.

Robert, F., Pokholok, D.K., Hannett, N.M., Rinaldi, N.J., Chandy, M., Rolfe, A., Workman, J.L., Gifford, D.K., and Young, R.A. 2004. Global position and recruitment of HATs and HDACs in the yeast genome. *Mol Cell* **16**(2): 199-209.

Robyr, D., Suka, Y., Xenarios, I., Kurdistani, S.K., Wang, A., Suka, N., and Grunstein, M. 2002. Microarray deacetylation maps determine genome-wide functions for yeast histone deacetylases. *Cell* **109**(4): 437-446.

Roguev, A. and Krogan, N.J. 2007. SIN-fully silent: HDAC complexes in fission yeast. *Nat Struct Mol Biol* **14**(5): 358-359.

Ruault, M. and Pillus, L. 2006. Chromatin-modifiying enzymes are essential when the *Saccharomyces cerevisiae* morphogenesis checkpoint is constitutively activated. *Genetics* **174**(3): 1135-1149.

Rundlett, S.E., Carmen, A.A., Kobayashi, R., Bavykin, S., Turner, B.M., and Grunstein, M. 1996. HDA1 and RPD3 are members of distinct yeast histone deacetylase complexes that regulate silencing and transcription. *Proc Natl Acad Sci USA* **93**(25): 14503-14508.

Rundlett, S.E., Carmen, A.A., Suka, N., Turner, B.M., and Grunstein, M. 1998. Transcriptional repression by UME6 involves deacetylation of lysine 5 of histone H4 by RPD3. *Nature* **392**(6678): 831-835.

Rusche, L.N., Kirchmaier, A.L., and Rine, J. 2003. The establishment, inheritance, and function of silenced chromatin in *Saccharomyces cerevisiae*. *Annu Rev Biochem* **72**: 481-516.

Rusche, L.N. and Rine, J. 2001. Conversion of a gene-specific repressor to a regional silencer. *Genes Dev* **15**(8): 955-967.

Sabet, N., Volo, S., Yu, C., Madigan, J.P., and Morse, R.H. 2004. Genome-wide analysis of the relationship between transcriptional regulation by Rpd3p and the histone H3 and H4 amino termini in budding yeast. *Mol Cell Biol* **24**(20): 8823-8833.

Schacherer, J., Ruderfer, D.M., Gresham, D., Dolinski, K., Botstein, D., and Kruglyak, L. 2007. Genome-wide analysis of nucleotide-level variation in commonly used *Saccharomyces cerevisiae strains*. *PLoS One* **2**(3): e322.

Schmidt, A., Hall, M.N., and Koller, A. 1994. Two FK506 resistance-conferring genes in *Saccharomyces cerevisiae*, *TAT1* and *TAT2*, encode amino acid permeases mediating tyrosine and tryptophan uptake. *Mol Cell Biol* **14**(10): 6597-6606.

Sertil, O., Vemula, A., Salmon, S.L., Morse, R.H., and Lowry, C.V. 2007. Direct role for the Rpd3 complex in transcriptional induction of the anaerobic *DAN/TIR* genes in yeast. *Mol Cell Biol* **27**(6): 2037-2047.

Shahbazian, M.D. and Grunstein, M. 2007. Functions of site-specific histone acetylation and deacetylation. *Annu Rev Biochem* **76**: 75-100.

Sharma, V.M., Tomar, R.S., Dempsey, A.E., and Reese, J.C. 2007. Histone deacetylases RPD3 and HOS2 regulate the transcriptional activation of DNA damage-inducible genes. *Mol Cell Biol* **27**(8): 3199-3210.

Sheldon, K.E., Mauger, D.M., and Arndt, K.M. 2005. A Requirement for the Saccharomyces cerevisiae Paf1 complex in snoRNA 3' end formation. *Mol Cell* **20**(2): 225-236.

Shimazu, T., Horinouchi, S., and Yoshida, M. 2007. Multiple histone deacetylases and the CREB-binding protein regulate pre-mRNA 3'-end processing. *J Biol Chem* **282**(7): 4470-4478.

Sikorski, R.S. and Hieter, P. 1989. A system of shuttle vectors and yeast host strains designed for efficient manipulation of DNA in *Saccharomyces cerevisiae*. *Genetics* **122**(1): 19-27.

Smith, B.C. and Denu, J.M. 2009. Chemical mechanisms of histone lysine and arginine modifications. *Biochim Biophys Acta* **1789**(1): 45-57.

Smith, E.R., Eisen, A., Gu, W., Sattah, M., Pannuti, A., Zhou, J., Cook, R.G., Lucchesi, J.C., and Allis, C.D. 1998a. ESA1 is a histone acetyltransferase that is essential for growth in yeast. *Proc Natl Acad Sci USA* **95**(7): 3561-3565.

Smith, J.S., Brachmann, C.B., Pillus, L., and Boeke, J.D. 1998b. Distribution of a limited Sir2 protein pool regulates the strength of yeast rDNA silencing and is modulated by Sir4p. *Genetics* **149**(3): 1205-1219.

Steinmetz, E.J. and Brow, D.A. 1996. Repression of gene expression by an exogenous sequence element acting in concert with a heterogeneous nuclear ribonucleoprotein-like protein, Nrd1, and the putative helicase Sen1. *Mol Cell Biol* **16**(12): 6993-7003.

Sterner, D.E., Belotserkovskaya, R., and Berger, S.L. 2002. SALSA, a variant of yeast SAGA, contains truncated Spt7, which correlates with activated transcription. *Proc Natl Acad Sci USA* **99**(18): 11622-11627.

Sterner, D.E. and Berger, S.L. 2000. Acetylation of histones and transcription-related factors. *Microbiol Mol Biol Rev* **64**(2): 435-459.

Stone, E.M., Heun, P., Laroche, T., Pillus, L., and Gasser, S.M. 2000. MAP kinase signaling induces nuclear reorganization in budding yeast. *Curr Biol* **10**(7): 373-382.

Suka, N., Carmen, A.A., Rundlett, S.E., and Grunstein, M. 1998. The regulation of gene activity by histones and the histone deacetylase RPD3. *Cold Spring Harb Symp Quant Biol* **63**: 391-399.

Suka, N., Luo, K., and Grunstein, M. 2002. Sir2p and Sas2p opposingly regulate acetylation of yeast histone H4 lysine16 and spreading of heterochromatin. *Nat Genet* **32**(3): 378-383.

Suka, N., Suka, Y., Carmen, A.A., Wu, J., and Grunstein, M. 2001. Highly specific antibodies determine histone acetylation site usage in yeast heterochromatin and euchromatin. *Mol Cell* **8**(2): 473-479.

Sun, Z.W. and Hampsey, M. 1999. A general requirement for the Sin3-Rpd3 histone deacetylase complex in regulating silencing in *Saccharomyces cerevisiae*. *Genetics* **152**(3): 921-932.

Tamburini, B.A. and Tyler, J.K. 2005. Localized histone acetylation and deacetylation triggered by the homologous recombination pathway of double-strand DNA repair. *Mol Cell Biol* **25**(12): 4903-4913.

Thomas, B.J. and Rothstein, R. 1989. Elevated recombination rates in transcriptionally active DNA. *Cell* **56**(4): 619-630.

Tong, A.H., Evangelista, M., Parsons, A.B., Xu, H., Bader, G.D., Page, N., Robinson, M., Raghibizadeh, S., Hogue, C.W., Bussey, H., Andrews, B., Tyers, M., and Boone, C. 2001. Systematic genetic analysis with ordered arrays of yeast deletion mutants. *Science* **294**(5550): 2364-2368.

van Leeuwen, F. and Gottschling, D.E. 2002. Assays for gene silencing in yeast. *Methods Enzymol* **350**: 165-186.

Vannier, D., Balderes, D., and Shore, D. 1996. Evidence that the transcriptional regulators *SIN3* and *RPD3*, and a novel gene (*SDS3*) with similar functions, are involved in transcriptional silencing in *S. cerevisiae*. *Genetics* **144**(4): 1343-1353.

Vidal, M. and Gaber, R.F. 1991. *RPD3* encodes a second factor required to achieve maximum positive and negative transcriptional states in Saccharomyces cerevisiae. *Mol Cell Biol* **11**(12): 6317-6327.

Vogelauer, M., Rubbi, L., Lucas, I., Brewer, B.J., and Grunstein, M. 2002. Histone acetylation regulates the time of replication origin firing. *Mol Cell* **10**(5): 1223-1233.

Voth, W.P., Jiang, Y.W., and Stillman, D.J. 2003. New 'marker swap' plasmids for converting selectable markers on budding yeast gene disruptions and plasmids. *Yeast* **20**(11): 985-993.

Wang, A., Kurdistani, S.K., and Grunstein, M. 2002. Requirement of Hos2 histone deacetylase for gene activity in yeast. *Science* **298**(5597): 1412-1414.

Wilson, S.M., Datar, K.V., Paddy, M.R., Swedlow, J.R., and Swanson, M.S. 1994. Characterization of nuclear polyadenylated RNA-binding proteins in *Saccharomyces cerevisiae*. *J Cell Biol* **127**(5): 1173-1184.

Winzeler, E.A., Castillo-Davis, C.I., Oshiro, G., Liang, D., Richards, D.R., Zhou, Y., and Hartl, D.L. 2003. Genetic diversity in yeast assessed with whole-genome oligonucleotide arrays. *Genetics* **163**(1): 79-89.

Winzeler, E.A., Shoemaker, D.D., Astromoff, A., Liang, H., Anderson, K., Andre, B., Bangham, R., Benito, R., Boeke, J.D., Bussey, H., Chu, A.M., Connelly, C., Davis, K., Dietrich, F., Dow, S.W., El Bakkoury, M., Foury, F., Friend, S.H., Gentalen, E., Giaever, G., Hegemann, J.H., Jones, T., Laub, M., Liao, H., Liebundguth, N., Lockhart, D.J., Lucau-Danila, A., Lussier, M., M'Rabet, N., Menard, P., Mittmann, M., Pai, C., Rebischung, C., Revuelta, J.L., Riles, L., Roberts, C.J., Ross-MacDonald, P., Scherens, B., Snyder, M., Sookhai-Mahadeo, S., Storms, R.K., Veronneau, S., Voet, M., Volckaert, G., Ward, T.R., Wysocki, R., Yen, G.S., Yu, K., Zimmermann, K., Philippsen, P., Johnston, M., and Davis, R.W. 1999. Functional characterization of the *S. cerevisiae* genome by gene deletion and parallel analysis. *Science* **285**(5429): 901-906.

Wu, P.Y. and Winston, F. 2002. Analysis of Spt7 function in the *Saccharomyces cerevisiae* SAGA coactivator complex. *Mol Cell Biol* **22**(15): 5367-5379.

Yang, B. and Kirchmaier, A.L. 2006. Bypassing the catalytic activity of SIR2 for SIR protein spreading in *Saccharomyces cerevisiae*. *Mol Biol Cell* **17**(12): 5287-5297.

Yang, X.J. and Seto, E. 2008. The Rpd3/Hda1 family of lysine deacetylases: from bacteria and yeast to mice and men. *Nat Rev Mol Cell Biol* **9**(3): 206-218.

Zhang, Y., Sun, Z.W., Iratni, R., Erdjument-Bromage, H., Tempst, P., Hampsey, M., and Reinberg, D. 1998. SAP30, a novel protein conserved between human and yeast, is a component of a histone deacetylase complex. *Mol Cell* **1**(7): 1021-1031.

Zhao, S., Xu, W., Jiang, W., Yu, W., Lin, Y., Zhang, T., Yao, J., Zhou, L., Zeng, Y., Li, H., Li, Y., Shi, J., An, W., Hancock, S.M., He, F., Qin, L., Chin, J., Yang, P.,

Chen, X., Lei, Q., Xiong, Y., and Guan, K.L. 2010. Regulation of cellular metabolism by protein lysine acetylation. *Science* **327**(5968): 1000-1004.

Zhou, J., Zhou, B.O., Lenzmeier, B.A., and Zhou, J.Q. 2009. Histone deacetylase Rpd3 antagonizes Sir2-dependent silent chromatin propagation. *Nucleic Acids Res* **37**(11): 3699-3713.